7. Mountain Glaciers and Ice Caps

Coordinating Lead Author: Martin Sharp

Lead Authors: Maria Ananicheva, Anthony Arendt, Jon-Ove Hagen, Regine Hock, Edward Josberger, R. Dan Moore, W. Tad Pfeffer, Gabriel J. Wolken

Contributing Authors: Helgi Björnsson, Carl Egede Bøggild, Tobias Bolch, Igor Buzin, John J. Clague, J. Graham Cogley, Mattias de Woul, Julian A. Dowdeswell, Mark B. Dyurgerov, Andrey Glazovsky, Hester Jiskoot, Tómas Jóhannesson, Alexander Klepikov, Alexander Krenke, Mark F. Meier, Brian Menounos, Alexander Milner, Yaroslav Muravyev, Matt Nolan, Finnur Palsson, Valentina Radić

Contents

Key Findings

- Mountain glaciers and ice caps in the Arctic cover an area of around 402 000 km^2 and contain about 0.41 m sea-level equivalent of water.
- Over the past century, nearly all have retreated from maximum extents reached during the Little Ice Age, which ended in the late 19th century. This period of glacier retreat has been associated with an overall reduction in glacier mass during the period of record, which extends to more than 60 years in some cases. Surface mass balance measurements showed negative or nearly balanced conditions and generally showed no trend until the mid-1990s, but since then reveal significantly higher rates of mass loss in Alaska, the Canadian Arctic, and Iceland.
- The fraction of ablation that occurs through iceberg calving can be as much as 40% in regions where it has been measured, but it has not been measured over large areas of the Arctic. Estimation of calving fluxes is therefore a major source of uncertainty in estimates of current and future rates of mass loss from mountain glaciers and ice caps in the Arctic.
- Mass loss (surface mass balance plus calving) from Arctic glaciers probably exceeded 150 Gt/y in the past decade, when it was similar to mass loss from the Greenland Ice Sheet. This suggests that glacier and ice sheet change in the Arctic is probably now the dominant contributor to the eustatic (water mass) component of global sea level rise.
- Under the IPCC A1B emissions scenario, the total volume of Arctic glaciers is projected to decline by between 13% and 36% by 2100 (corresponding to an increase of 51 to 136 mm sea-level equivalent), depending on the choice of general circulation model. These projections are a lower bound since they do not include mass losses by iceberg calving. Regardless, mountain glaciers and ice caps will continue to influence global sea-level changes beyond the 21st century.
- In many parts of the Arctic, climate warming should cause glacier runoff to increase for a few decades or longer, but glacier area reduction will ultimately cause glacier runoff to decline. These changes in glacier runoff will have impacts on water supplies; water quality; hydroelectric power generation; flood hazards; freshwater, estuarine and coastal habitats; and ocean circulation patterns.
- Iceberg hazards to shipping and offshore activities related to exploration for and exploitation of offshore hydrocarbon and mineral resources may increase if changes in tidewater glacier dynamics result in more iceberg production and/or larger bergs, and reductions in sea-ice cover allow icebergs to become more mobile.

Summary

In addition to the Greenland Ice Sheet, the Arctic contains a diverse array of smaller glaciers ranging from small cirque glaciers to large ice caps with areas up to 20 000 km^2. Together, these glaciers cover an area of more than 400 000 km^2, over half the global area of mountain glaciers and ice caps. Their total volume is sufficient to raise global sea level by an average of about 0.41 m if they were to melt completely.

These glaciers exist in a range of different climatic regimes, from the maritime environments of southern Alaska, Iceland, western Scandinavia, and Svalbard, to the polar desert of the Canadian Arctic. Glaciers in all regions of the Arctic have decreased in area and mass as a result of the warming that has occurred since the 1920s (in two pulses – from the 1920s to the 1940s and since the mid-1980s). A new phase of accelerated mass loss began in the mid-1990s, and has been most marked in Alaska, the Canadian Arctic, and probably Greenland. Current rates of mass loss are estimated to be in the range 150 to 300 Gt/y; comparable to current mass loss rates from the Greenland Ice Sheet. This implies that the Arctic is now the largest regional source of glacier contributions to global sea-level rise.

Most of the current mass loss is probably attributable to a change in surface mass balance (the balance between annual mass addition, primarily by snowfall, and annual mass loss by surface melting and meltwater runoff). Iceberg calving is also a significant source of mass loss in areas such as coastal Alaska, Arctic Canada, Svalbard, and the Russian Arctic. However, neither the current rate of calving loss nor its temporal variability have been well quantified in many regions, so this is a significant source of uncertainty in estimates of the total rate of mass loss. It is, however, clear that the larger Arctic ice caps have similar variability in ice dynamics to that of the Greenland Ice Sheet. That is to say, areas of relatively slow glacier flow (which terminate mainly on land) are separated by faster-flowing outlet glaciers (which terminate mainly in the ocean). Several of these outlet glaciers exhibit surge-type behavior, while others have exhibited substantial velocity changes on seasonal and longer timescales. It is very likely that these changes in ice dynamics affect the rate of mass loss by calving both from individual glaciers and the total ice cover.

Projections of future rates of mass loss from mountain glaciers and ice caps in the Arctic focus primarily on projections of changes in the surface mass balance. Current models are not yet capable of making realistic forecasts of changes in losses by calving. Surface mass balance models are forced with downscaled output from climate models driven by forcing scenarios that make assumptions about the future rate of growth of atmospheric greenhouse gas concentrations. Thus, mass loss projections vary considerably, depending on the forcing scenario used and the climate model from which climate projections are derived. A new study in which a surface mass balance model is driven by output from ten general circulation models (GCMs) forced by the IPCC (Intergovernmental Panel on Climate Change) A1B emissions scenario yields estimates of total mass loss of between 51 and 136 mm sea-level equivalent (SLE) (or 13% to 36% of current glacier volume) by 2100. This implies that there will still be substantial glacier mass in the Arctic in 2100 and that Arctic mountain glaciers and ice caps will continue to influence global sea-level change well into the 22nd century.

As glaciers and ice caps shrink in a warming climate, runoff initially increases in response to higher rates of surface melting. Ultimately, however, runoff will decline as reductions in glacier area outweigh the effect of more rapid melting. This phase of declining runoff does not yet seem to have begun in most regions of the Arctic, but it may begin soon in the Russian Arctic mountains. In the Yukon River basin, Greenland, Iceland, and Norway, glacier runoff is an important resource for hydroelectric power generation, and the viability of hydroelectric projects may ultimately be compromised by runoff decreases associated with glacier shrinkage.

Changes in glacier runoff also result in changes in stream temperature, sediment load, and nutrient export (both magnitude and type) that can be expected to initiate changes in the ecology and productivity of downstream river, lake, and fjord environments. Increased rates of glacier melt may accelerate the release of a range of 'legacy' pollutants stored in firn (partially compacted snow that is the intermediate stage between snow and glacier ice) and glacier ice back into the environment. Increasing freshwater fluxes to fjords and other nearshore marine environments will alter the characteristics of surface water masses and drive changes in circulation. Circulation changes may also follow the retreat of tidewater glaciers onto land, particularly in regions of upwelling close to the termini of these glaciers. These changes can decrease the availability of feeding and resting habitats that are important for marine mammals and seabirds.

The number and size of icebergs produced is likely to change as tidewater glaciers retreat, ultimately reaching zero as their termini emerge onto land. Break-up of floating glacier tongues and ice shelves, a process that has accelerated in the past decade along the northern coast of Ellesmere Island, results in large tabular bergs, while accelerated flow of tidewater glaciers tends to result in accelerated production of small bergs unless flotation of the glacier terminus occurs, when large tabular bergs may be produced. Cessation of small berg production when tidewater termini retreat onto land can reduce the number of such bergs that become grounded in fjords, decreasing the availability of important resting habitat for seals. Circulating icebergs are a potential hazard for shipping, drilling platforms, and seafloor pipelines in the Arctic. Circulation patterns and longevity of bergs may change as the Arctic sea-ice cover declines. Thinner and less extensive sea ice is likely to result in greater berg mobility, while warmer surface waters may result in more rapid melting and disintegration of bergs. A knowledge of the size distributions of bergs produced and circulating in different regions is critical to evaluating the risk of bergs contacting the sea floor and damaging seafloor pipelines.

Glacier retreat will be associated with changes in the magnitude and frequency of a range of geomorphological hazards, most notably outburst floods from ice-marginal and moraine-dammed proglacial lakes, and mass movements from newly deglaciated valley walls. The degree of risk from such phenomena will, however, be highly variable, depending upon the nature of the deglaciated terrain, the size of local populations, and the amount of infrastructure present in individual regions.

Finally, it should be emphasized that the ability to monitor and predict changes in the Arctic's mountain glaciers and ice caps is still quite limited. Basic inventory data for Arctic glaciers are lacking. The number of glaciers on which mass balance is measured is small and declining, and the distribution of measurement sites is highly non-uniform. There are no measurement sites at all in some areas with large glacier areas (such as the Russian Arctic and the Yukon). There is no routine monitoring of mass losses by iceberg calving, and understanding of what controls calving rates is rudimentary. This severely constrains the ability to model calving losses into the future. Studies of the socio-economic impacts of Arctic glacier change are currently few and limited in scope, so most statements about such impacts are based solely on general principles. As such, they do not provide a strong basis for either the formulation or enactment of a policy response to Arctic glacier change. Some of the largest impacts of the ongoing changes in Arctic glaciers (such as global sea-level rise) will be felt in regions of the world that are very far from the Arctic. They may, however, still have social, political, and economic repercussions for Arctic nations – repercussions that need to be explored more thoroughly.

7.1. Introduction

- Mountain glaciers and ice caps cover an area of nearly 402 000 km^2 in the Arctic. Over half of this area is in western North America and the Canadian Arctic.
- The combined volume of these glaciers is sufficient to raise sea level by around 0.41 m if they all melted.
- Glacier types range from small cirque glaciers to large ice caps, with areas of up to 20 000 km^2. These ice caps are dynamically complex, and are drained in part by fast-flowing outlet glaciers that often reach the ocean and lose mass by calving icebergs.
- In many regions, a proportion of the glaciers exhibit 'surge-type' behavior, in which long periods of flow at relatively low speeds are punctuated by short-lived episodes of very rapid flow.
- Long-term changes in the extent, volume, and mass of these glaciers are driven by changes in climate and oceanographic conditions that alter their 'mass balance' – the annual balance between mass gains (due mainly to snowfall) and mass losses (due mainly to surface melting and runoff, and iceberg calving).
- Changes in the thermal structure and flow of glaciers can play an important role in how, and how rapidly, they respond to changing climate and oceanographic conditions.

7.1.1. Background

Glacier ice (including mountain glaciers, ice caps and the Greenland Ice Sheet) occupies about 2.16 million km^2 of the Arctic land surface. This chapter deals with all mountain glaciers and ice caps (hereafter referred to as glaciers), including those in Greenland that are not connected to the ice sheet. The Greenland Ice Sheet itself is addressed in Chapter 8. Mountain glaciers are ice bodies whose geometry and boundaries are controlled by bedrock topography, while ice caps are dome-shaped ice bodies that submerge the underlying bedrock topography. Table 7.1 presents the regional distribution of the

Table 7.1. The areas (rounded to three significant figures) and estimated volumes, in mm sea-level equivalent (SLE), of ice caps and glaciers in the Arctic compared to global values and the ice sheets in Greenland and Antarctica.

Region	Ice-covered area, km^2	Volume[a], mm SLE	Source, area
Canadian Arctic	1 51 000	199 ± 30	Ommanney, 1970
Northwestern North America	91 800	71 ± 8	Berthier et al., 2010; ESRI, 2003
Russian Islands[b]	56 700	44 ± 8	Radić and Hock, 2010
Greenland[c]	48 600	44 ± 7	Weng, 1995
Svalbard	36 500	26 ± 2	Hagen et al., 1993
Iceland	11 000	12 ± 6	Björnsson and Pálsson, 2008
Scandinavia	3 100	6 ± 0	Østrem et al., 1973, 1988
Russian Arctic	2 900	4 ± 0	Radić and Hock, 2010
Total (Arctic)	401 600	410 ± 30	
Mountain glaciers and ice caps (global)	741 400	600 ± 70	Radić and Hock, 2010
Greenland Ice Sheet	1 755 600	7500	Bamber et al., 2001
Antarctic ice sheet Antarctic ice shelves	12 348 000 1 555 000	57 000	Fox and Cooper, 1994 (areas) Lythe et al., 2001 (volume)

[a] Volumes of all mountain glaciers and ice caps are from Radić and Hock (2010); [b] Franz Josef Land (13 700 km^2), Novaya Zemlya (23 600 km^2), Severnaya Zemlya (19 400 km^2); [c] Greenland excluding the ice sheet: only the glaciers physically disconnected from the ice sheet are considered here. Areas over 70 000 km^2 have been reported (Holtzscherer and Bauer, 1954; Weidick and Morris, 1998); however, these estimates have included some glaciers that are connected to the ice sheet but considered independent of the ice sheet in a dynamic sense or that were, by their morphology, discernible as units independent of the ice sheet. Nevertheless, the estimate by Weng (1995) is a minimum estimate because it is based on a 1:2 500 000 map, a scale too coarse to allow identification of many small glaciers.

area and volume of glacier ice in the Arctic. Here, the ice volume is given in units of mm sea-level equivalent (SLE), which is the volume of water (in m^3) stored as glacier ice, divided by the surface area of the global ocean (in m^2) multiplied by 1000.

7.1.2. Context: What did the Arctic Climate Impact Assessment report say about mountain glaciers and ice caps?

The SWIPA report is an update of knowledge on the state of the Arctic cryosphere relative to the Arctic Climate Impact Assessment (ACIA, 2005). This dealt with mountain glaciers, ice caps, and the Greenland Ice Sheet in a single section of Chapter 6, '*Cryosphere and Hydrology*'. It gave a regional summary of glacier changes since around 1950 with an emphasis on measurements of surface mass balance and, for regions where mass balance measurements were lacking, changes in glacier area. Mass losses by iceberg calving were mentioned but not discussed in detail. The major ACIA contribution was a series of projections of changes in the surface mass balance of Arctic glaciers for the period until 2100. These mass balance projections were computed using regional seasonal sensitivity characteristics (a measure of the expected change in the annual surface mass balance due to prescribed changes in monthly mean air temperature and precipitation amounts) and projected changes in temperature and precipitation derived from a suite of five GCMs forced by the IPCC B2 emissions scenario. The mass balance projections were used to estimate the potential contributions of different regions of the Arctic to sea level rise over the 21st century. The ACIA report also commented on the potential impacts of changes in glaciers for other parts of the physical system, ecosystems, and people, and gave an assessment of critical research needs that remains valid today.

7.1.3. Geographic setting

The glacierized areas (i.e. those presently overlain by glaciers) addressed in this chapter are shown in Figure 7.1. Most of the glaciers are located north of 60° N, but some more southerly glaciers, in Kamchatka, Alaska, and northwestern Canada are also included (Table 7.1). The total glacier-covered area is approximately 402 000 km^2, which is about 54% of all glaciers in the world excluding the large ice sheets (~741 400 km^2, Radić and Hock, 2010).

Arctic glaciers are irregularly distributed in space (Figure 7.1), and are located in a range of very different climatic regimes (Braithwaite, 2005). In southern Alaska, Iceland, western Scandinavia, and western Kamchatka, the climate is maritime with a relatively small annual temperature range and precipitation rates of a few metres per year, while in the Canadian High Arctic it is very dry, cold and continental, with short summers, a very large annual temperature range (greater than 50 °C), and annual precipitation that ranges from 0.1 to 0.7 m/y. Conditions on Svalbard and in the Russian Arctic islands fall between these two climatic extremes. In northwestern North America, most of the ice cover is in the mountain ranges adjacent to the Gulf of Alaska, while in Arctic Canada the most heavily glacierized regions are in the mountains on Devon and Ellesmere Islands, which are nourished in part by moisture from a large persistent polynya in northern Baffin Bay (the North Open Water).

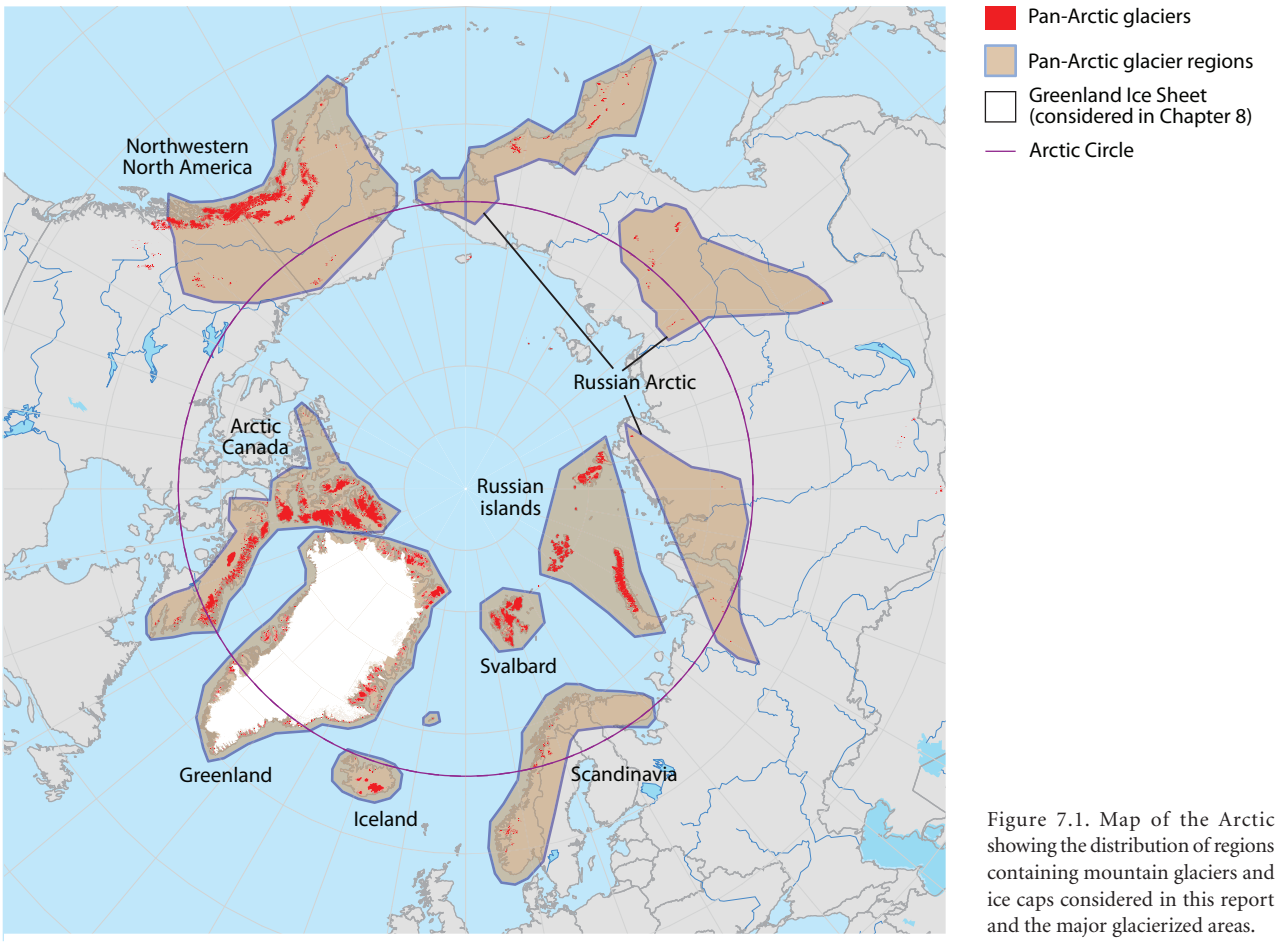

Figure 7.1. Map of the Arctic showing the distribution of regions containing mountain glaciers and ice caps considered in this report and the major glacierized areas.

7.1.4. Characteristics of Arctic mountain glaciers and ice caps

7.1.4.1. Morphology

Arctic glaciers have a range of forms. Dome-shaped ice caps have lobes and outlet glaciers that drain ice away from the accumulation area, where annual snowfall exceeds annual surface melt, to lower-lying regions (ablation areas) where the reverse is true, and in some cases to tidewater margins where the ice reaches the ocean and icebergs are calved. Large ice caps are found in the Canadian Arctic, Iceland, Svalbard, the Russian Arctic islands, and in Greenland beyond the margins of the ice sheet (Figure 7.2). In other regions, large glaciers originate from icefields that fill basins within mountain ranges (e.g., in southern Alaska). Many regions, for example Svalbard, also have a large number of individual valley glaciers that occupy valleys and basins in the landscape.

Much of the Arctic ice mass is contained in relatively large ice caps with areas of up to 20 000 km^2, although there are large numbers of independent glaciers with areas ranging from 0.1 to several thousand km^2 (Dowdeswell and Hagen, 2004). The largest ice masses in the Arctic are found in Arctic Canada, and include the Agassiz Ice Cap (17 300 km^2) and Prince of Wales Icefield (19 400 km^2) on Ellesmere Island, the Devon Island Ice Cap (about 14 400 km^2), and the Barnes and Penny Ice Caps (each almost 6000 km^2) on Baffin Island. On Greenland, the largest independent ice cap is the ~9000 km^2 Flade Isblink in the northeast, while the more northerly Hans Tausen Ice Cap, at 3975 km^2, is probably the best studied (Reeh et al., 2001). Austfonna on Nordaustlandet in eastern Svalbard (8120 km^2) is the largest ice cap in the Eurasian Arctic (Dowdeswell, 1986; Hagen et al., 1993). The largest Russian ice cap is the Academy of Sciences Ice Cap (5575 km^2) on Severnaya Zemlya (Dowdeswell et al., 2002), although the northern island of Novaya Zemlya has a larger ice-covered area with many outlet glaciers. In Iceland, Vatnajökull has an area of 8100 km^2 (Björnsson and Pálsson,

Figure 7.2. Small plateau ice caps on Axel Heiberg Island, Arctic Canada, with a larger ice cap in the distance. Note the clear contrast between the snow-covered accumulation area and the greyer ablation area, and the outlet glaciers draining into valleys leading away from the ice cap. Source: Martin Sharp, University of Alberta.

2008). Among the mountain glaciers (Figure 7.3), the largest is Bering Glacier in Alaska, with an area of 3630 km^2.

The larger Arctic ice caps and icefields (Figure 7.4) have complex dynamics involving a mix of fast- and slow-flowing elements that can vary in how they respond to climate changes and variability. Vestfonna on Nordaustlandet in eastern Svalbard is a good example, where four fast-flowing outlet glaciers are embedded within a largely slower-flowing ice cap of 2500 km^2 (Dowdeswell and Collin, 1990). Typical surface velocities may be less than 10 m/y close to the equilibrium-line altitude of valley and cirque glaciers that terminate on land. They can reach many hundreds of metres per year on major calving outlet glaciers, on which seasonal velocity variations can be large, with summer velocities up to an order of magnitude greater than winter velocities (Williamson et al., 2008). Interannual velocity variations can also be significant on such glaciers.

7.1.4.2. Thermal regime

Most glaciers in Iceland, Scandinavia, and central and southern Alaska are predominantly temperate (composed of ice at the pressure melting point). Elsewhere in the Arctic, glaciers tend to have polythermal temperature regimes (composed of a mixture of ice at and below the pressure melting point), and their dynamics may be strongly affected by climate-driven changes in the thermal regime. In some parts of polythermal glaciers, the ice temperature at the glacier bed is below the melting point, implying that the glacier is frozen to its bed. In some smaller (cold) glaciers, all the ice is at temperatures below the melting point, except at the surface where the ice temperature may reach the melting point in summer. The thermal regime of glaciers is determined by the prevailing climatic conditions (snow accumulation and surface energy balance). Climatic change can alter the thermal regime of a glacier, and potentially also its dynamics, because ice deforms more rapidly at higher temperatures and glacier flow can be enhanced by the lubricating effect of meltwater at the glacier bed. Most cold-based and polythermal glaciers are found in dry regions with low accumulation rates. It takes a long time for a climate change signal to penetrate into such glaciers, and changes in the temperature regime are probably not very large on a 100-year timescale. However, in areas where penetration of surface meltwater into cold firn on the glacier surface increases, the release of latent heat when this meltwater refreezes can cause a more rapid change in the thermal regime.

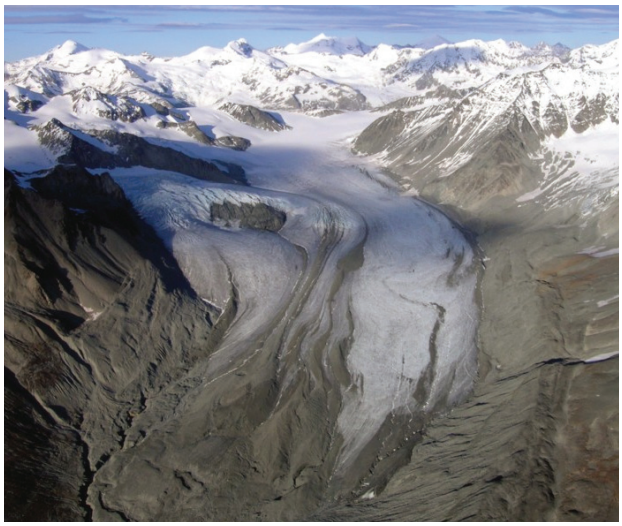

Figure 7.3. Gulkana Glacier in Alaska is a typical mountain glacier and a long-term mass balance monitoring site. Note the end moraines surrounding the glacier terminus that indicate that the glacier was more extensive and thicker in the past. Source: U.S. Geological Survey.

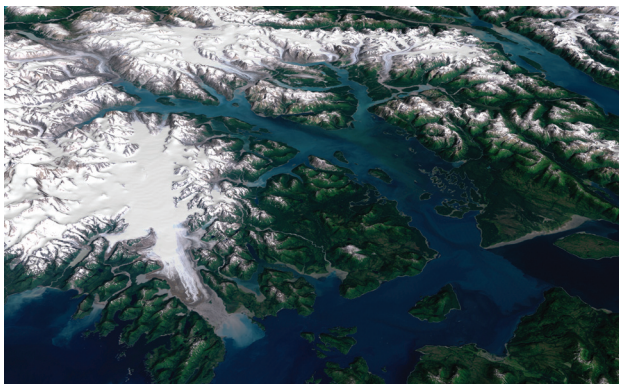

Figure 7.4. The Glacier Bay Icefield, Alaska. Outlet glaciers drain outward from a central accumulation area within the mountains. Source: Landsat imagery courtesy of NASA Goddard Space Flight Center and U.S. Geological Survey.

Owing to the polythermal nature of many Arctic glaciers, the formation of superimposed ice by meltwater refreezing on the glacier surface and internal accumulation (where percolating meltwater freezes in cold snow and firn) can be important processes of mass accumulation. When these processes occur, the refrozen water has to be melted again to become meltwater runoff, complicating the measurement and modeling of the surface mass balance. Neglecting or inadequately accounting for these processes in mass balance measurements overestimates mass loss. Superimposed ice formation is important on many Arctic glaciers and is the dominant form of accumulation on some (Koerner, 1970).

Surge-type glacier behavior is common in many parts of the Arctic and can be a source of significant hazards. In a glacier surge, surface velocities increase by an order of magnitude or more and glacier fronts can advance many kilometres (sometimes more than 10 km) in a matter of years. When tidewater glaciers surge, iceberg production increases and can be an important process of mass loss from the glacier (Liestøl, 1973; Dowdeswell, 1989). While the occurrence of individual surges is not directly related to climate change, climate change may alter the frequency of surging (Dowdeswell et al., 1991; Eisen et al., 2001), or even cause glaciers to cease being of the surge type (Dowdeswell et al., 1995). Changes in the number of actively surging glaciers in a region that extend into tidewater can have a large short-term impact on the regional glacier mass balance through changes in the overall calving flux to the ocean.

7.1.4.3. Tidewater glaciers

Iceberg calving plays a major role in the overall mass balance of tidewater glaciers and Arctic ice caps that have significant tidewater margins (Dowdeswell et al., 1997, 2008; Dowdeswell and Hagen, 2004; Błaszczyk et al., 2009) (Figure 7.5). However, accurate calculation of the calving flux requires information that is frequently not available (e.g., ice thickness at the glacier terminus), and modeling of calving flux is challenging because

Figure 7.5. Time-lapse camera overlooking the calving terminus of the tidewater glacier, Kronebreen, in Svalbard. Kronebreen is a focus of study within the IPY GLACIODYN project. Source: Monica Sund, University Centre, Svalbard.

of the lack of a widely accepted calving law. Although individual ice caps may have multiple tidewater glacier outlets, the mass loss by calving is often dominated by one or two of these outlets (Krenke, 1982; Dowdeswell et al., 2002, 2008; Burgess et al., 2005; Williamson et al., 2008; Mair et al., 2009), but calving fluxes from individual glaciers can show large temporal variability.

Recent increases in calving flux from the Greenland Ice Sheet have been associated with acceleration, retreat, and thinning of major outlet glaciers (Howat et al., 2005; Rignot and Kanagaratnam, 2006). Similar changes are observed in Alaska and on some large Arctic ice caps, and may be caused by changes in glacier dynamics related to increased surface melting, penetration of meltwater to glacier beds, and subsequent lubrication of the ice-bed interface allowing increased flow by basal sliding. Other possible causes of calving flux increases include increased melt of the underwater part of terminal ice cliffs due to increasing ocean temperature (Holland et al., 2008), thermal transitions (from cold-based to warm-based) in polythermal glaciers, and break-up and removal of floating ice tongues that formerly restrained the flow of the glacier. Such dynamic changes may be larger and more rapid than those induced by changes in surface mass balance alone.

7.1.4.4. Response to climate change

Glaciers respond to climate change over very different timescales depending on their size, shape, and thermal regime. Among glaciers that terminate on land, smaller glaciers tend to respond more quickly, changing their shape, flow, and terminus position over years or decades. The hypsometry (area-altitude distribution) of a glacier plays an important controlling role in determining its response to changes in climate. In a given region, low-lying glaciers may shrink and retreat quickly at the same time as glaciers at higher elevations grow or maintain their size. Changes in the temperature and salinity of the ocean water adjacent to calving ice fronts can trigger rapid changes in the terminus position, flow velocity, and calving flux of tidewater glaciers, so that large tidewater glaciers may alter their form more rapidly than small glaciers that terminate on land (Holland et al., 2008; Rignot et al., 2010; Straneo et al., 2010). Although Arctic glaciers show a variety of responses to changing climate, it is something to which they are all sensitive. It is worth noting that the surface mass balance of glaciers in the Arctic may be affected indirectly by changes in other components of the Arctic cryosphere, such as the regional snow cover and extent of sea ice, that affect the surface energy balance, atmospheric circulation, and availability of open water as a source of water vapor (e.g., Rennermalm et al., 2009).

7.1.5. Significance and impacts of glacier changes

According to recent estimates, glaciers contributed about 0.8 to 1 mm annually to global sea-level rise during the period 2001 to 2004. The upper limit of the estimates includes the contribution from glaciers surrounding the Greenland and Antarctic ice sheets (Kaser et al., 2006; Solomon et al., 2007). Meier et al. (2007) gave a slightly higher estimate of 1.1 mm for 2006. This is about one third of the total current sea-level rise, or about 60% of that component of the rise attributable to the addition of water mass to the oceans, as opposed to the thermal expansion of ocean waters. The remaining 40% of that component comes from the combined contribution of the Greenland and Antarctic ice sheets. Meier et al. (2007) predicted that a large contribution to sea-level rise over the period to 2100 will still come from glaciers and ice caps. As more than half of the world's glacier and ice cap area is found in the Arctic, it is very important to reduce the uncertainty in estimates of the current and future mass balance of the Arctic glaciers and ice caps.

It is also important to evaluate the impacts of ongoing and future changes in glacier extent and volume on regional water resources, water quality, and the incidence of glacier-related natural hazards. Glacier runoff is exploited as a source of hydroelectric power in Scandinavia, Iceland, Greenland, western Canada, and Alaska. Increasingly negative surface mass balance of the glaciers, and reductions in glacier area may have a direct impact on the water balance of basins used for hydroelectric power generation. Increased freshwater flux from glaciers to nearby fjords and oceans may have an impact on the marine ecosystem via freshening of ocean water and increased transport of nutrients and contaminants from land to sea. Freshening of ocean water may have an impact on fjord circulation and on global ocean thermohaline circulation. Changes in the frequency and magnitude of iceberg calving events may impact infrastructure development, marine transport, fisheries, and oil and gas exploration and production on Arctic continental shelves, where human activity is expected to increase significantly over the coming decades.

Changes in the extent and thickness of Arctic glaciers can destabilize the surrounding terrain and generate geomorphological hazards (rock slides, debris flows, ice avalanches, glacial mudflows, outburst floods), especially when combined with changes in the extent and thickness of permafrost on surrounding slopes. They also create a threat of floods (*jökulhlaups*) from ice-dammed and subglacial lakes, especially in volcanic areas such as Iceland, Alaska, and Kamchatka.

Glacier related tourism is important to some local economies, and shrinking or even disappearing glaciers may have a direct economic impact.

7.1.6. Challenges

The ACIA report (ACIA, 2005) stated that the most difficult task in a regional-scale assessment of glacier behavior is to generalize results from a few glaciers and ice caps to all ice masses in the Arctic. This statement is still valid today. Neither the remote sensing tools nor the glacier and ice sheet models currently available are well suited to studies of regional ice covers that comprise a multitude of glaciers of varying sizes in regions with complex surface topography.

Direct measurements of the mass balance of Arctic glaciers are limited to a small number of glaciers across the Arctic (50 in the 2000 to 2004 pentad); 31 of these were in Scandinavia, which contains only 3.5% of the total mountain glacier and ice cap area in the Arctic. In the past 35 years, the number of *in situ* glacier monitoring sites in the Canadian Arctic and Arctic Russia (regions which contain over 50% of the area of mountain glaciers and ice caps in the Arctic) has declined from 16 in the 1970 to 1975 period, to just six in the period 2000 to 2005, with no measurements in Arctic Russia since 1990 and only one set since 1980 (Dyurgerov and Meier, 2005). There is a pressing need for an updated regional-scale assessment of glacier and ice cap mass balance, the last assessment having been made in 2005. The uncertainties associated with such regional-scale assessments are large owing to the small number of *in situ* measurements and their uneven spatial distribution relative to the distribution of glacier ice.

In situ measurements are critical for quantifying regional mass balance, enhancing process understanding, and validating remote sensing techniques and model predictions. Given the limited number and distribution of such measurements, it is essential to improve and sustain remote sensing capabilities for monitoring ongoing changes in glacier extent, surface elevation and thickness, surface mass balance, ice dynamics, and iceberg production. Although there has been some progress on these issues, there is also a need for repeated, regional-scale mapping of parameters that provide simple indices of glacier mass balance (such as equilibrium-line altitude, glacier facies zones, and summer melt duration; see section 7.4.2) to be used to evaluate year-to-year variability in climate effects on glacier health.

7.2. Climate evolution in glacierized regions of the Arctic

- While some Arctic glaciers have existed throughout the period since the end of the last glaciation, most disappeared during a warm period between 10 000 and 6000 years ago. Many of today's glaciers, therefore, formed in a cooler period after 5000 years ago.
- Although there were several warmer intervals within this cool period, the 20th century appears to have been the warmest century in the past 2000 years, with the warmest conditions occurring between the 1930s and early 1960s and since the mid-1980s.
- Across much of the Arctic, low winter precipitation means that most of the year-to-year variability in glacier mass balance arises from changes in summer temperature. In more maritime regions such as southern Alaska, Iceland, western Scandinavia and Svalbard, variability in winter precipitation can be an important influence on mass balance variability.

7.2.1. Holocene climate

Ice formed during the last glaciation is found in some ice caps in the Canadian Arctic (Koerner and Fisher, 2002; Zdanowicz et al., 2002) and Severnaya Zemlya (Kotlyakov et al., 1991). The absence of such ice in ice caps in Svalbard and other parts of the Russian Arctic is evidence for substantial retreat (or even disappearance) of glaciers and ice caps across much of the Arctic outside Greenland in the early Holocene (Koerner and Fisher, 2002). Therefore, the genesis of much of the present-day Arctic glacier cover may lie in the climate of the middle and late Holocene.

Many climate proxy records suggest that the warmest period of the Holocene in the Arctic was between 10 000 and 6000 years BP, after which the climate cooled, possibly because of a decrease in incident solar radiation at high latitudes due to changes in the Earth's orbital parameters (Koerner and Fisher, 1990; Vinther et al., 2009). Air temperature reconstructions based on ice-core oxygen isotope records from the Agassiz Ice Cap (Canadian Arctic) and Renland (eastern Greenland) suggest peak temperatures slightly in excess of 2 °C warmer than at present during this period (Vinther et al., 2009), which is often referred to as the Holocene Thermal Maximum. However, the exact timing of peak air temperatures during this period seems to have varied across the Arctic. In North America, it was later in the eastern Arctic than in the western Arctic, probably because the residual Laurentide Ice Sheet had a cooling effect on the climate in the east. During the Thermal Maximum, around 7500 years BP, summer temperatures were about 1.6 ± 0.8 °C warmer than in the 20th century (Kaufman et al., 2004). Records of summer melt and oxygen isotope ratios from ice cores in the Canadian and Russian Arctic indicate that cooling following the Thermal Maximum was underway by no later than 6000 years BP (Koerner and Fisher, 2002) (Figure 7.6).

A 2000-year, decadally-resolved, multi-proxy record of Arctic summer surface temperatures (which includes the temperature reconstructions from Agassiz Ice Cap and Renland) shows a cooling trend from 2000 to 100 years BP (Kaufman et al., 2009) (see Fisher, 2002, for an analysis of the reliability of multi-proxy temperature reconstructions). This trend (-0.22 °C/millennium) was probably driven by the orbitally-forced trend in summer insolation at high latitudes over the same period, but may have been amplified in some regions by feedbacks involving the progressive expansion of Arctic sea ice (England et al., 2008; Vare et al., 2009) and seasonal snow cover. The record also shows centennial-scale anomalies about the long-term trend, with the period 450 to 700 AD being cooler than the long-term trend and the period 900 to 1050 being warmer. The coldest period in the record occurred between 1600 and 1850, during the Little Ice Age (Kaufman et al., 2009). There is evidence that this cold period was associated with a persistently negative phase of the North Atlantic Oscillation (Trouet et al., 2009). Although the decline in orbitally-driven summer insolation continued throughout the 20th century, reconstructed Arctic summer temperatures rose sharply, reaching the highest values in the 2000-year record in the period after 1950. On the basis of this reconstruction and recent instrumental data, Kaufman et al. (2009) concluded that the decade 1999 to 2008 had the warmest summers in the 2000-year record (Kaufman et al., 2009).

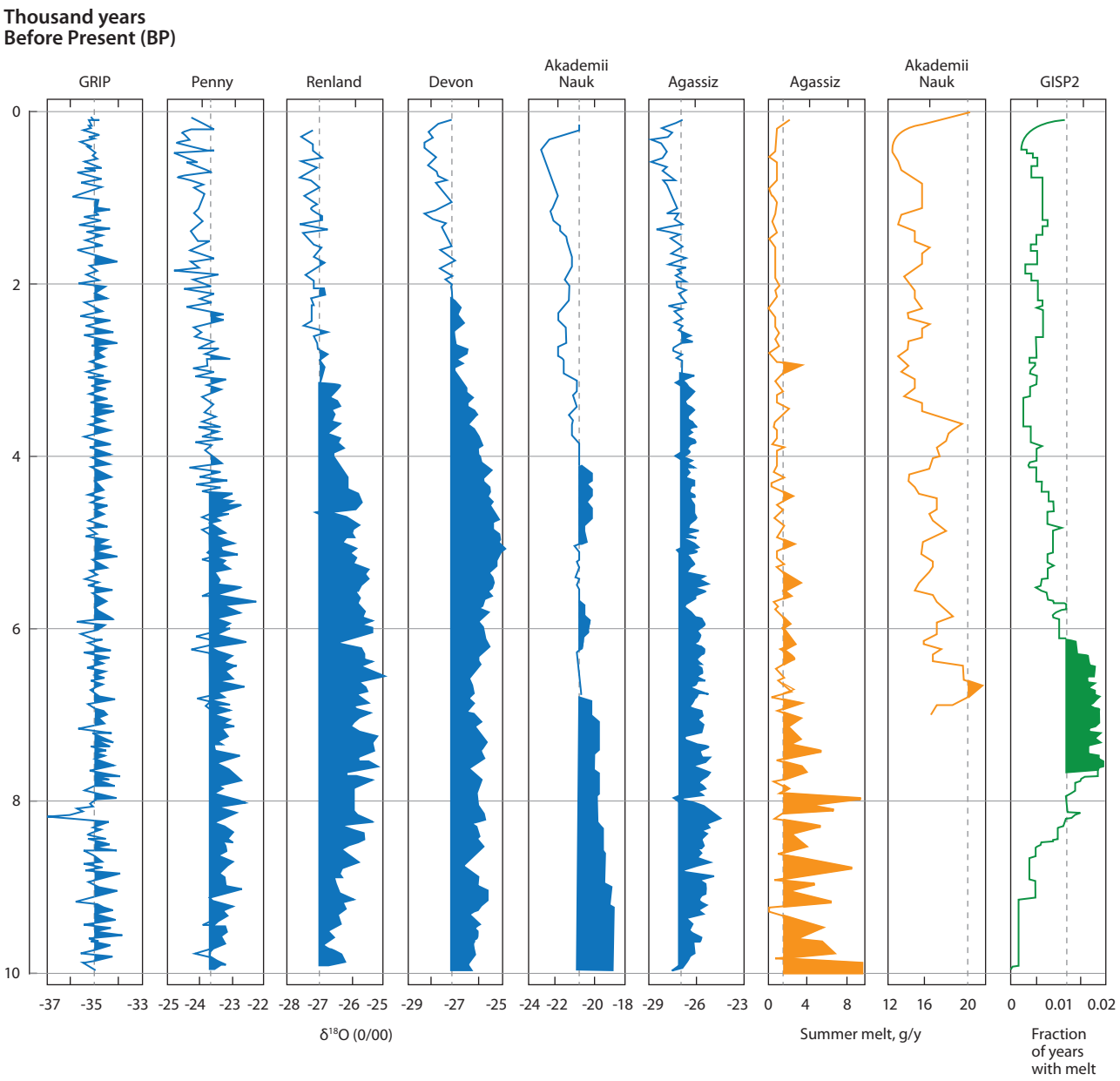

Figure 7.6. Holocene sections of ice cores from Greenland (GRIP, GISP2, Renland), Arctic Canada (Agassiz, Devon, Penny), and Severnaya Zemlya (Akademii Nauk) showing records of $\delta^{8}O$ (negative values) and summer melt (positive values), which are proxies for air temperature over the ice caps / ice sheet. Shaded sections suggest conditions warmer than those of today. Source: Koerner and Fisher (2002).

7.2.2. Arctic ice cores: Holocene climate records from glacierized regions

Ice cores from the larger Arctic ice caps yield records of past environmental conditions in glacierized regions that span the full Holocene. The longest records are from the Canadian Arctic, Mount Logan (Yukon), and Severnaya Zemlya (Koerner and Fisher, 1990, 2002; Kotlyakov et al., 1991; Fisher et al., 1995, 2008; Koerner, 1997; Zdanowicz et al., 2002; Kinnard et al., 2008). The melt layer record from the Agassiz Ice Cap and the oxygen isotope record from Severnaya Zemlya show a temperature maximum in the early Holocene, before 8000 BP, while oxygen isotope records from Arctic Canada typically show a later thermal maximum – as late as 5000 BP on Devon Island (Paterson et al., 1977). Melt layer records show a persistent cooling trend from about 8000 BP until the mid-19th century, after which there is renewed warming. Oxygen isotope records also show cooling, but the timing of this is delayed until after about 5000 BP in some records (Koerner and Fisher, 2002). The melt records suggest maximum summer cooling from the Holocene Thermal Maximum of 2.0 to 2.5 °C, while the oxygen isotope records suggest cooling of 1.3 to 3.5 °C (Koerner and Fisher, 2002). Part of the early Holocene warming recorded in the ice core records must be due to the effects of surface lowering due to ice cap thinning, although this would have been partly offset by cooling induced by isostatic uplift of the land surface as the ice cover thinned and shrank (Koerner and Fisher, 2002; Vinther et al., 2009).

Oxygen isotope records from ice cores from smaller ice caps in Arctic Canada, northern Greenland, Svalbard, and the Russian Arctic islands show temporal variability but not the long-term cooling trend apparent in the records from the larger ice caps. This suggests that the small ice caps began to re-grow in the latter part of the Holocene after melting away during the

Thermal Maximum (Hammer et al., 2001; Landvik et al., 2001; Koerner and Fisher, 2002). The record from the upper 125 m of the ice core from Hans Tausen Iskappe in northern Greenland suggests a warm period between 900 and 1100 AD, and that the period 1700 to 1900 was the coldest in the past 2000 years. There was strong warming from the 1920s to the early 1960s (making the 20th century the warmest part of the record), but no clear trend in temperatures thereafter (Hammer et al., 2001). New oxygen isotope records from Austfonna and Lomonosovfonna in Svalbard span the past 600 to 800 years and show gradual cooling to a minimum in the 19th century, followed by rapid warming around 1900 that made the 20th century the warmest century in the past 600 years (Isaksson et al., 2003, 2005). A 275-year oxygen isotope record from Akademii Nauk Ice Cap on Severnaya Zemlya shows the coldest conditions around 1790, and then continuous warming until 1935. It also shows that the 20th century was the warmest period in this region (Fritzsche et al., 2005). A reconstruction of snow accumulation rates on Lomonosovfonna shows an increase of 25% in the late 1940s (Pohjola et al., 2002). A similar increase is recorded on Severnaya Zemlya after 1935 (Opel et al., 2009).

The oxygen isotope record from Mount Logan is unusual in that it appears to be a proxy for changes in the moisture source region for precipitation, rather than air temperature (Fisher et al., 2008). Major changes in moisture source region seem to be associated with switches between strong, frequent El Niño conditions (associated with meridional patterns of atmospheric flow and water vapor transport towards the Yukon) and strong, frequent La Niña conditions (associated with more zonal flow and moisture transport towards the Pacific Northwest). La Niña periods are associated with reduced precipitation (and snow accumulation) in the southern Yukon, while the reverse is true for El Niño periods. Periods of enhanced meridional flow seem to have occurred around 4200 BP and between 8000 and 7000 BP, while the modern El Niño Southern Oscillation regime seems to have been initiated after 4200 BP (Fisher et al., 2008).

Chemically-based melt indices from the Lomonosovfonna ice core show very high melt in the 12th century (Grinsted et al., 2006), as do melt layer records from the Canadian Arctic. This suggests a warm episode in medieval times in these parts of the Arctic. This warm episode was followed by a long period of reduced melt lasting to the mid- to late 19th century, after which melt increased sharply. For example, the melt layer record from Akademii Nauk Ice Cap shows maxima in the 1840s, 1880s, and from 1900 to 1970, after which melt layer content dropped sharply (Opel et al., 2009). However, the increase in melt was delayed until about 1925 in the new record from Prince of Wales Icefield, Ellesmere Island (Kinnard et al., 2008). The first principal component of seven Arctic melt layer records spanning the period 1551 to 1956 explains 34% of the variance in these records. It shows a strong increase in melt layers starting around 1830 and peaking in the mid-20th century (Kinnard et al., 2008) and has a similar form to a multi-proxy summer temperature reconstruction for the Arctic (Overpeck et al., 1997). Melt layer records from multiple sites on the Devon Island Ice Cap show an increase in ice fraction of over 50% after 1989 relative to the period 1963 to 1988 (Colgan and Sharp, 2008), consistent with a shift to increasingly negative surface mass balance after 1987 (Gardner and Sharp, 2007).

7.2.3. Climate records for glacierized regions of the Arctic derived from instrumental observations and climate re-analysis

Observational records of past surface air temperature from around 70 stations in the Arctic (north of 62° N) since 1875 show large multi-decadal fluctuations. Maxima in mean annual air temperatures occurred in the 1930s and 1940s and in the past two decades, with minima before 1920 and from about 1955 to 1985 (Polyakov et al., 2003). The same trends are apparent for the region 68° to 90° N in the 250-km smoothed air temperature dataset from the Goddard Institute for Space Studies. Mean summer 2-m air temperature anomalies in this dataset show a similar history to mean annual anomalies, but the range of summer anomalies is smaller than for the mean annual air temperature. In addition, there is a period of high mean summer air temperature in the 1950s that is not apparent in the record of mean annual air temperature (Figure 7.7).

Correlations between surface air temperature measured at coastal weather stations and the monthly North Atlantic Oscillation index are positive for a region that includes northern Scandinavia, Svalbard, and the Eurasian Arctic islands, and negative for a region that covers most of Greenland and the Canadian Arctic (Polyakov et al., 2003). Since the late 1990s, surface air temperature anomalies over the Arctic Ocean have become increasingly positive in autumn, especially over those regions where there has been a strong decrease in September sea-ice extent (Serreze et al., 2009). This trend may have resulted in longer melt seasons over glacierized regions of the Canadian and Eurasian Arctic.

In most regions of the Arctic, low winter precipitation means that interannual variability in annual glacier mass balance arises from variability in the summer balance, which is strongly controlled by summer air temperature. Gardner et al. (2009) found positive correlations between mean lower-troposphere summer air temperature from climate re-analyses and surface air temperature measured at the summit elevations

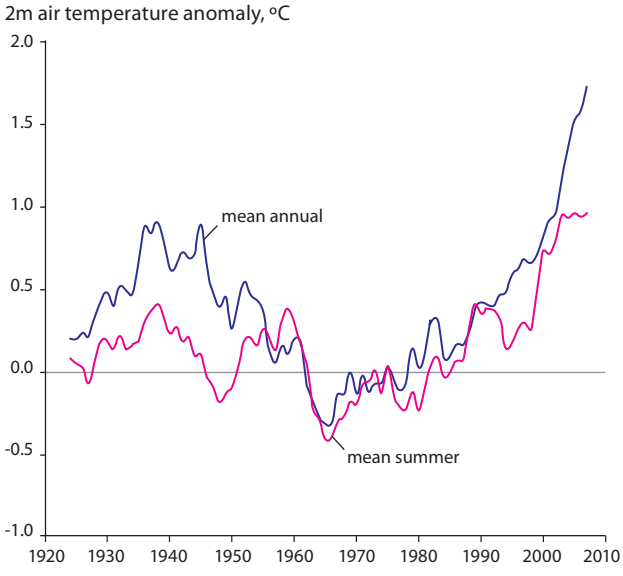

Figure 7.7. Five-year running means for mean annual and mean summer (June – August) 2-m air temperature anomalies (relative to the mean for 1951 to 1980) for the region 68° to 90° N from the Goddard Institute for Space Studies 250-km smoothed dataset.

of Arctic ice caps. Sharp and Wang (2009) reported similar correlations between lower tropospheric summer mean air temperature from climate re-analyses and melt season duration on Eurasian Arctic ice caps. For the period 1948 to 2008, NCEP/NCAR (U.S. National Weather Service National Centers for Environmental Prediction and the National Center for Atmospheric Research) Reanalysis (Kalnay et al., 1996) decadal mean 700 hPa air temperatures over glacierized regions of the Arctic in June to August were warmest in either the 1950s (Russian Arctic, northern Ellesmere and Axel Heiberg Islands) or the 2000s (Alaska, Iceland, Svalbard, and the rest of the Canadian Arctic). They were coldest in the 1990s in the Eurasian Arctic and the 1960s and 1970s over Iceland, Alaska, and the Canadian Arctic.

In the more maritime regions of the Arctic (such as Alaska, Iceland, Svalbard, and western Scandinavia), high variability in winter accumulation can also induce interannual variability in the annual mass balance. According to the NCEP/NCAR Reanalysis, decadal mean winter (September to May) precipitation anomalies were most negative in the 1950s over Alaska, the 1960s over Iceland, and the 1980s over Svalbard. They were most positive in the 2000s over Alaska and the 1950s over Iceland and Svalbard.

High summer precipitation keeps glacier surface albedo relatively high and reduces summer melt, while low summer precipitation has the opposite effect. In the Eurasian Arctic islands, decadal mean summer precipitation anomalies were typically positive from the 1950s through the 1970s and negative from the 1980s to 2000s. The opposite trend was observed in Iceland.

7.3. Changes in glacier extent, volume and total mass

- Following the early Holocene warm period, the cooler climate between 6000 years BP and the end of the Little Ice Age resulted in glacier growth and advances across the Arctic.
- In some cases, maximum glacier extents were reached as early as the mid-17th century, but in most regions glaciers were at or close to their maximum extents in the late 19th and/or early 20th centuries.
- Across the Arctic, glaciers began retreating and losing mass in the early 20th century. This trend continued through the mid-20th century, although glaciers in some regions experienced brief episodes of slower retreat, reduced mass loss, or even mass gain. Overall, there were substantial reductions in glacier area and mass across the entire Arctic over the 20th century.
- Mass loss has accelerated across most regions of the Arctic since the mid-1990s.
- In some regions, the timing and duration of episodes of relatively positive or negative mass balance were tied to major changes in atmospheric circulation related to phenomena such as the North Atlantic Oscillation (Iceland, western Scandinavia), the Pacific Decadal Oscillation (western Canada, southern Alaska), and the location and intensity of the summer circumpolar vortex (Arctic Canada).

7.3.1. Arctic glacier changes during the Holocene

Reconstructions of dated lateral and terminal moraine positions (and associated stratigraphy) are the primary source of information on glacier changes during the Holocene. In western North America, the Cordilleran ice sheet reached its maximum extent and thickness by 16 000 BP. Between 15 000 and 11 000 BP, climate conditions allowed some lobes of the ice sheet to advance (Menounos et al., 2009), and alpine glaciers also advanced in the southern and north-central ranges of the Cordillera, but by 11 000 BP glacier extent was comparable to that at present (Clague et al., 1982). Glacier extent reached a minimum between about 11 500 to 9000 BP, with temperatures 2 to 3 °C above present and generally drier conditions (Kaufman et al., 2004). Subsequently, periods of glacier advance occurred from 8600 to 8200 BP, 7400 to 6500 BP, 4400 to 4000 BP, 3500 to 2800 BP, and 1700 to 1300 BP (Menounos et al., 2009), and maximum Holocene extents were reached during the early 18th or mid-19th centuries AD.

A number of ice caps in Arctic Canada (Devon, Agassiz, Barnes, Penny) contain ice dating from the last glaciation (Paterson et al., 1977; Hooke and Clausen, 1982; Fisher et al., 1983, 1995, 1998; Zdanowicz et al., 2002) and must therefore have survived throughout the Holocene. During deglaciation, the margins of the last Innuitian ice sheet covering the Queen Elizabeth Islands reached the current margins of ice caps on Devon, Ellesmere, and Axel Heiberg Islands between 10 000 and 7500 ^{14}C years BP (England et al., 2006). Many of the smaller ice caps and glaciers in this region disappeared during this period (Koerner and Fisher, 2002). Glaciers began to grow again after 1000 ^{14}C years BP (Blake, 1981), reaching maximum extents in the late 19th or early 20th centuries. On Baffin Island, the Laurentide Ice Sheet retreated progressively throughout the Holocene to its current margin, that of the Barnes Ice Cap. Deglaciation was especially rapid around 7000 BP, when the ice cover in Foxe Basin collapsed (Briner et al., 2009). The early Holocene ice extent in this region is poorly constrained but glaciers began to advance again as early as 6000 BP, reaching extents similar to those of the Little Ice Age (the Holocene maximum for alpine glaciers on Baffin Island) by 3500 to 2500 BP (Briner et al., 2009). Small ice caps have been present in the northern interior of Baffin Island for 1600 to 2800 years, but they were absent for much of the middle Holocene. These ice caps started to expand after 1280 AD, and especially after 1450 (Anderson et al., 2008).

Most glaciers in Greenland were smaller during the early Holocene than at present and some areas that are currently occupied by mountain glaciers and ice caps may have become completely ice free in that period (Hammer et al., 2001). Neoglacial moraines have been reported (from western and southeastern Greenland), but in most regions historical advances were the most extensive after the early Holocene. In all areas apart from northern Greenland (where many ice margins are stationary), local glaciers are currently receding from their historical maximum extents (Kelly and Lowell, 2009).

Iceland was largely ice free during the early Holocene (8000 to 6000 BP), after which Neoglacial cooling began. Glacier extent increased between 4500 and 4000 BP, and again between 3000 and 2500 BP. The most extensive Holocene ice extent was

reached during the period 1250 to 1900 AD – probably in the latter part of that period between 1700 and 1850 (Geirsdóttir et al., 2009). However, some steep alpine glaciers reached their maximum extents earlier, probably around 2500 BP, when the present ice caps are also likely to have formed. A general glacier recession that began in the 1890s accelerated after 1930. Retreat slowed by the 1960s as a result of cooler summers beginning in the 1940s, and many steep glaciers were advancing in the 1970s. Renewed climate warming since 1985 has led to a new episode of retreat, and all major non-surging outlet glaciers have been retreating since 1995, at rates of up to 100 m/y. The southern outlets of Vatnajökull eroded down into soft sediments during the pre-1890 advance and have been especially susceptible to rapid retreat since then. The volume of Vatnajökull has decreased by about 300 km^3 (10%) since 1890 (Björnsson and Pálsson, 2008).

In northern Scandinavia, retreat of the Scandinavian Ice Sheet during the Late Glacial and early Holocene was punctuated by numerous readvances in the period 11 200 to 8000 BP. Most glaciers disappeared completely at some point in the early to mid-Holocene, and ice cover is likely to have reached a minimum between 6600 and 6300 BP (Nesje, 2009). Subsequently, there was a period of renewed glacier growth during which there were numerous century- to millennium-long 'Neoglacial' events. Glaciers in northern Sweden were probably at their Little Ice Age maximum extent in the 17th and early 18th centuries (Karlén, 1988), while those in Norway reached their maxima in the mid-18th century (Winkler, 2003; Nesje, 2009), or even later in some parts of northern Norway (Bakke et al., 2005). Most Swedish glaciers reached an extent close to their Holocene maximum at the beginning of the 20th century (Holmlund, 1993). Since then, Scandinavian glaciers have generally retreated, particularly since the 1930s (Nesje, 2009). Increased snow accumulation caused some glaciers to advance in the 1990s (Dowdeswell et al., 1997).

In northeast Svalbard, many glaciers started to retreat after the Last Glacial Maximum by about 9500 BP (Blake, 1989). During this period of deglaciation, variations of the glaciers and ice caps in Svalbard were similar to those of glaciers in Scandinavia. However, the Younger Dryas advance was apparently small due to a very dry climate, and the Little Ice Age maximum extent was larger than the Younger Dryas advance (Mangerud and Landvik, 2007). In the early Holocene, glaciers were much smaller than at present and perhaps even completely absent. A period of glacier growth from 3000 to 2500 BP was followed by a warmer period with smaller glaciers (Svendsen and Mangerud, 1997). Dating of relict vegetation found under the cold-based Longyearbreen indicates that late Holocene glacier growth started about 1100 BP. This period of glacier growth culminated in the Little Ice Age maximum with the greatest Holocene glacier extent. Many ice-cored moraines were formed at this time, which may have been as recently as around 1900 (Humlum et al., 2005). Surging of Svalbard glaciers is common and the maximum extent of many glaciers may be a result of surge dynamics (Hagen et al., 1993). Since the Little Ice Age maximum, the glaciers have generally retreated in response to early 20th century warming (Lefauconnier and Hagen, 1991; Hagen et al., 2003a,b).

In the Russian Arctic, outlet glaciers in northwestern Novaya Zemlya retreated from the outer coast by the earliest Holocene. Prior to about 9500 BP the terminus of the tidewater Shokal'sky Glacier was over 1 km behind its present margin, allowing incursion of the sea (Zeeberg, 2001). A sediment core from Russkaya Gavan spans a period of 800 years and allows reconstruction of the recent history of Shokal'sky Glacier. A noticeable advance around 1400 AD was followed by a major retreat by about 1600. Increased melting in the 1900s is suggested by an increase in sedimentation rates (Polyak et al., 2004). On Franz Josef Land, glaciers were less extensive than at present throughout the period 10 300 to 4400 ^{14}C years BP, but re-expanded to their present margins by 2000 ^{14}C years BP (Lubinski et al., 1999). A major advance occurred during the past 1000 years, with maxima around 1200, 1400, and in the mid-17th century. Glaciers were more extensive than now at the start of the 20th century; since then there has been widespread glacier retreat.

7.3.2. Arctic glacier changes in the 20th and 21st centuries

7.3.2.1. Methods for determining glacier mass balance

Mass balance is the change in mass of a glacier, quantified as the difference between mass gains (accumulation) and mass losses (ablation), over a specified time period. A summary of the processes that determine the mass balance of a glacier is provided in Appendix 7.1 (see also Box 7.1). Over the 20th and beginning of the 21st centuries, many new methods have been developed for measuring glacier mass balance. Each method provides information at unique spatial and temporal resolutions, and samples specific parameters to characterize glacier evolution over time. Important challenges for global mass balance inventories include the integration of these different datasets and quantification of the errors in each approach.

Long-term records of surface mass balance that form the basis of existing global datasets have been acquired from direct sampling of individual glaciers using glaciological methods (Østrem and Brugman, 1991; Cogley, 2005). In this approach, measurements of snow accumulation are acquired from snow probing or digging snow pits to measure snow depth and density (Figure 7.8). Glacier ablation is measured by determining the

Box 7.1. Units for mass balance measurements

Mass balance measurements have units of mass per unit time (see Appendix 7.1). It is also common to report the rate of change of mass per unit area, for example, kg/m^2 per year, which is numerically equivalent to the millimetres of water equivalent (w.e.) per year. In this report, mass balances are usually presented in units of gigatonnes per year (Gt/y) or metres of water equivalent per year (m w.e./y). Exceptions are those studies reporting cumulative mass balances, in which case they are not converted to a rate because it is not always clear what exact time period was used for the measurements, and those studies reporting volume changes, in which case they are not converted to a mass equivalent unless the density of the changing snow and ice volume is clearly stated.

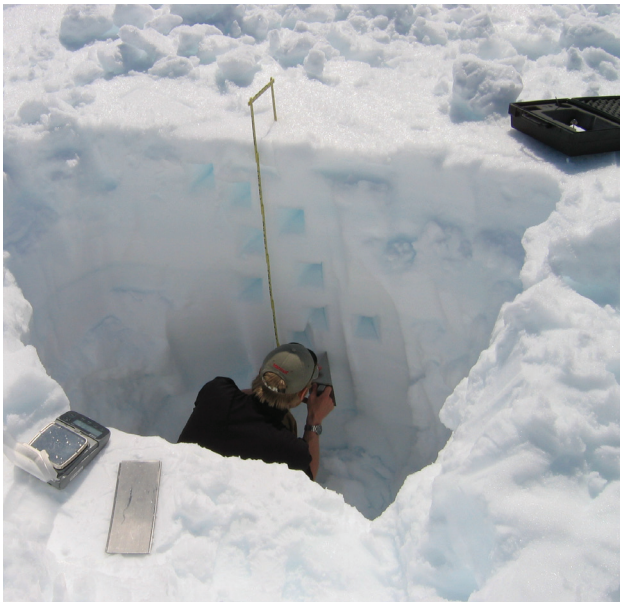

Figure 7.8. Measuring snow accumulation in a snow pit.

vertical change in distance from the glacier surface to a marker, fixed within the reference frame of the moving ice mass, and by assuming an appropriate density for the snow, firn, or glacier ice that melted. Annual mass balance is defined as the difference between the annual accumulation and the annual ablation. Point measurements of this quantity are extrapolated to the entire glacier. Two processes, internal accumulation and the formation of superimposed ice, involve the refreezing of some fraction of the annual melt and alter surface mass balance by reducing the amount of meltwater runoff. However, not all surface mass balance programs measure these processes owing to the difficulty of doing so, resulting in overestimates of the rate of mass loss. Regardless, glaciological mass balance measurements generally provide the most accurate sampling of mass balance at a point, but are limited in spatial extent.

Developments in ground surveying and remote sensing technologies have resulted in many geodetic mass balance methods. These calculate a volume balance determined from repeat measurements of surface elevation and area, from which the mass balance is obtained by estimating the density of the changing ice volume. Elevations are determined using overlapping aircraft or satellite imagery to determine the 3-dimensional position of the surface through stereoscopy, ground mapping of the glacier surface elevation using theodolite or Global Positioning System (GPS) surveying, or airborne / satellite altimetry using radar or laser ranging instruments. Geodetic methods provide a broad regional sampling of glacier changes, but can have large errors due to uncertainties in the density of the volume lost, especially over short periods, non-representative sampling of fast- and slow-flowing sectors of ice caps, or biases in the distribution of surface-elevation change measurements relative to the distribution of rates of elevation change (e.g., in aircraft altimetry where measurements are typically made along a glacier centerline where rates of thickness change may be larger than the glacier-wide mean; Berthier et al., 2010).

Recent advances in spaceborne geodesy provide gravimetric data to determine glacier mass variations via measurement of changes in Earth's gravity field. At present, this is achieved using the Gravity Recovery and Climate Experiment (GRACE) satellites that measure variations in Earth's gravitational potential. Corrections must be made to the satellite measurements to account for all non-glacier sources of mass variation, such as glacial isostatic adjustment and changes in terrestrial water, atmospheric, and ocean mass. Gravimetric methods circumvent the need for density corrections of measured volume changes, but are limited in spatial resolution (about 50 000 km^2) and can only effectively sample broad regions undergoing significant change.

Measurements of glacier thickness are essential for estimating glacier volume and for computing mass losses by iceberg calving. They are also needed as input to models of the dynamic response of glaciers to climate forcing. They are usually obtained using the technique of radio echo sounding from either ground-based or airborne platforms (Dowdeswell and Evans, 2004). Airborne campaigns are typically required for measurements of the thickness of larger glaciers and ice caps, as well as for regional-scale studies (Dowdeswell et al., 2002, 2004).

Area/volume scaling (Bahr et al., 1997) is used to estimate glacier volume when glacier areas are known but direct measurements of volume are lacking. This method is based on the observed power-law relationship between a glacier's volume and area. Glacier surface areas measured at different times are used to estimate corresponding glacier volumes, from which changes in glacier volume can be determined. This method can have large errors when data are not available to constrain the scaling relationship and determine suitable scaling coefficients (Radić et al., 2008). Therefore, it is most appropriately applied to entire populations of glaciers rather than to individual ice masses.

Changes in proxy indicators are also used to approximate mass balance trends, and these approaches are summarized in Section 7.4. The distribution and length of glaciological and geodetic mass balance records in the Arctic region are highly variable, but the longest continuous records (from Scandinavia) extend back to the 1940s (Figure 7.9). Records from individual regions are discussed in the following sections.

7.3.2.2. Northwestern North America

Northwestern North America includes all glaciers of Alaska (United States) and Yukon Territory (Canada) and those glaciers in British Columbia and Alberta (Canada) that drain into the Alaska Panhandle or into the Arctic Ocean via the northern tributaries of the Mackenzie River.

During the 20th century most land-terminating glaciers in northwestern North America retreated extensively from their Little Ice Age maximum extent (Kaufman et al., 2004). Most of the recession occurred between 1900 and 1950 and from 1980 to present, with a period of slower recession, and in some cases advance, between 1950 and 1980. Since 1980, nearly all glaciers have been in a state of retreat. For example, in British Columbia, the extent of glaciers in the northern Coast and St. Elias mountains changed by -7.7 ± 2.9% and -7.9 ± 2.6%, respectively, over the period 1985 to 2005 (Bolch et al., 2010). Between 1958/1960 and 2006/2008, the total glacier area in the Yukon Territory decreased by 2541 ± 189 km^2 (or 22% of the initial area of 11 622 km^2) (Barrand and Sharp, 2010).

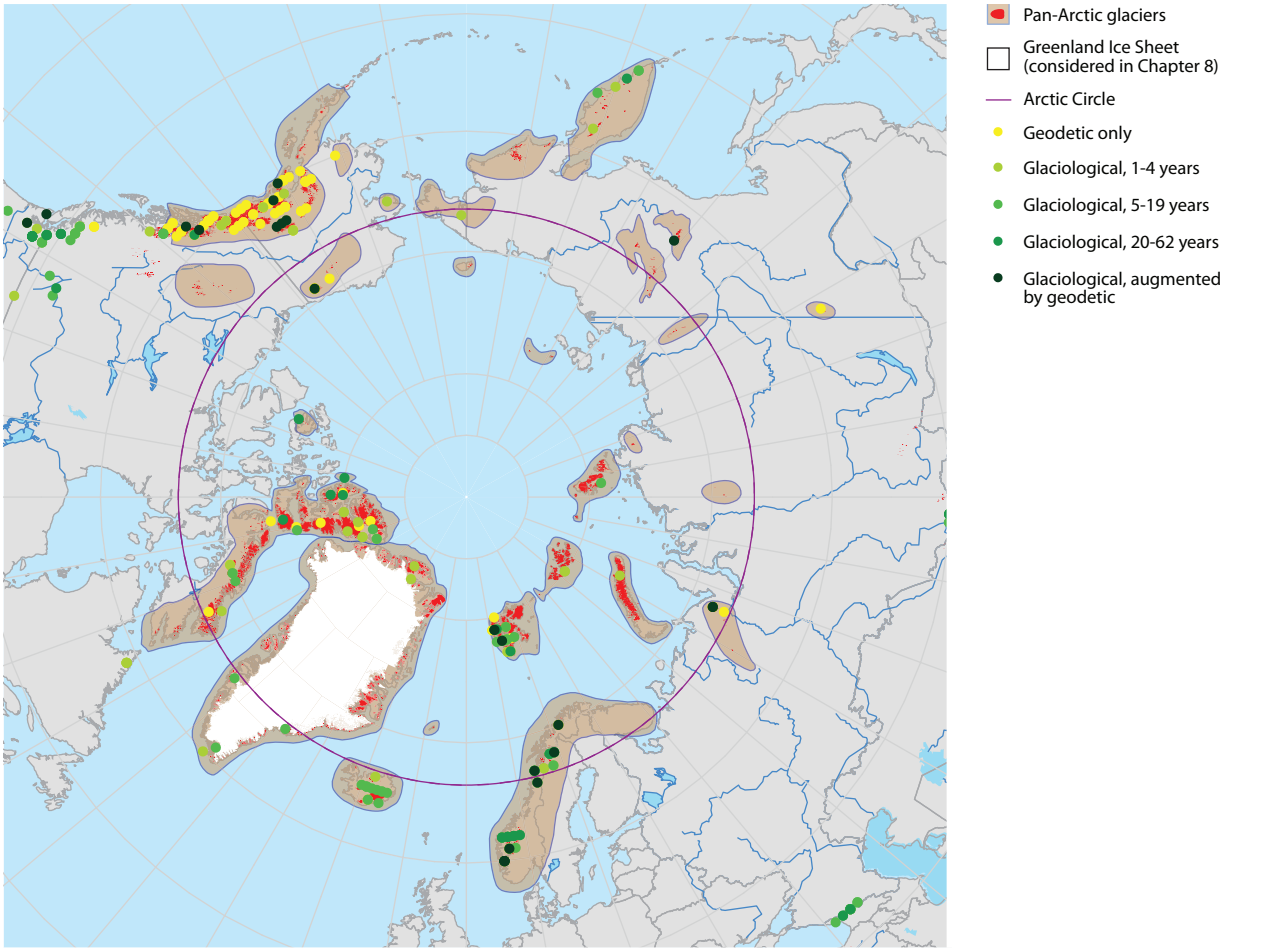

Figure 7.9. Glacierized regions in the Arctic and the locations where mass balance measurements have been made. The length of time of the geodetic and glaciological mass balance records are also indicated. Source: AMAP.

Regular glaciological mass balance measurements in Alaska began during the 1960s and trends generally agree with observed variations in glacier extent. Wolverine Glacier lost mass from 1966 to 1976 and gained mass from 1976 to 1988, while Gulkana Glacier lost mass at a constant rate from 1966 to 1973 and at an increasing rate from 1974 to 1985 (Josberger et al., 2007). After about 1988, both glaciers entered a period of accelerating mass loss (Figure 7.10).

Aircraft laser altimetry measurements showed that about 85% of 67 glaciers in northwestern North America had a mass balance of -52 ± 15 Gt/y between 1950/1970 and the early 1990s (Arendt et al., 2002; Echelmeyer et al., 1996). A repeat sampling of 28 of these glaciers between the early 1990s and late 1990s / early 2000s indicated a doubling of the rate of mass loss (-96 ± 35 Gt/y). A recent analysis compared digital elevation models (DEMs) from the 1950s/1970s against those from the 2000s, and argued that estimates based on centerline aircraft altimetry overestimated the mass loss of Alaskan glaciers by 34% (Berthier et al., 2010). These new estimates suggest a mass loss rate of -41.9 ± 8.6 Gt/y for the period 1962 to 2006.

Other geodetic measurements have been acquired through differencing of 1950s U.S. Geological Survey (USGS) and NASA's Shuttle Radar Topography Mission (SRTM) DEMs. Glacier mass balances in regions south of 60.5° N in southeastern Alaska and the Kenai Mountains were -15 ± 4.0 Gt/y (Larsen et al., 2007) and -1.2 ± 0.25 Gt/y (VanLooy et al., 2006), respectively, during a 30- to 50-year period ending in 2000. Another study using the SRTM data found the glaciers of the northern Coast and St. Elias mountains had a mass balance of -11.1 ± 2.0 Gt/y during the period 1985 to 2000 (Schiefer et al., 2007). Recent altimetry measurements for 2004 to 2008 suggest an acceleration of mass loss relative to the 1990s, especially for glaciers at low elevations (Lingle et al., 2008).

There are three estimates for the mass balance of glaciers surrounding the Gulf of Alaska based on data from GRACE: -110 ± 30 Gt/y for the period 2002 to 2004 (Tamisiea et al., 2005); -101 ± 22 Gt/y for the period 2002 to 2005 (Chen et al., 2006); and -84 ± 5 Gt/y for the period 2003 to 2008 (Luthcke et al., 2008).

7.3.2.3. Canadian Arctic

The Canadian Arctic region includes the Queen Elizabeth Islands (including Ellesmere, Devon, and Axel Heiberg Islands), and Bylot and Baffin Islands. Glaciers cover an area of about 150 000 km^2 in this region. Current and past glacier extents are known from aerial photography taken during the period 1956 to 1961 and from satellite imagery collected since the mid-1970s (and especially since 1999) (Sharp et al., 2003, in press; Dowdeswell et al., 2007; Wolken et al., 2008). Comparison of ice extents from around 1960 with trimline and end moraine positions visible on satellite imagery shows that there has been extensive ice retreat across the region from glacier maximum positions reached by the end of the Little Ice Age. The ice-

covered area on the Queen Elizabeth Islands decreased by 37% from a Little Ice Age maximum of 170 124 km² to about 107 735 km² in 1960, and all permanent ice was removed from most of the western islands (Dyke, 1978; Wolken et al., 2008). Further glacier retreat has occurred since 1960, with ice area reductions by 2000/2001 of 5.1% (253 km²) on Bylot Island (Dowdeswell et al., 2007) and 2.7% (2844 km²) on the Queen Elizabeth Islands (Sharp et al., 2003). The 14 400 km² Devon Island Ice Cap decreased in area by 338 ± 40 km² (2.4%) (Burgess and Sharp, 2004). The area of small plateau ice caps in interior northern Baffin Island decreased by 55% (from 150 km²) between 1958 and 2005 (Anderson et al., 2008), while the area of 264 glaciers on the Cumberland Peninsula in southeast Baffin Island decreased by about 294 km² (12.5%) between around 1920 and 2000 (Paul and Svoboda, 2009). In the latter study, proportional area reductions were greatest for the smallest glaciers, and the rate of area loss roughly doubled after 1975.

Glaciological mass balance measurements have been made in the Queen Elizabeth Islands since the late 1950s (Cogley et al., 1996; Koerner, 2005) (Figure 7.10), but there are no long-term records from Bylot or Baffin Islands, and no regular measurements since the mid-1980s (Hooke et al., 1987). In this region, variability in the annual mass balance arises almost entirely from variability in the summer balance (Koerner, 2005). The cumulative surface mass balance of all measured glaciers in the region has been negative over the measurement period (e.g., Devon Island Ice Cap -4.4 m w.e. from 1961 to 2007; White Glacier, Axel Heiberg Island -6.8 m w.e. from 1960 to 2007). Compared with the 1963 to 1987 period, the rate of mass loss accelerated significantly after 1987 (Gardner and Sharp, 2007). There have been a number of very negative mass balance years since 1997 (notably 1998, 2001, 2005, 2007, 2008, 2009) that suggest a further acceleration of mass loss since 1997. The cumulative mass loss from the Devon Island Ice Cap from 1997 to 2007 exceeds that for the period 1963 to 1997. Consistent with this trend, geodetic measurements on the Barnes Ice Cap suggest a progressive increase in rates of thinning from 0.12 m/y (1970 to 1984), to 0.76 ± 0.35 m/y (1984 to 2006), and 1.0 ± 0.14 m/y (2004 to 2006) (Sneed et al., 2008).

Iceberg calving also contributes to mass loss from many of the larger ice caps (Burgess et al., 2005). Separate estimates of surface mass balance and iceberg calving fluxes are available for two large ice caps in Arctic Canada: the Devon Island Ice Cap and Prince of Wales Icefield. For the Devon Island Ice Cap, the estimates equate to an overall mean annual balance of either -2.3 Gt/y (1963 to 2000) or -5.2 ± 1.7 Gt/y (1980 to 2006), depending on whether the net surface balance estimates of Mair et al. (2005) (-1.8 ± 0.8 Gt/y) or Gardner and Sharp (2009) (-4.7 ± 1.7 Gt/y) are added to the Burgess et al. (2005) estimate of mass loss due to iceberg calving (-0.5 Gt/y). The surface mass balance of the Prince of Wales Icefield (1963 to 2003) appears to be within an error of zero, so the overall negative balance (-2.0 ± 0.5 Gt/y) is similar to the annual calving flux (1.9 ± 0.2 Gt/y) (Mair et al., 2009).

Repeat airborne laser altimetry flown over some of the larger ice caps in the region in 1995 and 2000 showed that most ice caps were thickening or maintaining a constant thickness at elevations above 1600 m, and thinning at lower elevations (Abdalati et al., 2004). Rates of thinning were greater on Baffin Island ice caps (>1 m/y) than in the Queen Elizabeth Islands (< 0.5 m/y). Based on these data, Abdalati et al. (2004) suggested that the total mass balance of Arctic Canada in the period 1995 to 2000 was -22.9 Gt/y.

Thus, measurements of glacier extent, thickness, and surface mass balance are all consistent in showing progressive and possibly accelerating shrinkage of the Canadian Arctic land

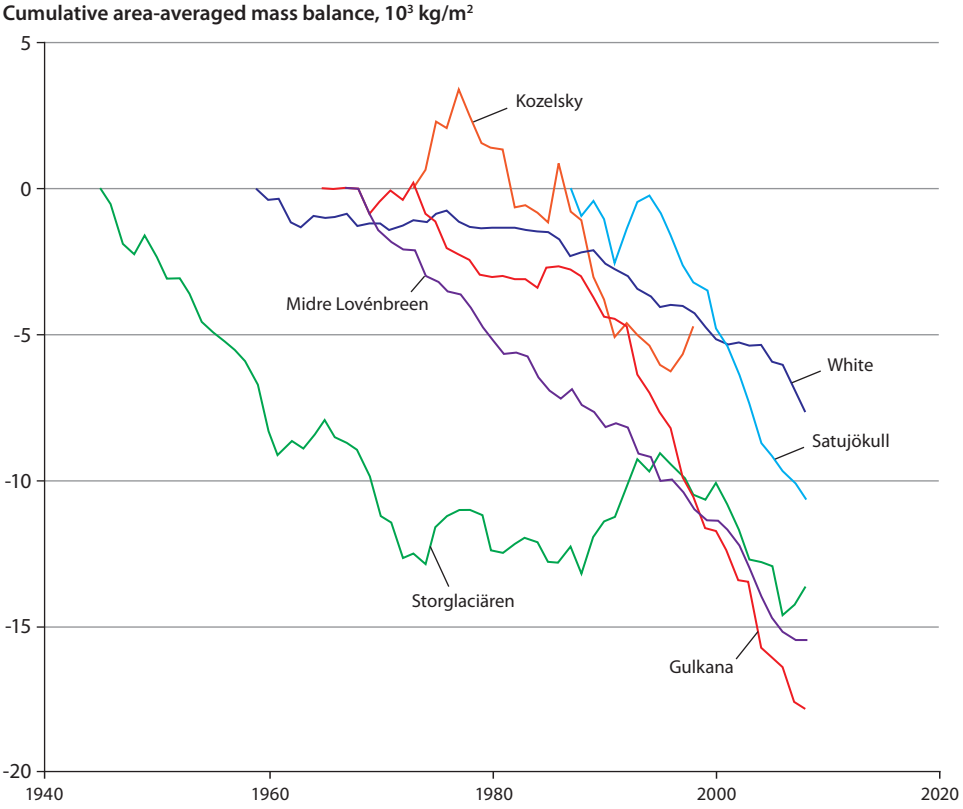

Figure 7.10. Cumulative area-averaged mass balance for six Arctic glaciers: White Glacier (Axel Heiberg Island), Gulkana Glacier (Alaska), Storglaciären (Sweden), Midre Lovénbreen (Svalbard), Satujökull (Hofsjökull, Iceland), and Kozelsky (Kamchatka) over the period of record. All records show a negative cumulative balance (net thinning) over the period of record and more rapid thinning after about 1990 (although the precise timing of this varies between regions). Source: AMAP.

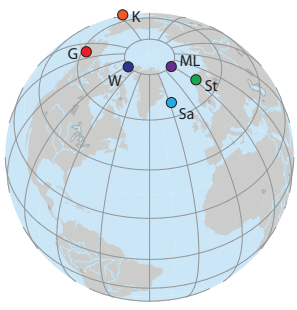

ice cover. Nonetheless, a precise and regionally comprehensive estimate of the magnitude of these changes and their implications for global sea level is not yet available.

7.3.2.4. Greenland (excluding Greenland Ice Sheet)

Glaciers occupy about one quarter of the peripheral area around the Greenland Ice Sheet (Thomsen and Weidick, 1992) (Figure 7.11). The glaciers of Disko Island (Qeqertarsuaq) and the Nuussuaq and Svartenhuk peninsulas, West Greenland, that covered an area of 3832 km^2 in 2001, lost between 16% and 21% of their area from the end of the Little Ice Age to 2001 (Citterio et al., 2009). There were no noticeable changes in the position of most calving glacier fronts between the late 19th century and the mid-1980s (Weidick, 1995). Between 1978 and 1991, major tidewater glacier termini along the northern coast of Kangerlussuaq and the southern part of Blosseville Kyst showed little change or a slight loss (0.1 to 0.5 km^2) in the glacier tongue area (Dwyer, 1995).

Extreme fluctuations of the terminus of the surge-type tidewater glacier Sortebrae involved a retreat of about 1.5 km between 1933 and 1943, a surge advance of about 10 km by 1950, a retreat of 8 km between 1950 and 1981, followed by stagnation between 1981 and 1992, and a second surge advance of over 5 km between 1992 and 1994 (Jiskoot et al., 2001). Another example of surge-related terminus fluctuations is shown by a small land-based Scoresby Sund glacier, which retreated 0.5 km between 1987 and 2000, and advanced by 2.8 km between 2000 and 2007 (Jiskoot and Juhlin, 2009). Neighboring glaciers did not change their terminus positions significantly during the same period.

7.3.2.5. Iceland

Glacier terminus variations in Iceland have been monitored regularly since 1930. Most non-surge-type glaciers retreated rapidly from 1930 to 1960, but more slowly in the 1960s. Glaciers began to advance in the 1970s and rates of advance peaked in the mid-1980s. In the 1990s, glaciers began to retreat again and all monitored glaciers were retreating by 2000. Terminus fluctuations follow changes in mean summer temperature with a delay of only a few years (Sigurðsson et al., 2007).

Mass balance measurements were initiated on Hofsjökull in 1987/1988 (Figure 7.10; Satujökull), Vatnajökull in 1991, and Langjökull in 1996. Vatnajökull's balance was positive from 1991 to 1994 and near zero in 1994 to 1995, but it has been negative ever since, with a cumulative specific balance of about -9.2 m w.e. (84 Gt, or 2.7% of the ice cap mass) from 1994 to 2006 (Björnsson and Pálsson, 2008). In the 1990s, mass loss from Vatnajökull due to basal melting resulting from geothermal activity and volcanic eruptions averaged 0.55 Gt/y, about 4% of the total surface ablation in a year of zero surface balance. However, the Gjalp volcanic eruption in 1996 melted about 4.0 Gt of ice. The net balance of Langjökull has been negative since measurements began and the cumulative specific net balance from 1996 to 2006 was about -12.8 m w.e. (13.1 Gt, 7% of the ice cap mass) (Björnsson and Pálsson, 2008). The current period of negative mass balance reflects a combination of high summer temperatures and low winter snowfall.

Figure 7.11. Mountain glaciers and ice caps occupy much of the peripheral areas of Greenland that lie beyond the margins of the Greenland Ice Sheet. Source: Anthony Arendt, University of Alaska.

7.3.2.6. Scandinavia

After their Little Ice Age maximum, Scandinavian glaciers retreated slightly until the 1930s/1940s, when there was a period of more rapid retreat that lasted into the 1950s for maritime outlet glaciers and the 1970s for more slowly responding outlets in the interior. Increased winter precipitation between 1988/1989 and 1994/1995 triggered a readvance of some glaciers in western Norway and Sweden, but higher summer air temperatures after 2001 induced an episode of rapid glacier retreat (Andreassen et al., 2005; Nesje, 2005, 2009). The longest mass balance records from Scandinavia date to the late 1940s (e.g., Holmlund et al., 2005), but the number of measurements increased in the early 1960s. Since that time, glaciers in inland Scandinavia (for which net balance variability is due largely to variability in the summer balance) have had a cumulative negative mass balance (Figure 7.10), while maritime glaciers in western Norway and some others such as Storglaciären in Sweden (for which net balance variability is due largely to variability in the winter balance) have had a cumulative positive net balance (especially in the 1990s when winter precipitation was unusually high) (Nesje, 2009). Since 2001, however, the mass balance of Norwegian glaciers has become predominantly negative. The North Atlantic Oscillation has a strong influence on the variability of the mass balance of maritime glaciers in western Norway (Reichert et al., 2001).

7.3.2.7. Svalbard

Over the past century, there has been a general trend toward retreat and thinning of Svalbard glacier fronts (Dowdeswell, 1986), excluding those that have surged during the period of observation, and thickening of higher elevation regions (Bamber et al., 2004; Nuth et al., 2007, 2010; Kohler et al., 2007; Moholdt et al., 2010a,b). Mass balance has been measured on two Svalbard glaciers (Austre Bröggerbreen and Midre Lovénbreen) since 1967 and on two more (Kongsvegen and Hansbreen) since the late 1980s (Hagen et al., 2003b). Almost all annual net balances are negative, the most notable exceptions being in 1987 and 1991 when all the measured balances were positive. There is no significant long-term trend in any of the annual balance records. Large annual variations are driven mainly by variations in the summer ablation. The cumulative balances of Austre Bröggerbreen (1967 to 2007) and Midre

Lovénbreen (1968 to 2007) were -20.3 and -15.3 m w.e., respectively, while that of Hansbreen (1989 to 2007) was -6.2 m w.e. (WGMS, 2009). Kongsvegen had a much smaller negative annual balance and a cumulative balance of -1.6 m w.e. (1987 to 2007) (WGMS, 2009), indicating that larger glaciers with high-elevation accumulation areas are experiencing more favorable mass balance conditions than smaller, low-lying glaciers. This is also the case for Austfonna in northeastern Svalbard, which had a surface net balance of -0.05 m/y w.e. for the five-year period 2004 to 2008 (Moholdt et al., 2010a). Shallow ice cores from Austfonna also indicated a net surface mass balance close to zero for the period between the Chernobyl fallout in 1986 and 1999 (Pinglot et al., 1999).

Hagen et al. (2003b) used the hypsometry (area-altitude distribution) of the glaciers and curves of net balance versus altitude for 13 regions to estimate the surface balance of Svalbard glaciers over the period 1968 to 1998. They found it to be slightly negative (-0.5 ± 0.1 Gt/y), or a mean specific surface net balance of -0.014 ± 0.003 m w.e./y. Mass loss by iceberg calving was estimated to be -4.0 ± 1.0 Gt/y (Dowdeswell and Hagen, 2004), making the total net balance of the archipelago significantly more negative, in total -4.5 Gt/y, or -0.12 ± 0.03 m w.e./y. A more recent estimate of the Svalbard calving flux (2000 to 2006) is -6.8 ± 1.7 Gt/y (Błaszczyk et al., 2009).

Geodetic measurements suggest that the rate of volume loss from a number of glaciers, especially low-lying glaciers close to the west coast, has increased by up to a factor of four since the early 1960s (Kohler et al., 2007). This is consistent with summer temperatures recorded at Longyearbyen, which increased by 0.04 °C/y from 1967 to 2006 and 0.17 **°C/y** from 1997 to 2006 (Førland and Hanssen-Bauer, 2003). Nuth et al. (2010) compared satellite altimetry from ICESat (2003 to 2007) to older topographic maps and digital elevation models (1965 to 1990) and estimated the geodetic mass change over the past 40 years for Svalbard, excluding Austfonna and Kvitøya, to be -9.7 ± 0.6 Gt/y (surface mass balance of -0.36 ± 0.02 m w.e./y). When the Austfonna estimate is added, this gives an overall mass balance for Svalbard of nearly -13 Gt/y. Moholdt et al. (2010b) used repeat track ICESat laser altimetry to assess mass and volume changes of Svalbard glaciers from 2003 to 2008. During this period, most regions experienced thinning at low elevations and thickening at high elevations. The geodetic mass balance for all of Svalbard's glaciers (not taking into account the effects of advance and retreat of calving glacier termini) was estimated to be -4.3 ± 1.4 Gt/y. The largest mass losses were in western and southern Svalbard, while Austfonna and glaciers in northeastern Spitsbergen gained mass over the period. Thus, available estimates of Svalbard net mass balance range from -4.3 to -14 Gt/y, depending upon the period of measurement and which calving flux estimate is used.

7.3.2.8. Russian Arctic islands

The major glacierized regions in the Russian Arctic are in the archipelagos of Franz Josef Land, Severnaya Zemlya, and Novaya Zemlya. Between 1952 and 2001, the glacierized areas decreased by 2.7% on Franz Josef Land, 0.4% on Severnaya Zemlya, and 1.4% on Novaya Zemlya. The total area reduction was about 725 km^2 (-375 km^2 on Franz Josef Land, -284 km^2 on Novaya Zemlya, and -65 km^2 on Severnaya Zemlya) (Glazovsky and Macheret, 2006). In Novaya Zemlya, net glacier recession has been greater on the west coast than on the east coast (Glazovsky, 2003). Using local area-volume scaling relationships, volume losses from the three archipelagos between 1952 and 2001 were estimated at -71 km^3 (Franz Josef Land), -24 km^3 (Severnaya Zemlya), and -150 km^3 (Novaya Zemlya). Assuming the volume was lost as ice, this gives a mean annual mass loss of -4.5 Gt/y from the three archipelagos (Glazovsky and Macheret, 2006).

Limited measurements of the surface mass balance of Shokal'sky Glacier on Novaya Zemlya, supplemented by reconstructions based on regression analyses between winter temperature / accumulation and summer temperature / ablation, suggest predominantly negative balances between 1930 and the mid-1990s (Zeeberg and Forman, 2001). Direct measurements on Vavilov Ice Cap (Severnaya Zemlya) between 1974 and 1988 also showed a slightly negative surface balance (-0.03 m w.e./y) (Barkov et al., 1992).

7.3.2.9. Russian mountains

The USSR glacier inventory mapped the glaciers of northeastern Siberia from aerial photography. Glacier changes have been determined by comparison with 2002/2003 Landsat7 ETM+ imagery. The area of glaciers of the Suntar Khayata mountain range (Figure 7.12) decreased from 200 km^2 in 1945 to 162 km^2 in 2002/2003, while that of glaciers in the Chersky mountain range decreased from 156 km^2 in 1970 to 113 km^2 in 2002/2003 (Ananicheva et al., 2006). The area of the Byrranga glaciers on the Taymir Peninsula decreased from 30.5 km^2 in 1967 to 24.4 km^2 in 2003, a reduction of 20%. South- and east-facing glaciers had the largest areal reductions, consistent with greater warming trends and smaller influence of westerly-derived cyclones on the eastern side of the mountain range (Ananichava and Kapustin, 2010).

On the Koryak Upland, a peninsula between Kamchatka and Chukotka, 248 glaciers were mapped from maps and aerial photographs dating from the 1950s and using Landsat 7 ETM+ and ASTER data from 2003. Their combined area decreased by 66.5%, from 176.6 km^2 to 54.4 km^2, over the intervening period. Glaciers with a northeasterly aspect showed the largest proportional area reductions. These glacier area changes are the largest recorded in the Russian sub-Arctic and reflect a

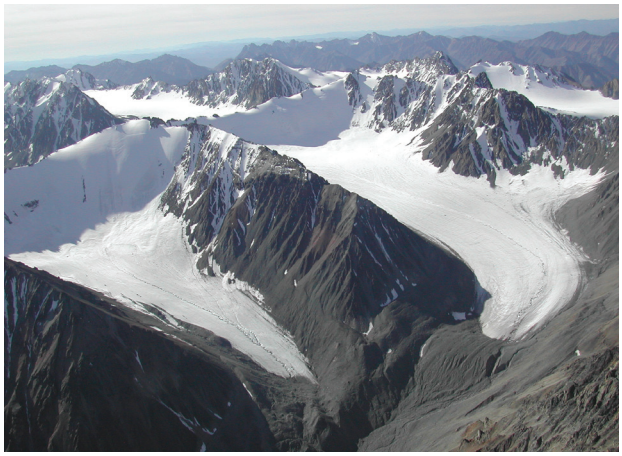

Figure 7.12. Mountain glaciers in the Suntar Khayata Range of northeastern Siberia. Note the well-developed meltwater drainage systems on the glacier surfaces. Source: Maria Ananicheva, Russian Academy of Science.

response to a combination of climate warming and decreased snowfall from Pacific sources (Ananichava and Kapustin, 2010).

At the end of the 1950s, there were 143 glaciers in the Ural Mountains with a total area of 28.7 km^2 (Osipova, 2006). From 1958 to 2001, mass balance observations were carried out on two Polar Ural glaciers (IGAN Glacier, area 0.73 km^2, and Obruchev Glacier, area 0.35 km^2). These records have been extended to cover the entire 20th century by correlation with local measurements of summer air temperature and winter precipitation. The resulting series show periods of negative balance between 1900 and 1920, in the late 1950s and 1960s, and since 1980. Positive balances occurred between 1920 and the mid-1950s (Kononov et al., 2005). From 1953 to 2000 (1981 for IGAN Glacier), the average area decrease rate of the four glaciers in the region (Obruchev, MGU, Chernov, IGAN) was 0.9% per year (Glazovsky et al., 2007).

7.3.2.10. Kamchatka

There are currently 448 glaciers in Kamchatka, with an area of about 874 km^2. The climate of Kamchatka is strongly influenced by intense storm activity from the Pacific Ocean, the thermal influence of the Sea of Okhotsk on the western side of the Peninsula, and the topography of the region. The mass balance of Kozelsky Glacier was positive from 1973 to 1978 and generally negative thereafter, with a cumulative mass balance of about -5 m w.e. over the period of record (1973 to 1997; Dyurgerov and Meier, 2005) (Figure 7.10).

7.3.2.11. Summary of regional changes

In general, glaciers across the Arctic began retreating and losing mass in the early 20th century. Area changes and mass loss continued through the mid-20th century, with some regions experiencing brief episodes of slower retreat, reduced mass loss, or even mass gain. The rate of mass loss increased during the past decade across most regions of the Arctic. This marks a change from the situation reported by Dowdeswell et al. (1997), who found that although most Arctic glaciers had experienced predominantly negative net surface mass balance over the previous few decades, there was no uniform trend in mass balance.

7.3.3. Links between mass balance and climate

Annual glacier mass balances often correlate over spatial scales as large as 1200 km (Cogley and Adams, 1998; Rasmussen, 2004) as a result of trends in climate that are consistent over broad regions. These trends often occur due to synoptic-scale teleconnections between the positioning of the polar jet stream, the phase of the El Niño Southern Oscillation (ENSO), and regional patterns in temperature and precipitation. The mass balance of glaciers in Alaska, western Canada, and the U.S. Pacific Northwest is strongly affected by a decadal ENSO-like phenomenon, otherwise known as the Pacific Decadal Oscillation (PDO), which is measured by variations in the sea-surface temperature of the Gulf of Alaska (Bitz and Battisti, 1999; Josberger et al., 2007). Mass balance measurements from Gulkana Glacier in interior Alaska, Wolverine Glacier in maritime Alaska, and South Cascade Glacier in coastal Washington State show the complex reaction of glacier mass balance to variations in the PDO that result in major changes in the positioning of the North Pacific storm track and the distribution of winter precipitation. From 1966 to 1977, the PDO was in a strong cold phase and the net balance of the three glaciers was slightly negative. In 1977, the PDO switched into a strong warm phase, and the mass balance of South Cascade became very negative, a trend that continues to present. The mass balance of Gulkana and Wolverine Glaciers began to increase as the storm track was diverted toward Alaska. From 1987 to present, the PDO warm phase has weakened, and the net balance of all three glaciers has become uniformly negative.

Gardner and Sharp (2007) showed that accelerated glacier surface mass loss in the Canadian Arctic after 1987 was associated with increased July mean air temperature and a shift in the mean position of the center of the July circumpolar vortex from the western hemisphere to the eastern hemisphere. This allowed increased intrusion of warm air from continental North America into the Queen Elizabeth Islands in summer. July vortex types associated with warm temperatures and negative mass balance anomalies were also more common from 1948 to 1962, so predominantly negative surface mass balances may also have characterized the 1950s.

Occasional periods of positive balance on Novaya Zemlya (especially in the late 1940s and early 1950s) occurred when the North Atlantic Oscillation (NAO) was in a positive phase, sea-surface temperatures in the southern Barents Sea were anomalously warm, and winter precipitation was increased (Zeeberg and Forman, 2001). Negative surface balances occurred whenever summer temperatures rose more than 1 °C above the 1933 to 1991 mean, most notably from the early 1950s to the late 1960s. Positive NAO conditions also coincided with the period of positive mass balances in western Scandinavia in the early 1990s (Pohjola and Rogers, 1997).

7.4. Proxy indicators of surface mass balance

- The number of *in situ* measurements of the surface mass balance of glaciers in the Arctic is small, and the distribution of monitored glaciers is uneven. Therefore, it is difficult to estimate accurately the surface mass balance of the regional ice cover (the quantity that needs to be known to determine the contribution of Arctic glaciers to global sea level change) on the basis of these measurements alone.
- There is, therefore, considerable interest in using remote sensing methods to repeatedly measure regional-scale patterns in parameters that vary in ways that are well-correlated with surface mass balance in order to generate records that may reflect the temporal trends and variability in surface mass balance.
- Parameters of interest include the length of the summer melt season, the distribution of snow and ice facies across mountain glaciers and ice caps, the equilibrium-line altitude, the accumulation area ratio, the surface albedo, and the surface temperature. These can be measured using active microwave methods or passive monitoring in the visible and infrared parts of the electromagnetic spectrum. To date, such measurements have been made more widely on the large ice sheets than on mountain glaciers and ice caps, but this is changing with improvements in sensor resolution.

- Pan-Arctic mapping of summer melt season duration and the end-of-summer distribution of snow and ice facies has been possible for the 1999 to 2009 decade due to the availability of enhanced resolution data products from the Seawinds scatterometer on QuikSCAT. That satellite is no longer functional and there is as yet no new data series to replace the one it generated.

7.4.1. Introduction

Glaciological (*in situ*) measurements of the surface mass balance of Arctic glaciers and ice caps are limited to a small number of glaciers that are unevenly distributed across the Arctic and are biased toward small, land-terminating glaciers. For many of these glaciers, the time series of surface mass balance measurements are discontinuous, of short duration, and not recent. In some regions of the Arctic, *in situ* surface mass balance data are simply nonexistent. Such limitations are mainly due to the remoteness of the Arctic and the intense logistical demands associated with establishing and maintaining *in situ* surface mass balance observations. However, common practice has been to produce regional-scale estimates of surface mass balance based on interpolation of the small number of *in situ* observations. This results in large uncertainties where data are sparse, so that it is not clear whether these estimates truly represent regional surface mass balance trends over the Arctic. Because of these limitations, there is a pressing need to develop alternative methods for estimating trends in surface mass balance and to be able to apply them repeatedly over large areas in order to monitor changes in surface mass balance at regional scales.

Proxy indicators of surface mass balance are parameters or indices that are directly related to the surface mass balance process and that can be used to infer changes in surface mass balance. For example, variations in the abundance of melt layers in ice cores have been used for this purpose (e.g., Koerner and Fisher, 1990; Kinnard et al., 2008). Currently, regional-scale proxy indicators of annual surface mass balance are typically developed from satellite-derived remote sensing data. Some of these proxies provide an indication of the sign of the surface mass balance change between consecutive mass balance years (e.g., Wolken et al., 2009), while others may be useful in the development of methodologies for up-scaling *in situ* surface mass balance measurements to the regional-scale glacier cover (e.g., Wang et al., 2005) or for validating predictions from surface mass balance models.

7.4.2. Proxy indicators, data sources, and methods of measurement

7.4.2.1. Melt duration

Spatial and temporal variability in the surface mass balance of many Arctic glaciers is controlled by the variability in surface melt (Koerner, 2005; Gardner and Sharp, 2007). Surface melt characteristics (extent and duration) can provide valuable information about the melt process and can be detected at regional scales by satellite remote sensing. Because melt usually occurs in all regions of Arctic glaciers and ice caps every summer, melt extent provides little information about variability in the summer melt process on these ice masses. Melt duration is a much better descriptor and is well correlated with the annual positive degree-day total (a parameter used to simulate snow and ice melt rates in temperature index melt and mass balance models) (Wang et al., 2005), and with summer mean temperatures and geopotential heights in the lower troposphere as derived from climate re-analyses (Wang et al., 2005, 2007; Sharp and Wang, 2009).

Microwave remote sensing is well suited for mapping melt duration on Arctic ice masses. Passive microwave remote sensing is commonly used for melt mapping on Greenland, but its coarse spatial resolution (≥25 km) precludes its use on the smaller Arctic glaciers and ice caps. Data from Ku- and C-band microwave scatterometers have been used successfully to map annual melt duration on ice caps and glaciers in the Arctic (Smith et al., 2003; Wang et al., 2005; Sharp and Wang, 2009; Sharp and Wolken, 2009, 2010; Wolken et al., 2009) (Figure 7.13). Annual melt duration is determined by calculating the number of days between the melt onset and freeze-up dates minus the duration of any intervening periods when melt was not detected. Wang et al. (2005) used time series of enhanced resolution data from the SeaWinds scatterometer aboard QuikSCAT (Early and Long, 2001; Long and Hicks, 2005) to determine melt onset and freeze-up dates and to determine annual melt season durations on ice caps in Arctic Canada (2000 to 2004). On these ice caps, annual mean melt duration varies with ice surface elevation ($r = -0.80$) and distance from Baffin Bay ($r = -0.44$) and is strongly linked to variations in geopotential height at the 500 hPa level. For the period 2000 to 2004, average melt duration for individual ice caps ranged from 26 days on the Agassiz Ice Cap to 62 days on the Manson Icefield. For the Queen Elizabeth Islands as a whole, the shortest melt season was 2002 and the longest was 2001.

In the Eurasian Arctic (Svalbard, Severnaya Zemlya, Novaya Zemlya), average melt duration (2000 to 2004) is well correlated with latitude, longitude, and elevation and is consistent with the steep climatic gradient across the region (i.e., warm and moist in the west to cool and dry with persistent sea ice in the east; Dowdeswell et al., 2002; Sharp and Wang, 2009). Average melt duration on Severnaya Zemlya (51 days) is significantly shorter than on Novaya Zemlya (75 days) and Svalbard (77 days). Data show that 2000 was the shortest melt season and 2001 the longest during the 2000 to 2004 period (Sharp and Wang, 2009). Variations in annual mean melt duration were strongly correlated with the mean (June and August) 850 hPa air temperature.

7.4.2.2. Snow and ice facies

Glacier surfaces are organized into zones on the basis of differences in the physical properties of surface and near-surface snow and ice (Benson, 1962). The differences between snow and ice facies are related to variations in the magnitude of summer melt, which are strongly correlated with elevation. Snow and ice facies on glaciers and ice caps in the Arctic include the following (from high to low elevation): dry snow facies – formed where no melt occurs and snow is converted to ice solely by compaction; percolation facies – formed where meltwater percolates into the snowpack and refreezes as lenses, layers and pipes, but the snowpack never reaches the melting point throughout the melt season; saturation facies – formed where

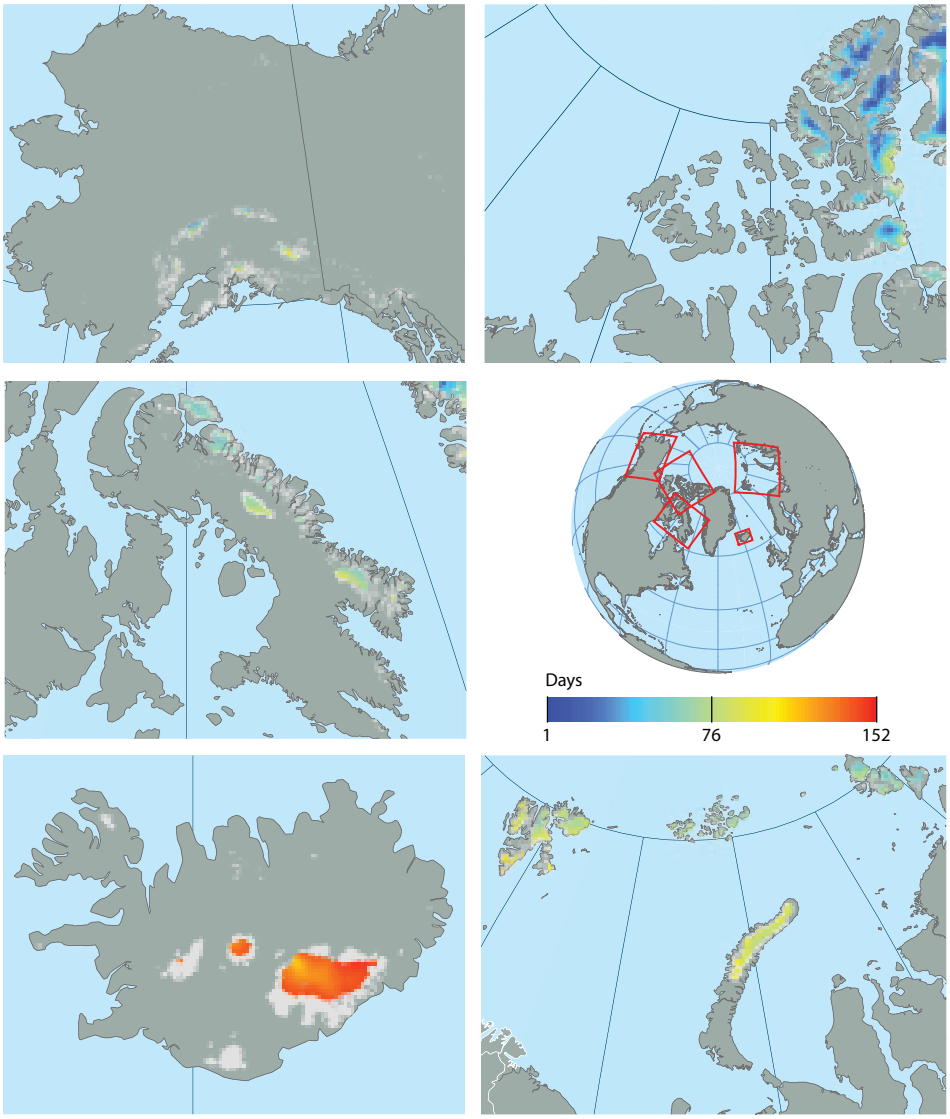

Figure 7.13. Mean annual melt duration (days) on larger Arctic ice masses for the period 1999 to 2008 based on QuikSCAT scatterometer data. Source: Gabriel Wolken, Alaska Division of Geological and Geophysical Surveys.

the temperature of the entire snowpack reaches the melting point sometime during the melt season and wet snow refreezes at the end of the melt season; superimposed ice facies – formed in a transitional zone in the lowest part of the accumulation area where meltwater freezes directly onto the glacier ice surface; and glacier ice facies – exposed in the ablation zone in summer when summer melt removes the annual snow accumulation and exposes glacier ice at the surface (Figure 7.14). There is often a transitional zone between snow and ice facies in which a mixture of these facies can be found. The distribution of snow and ice facies can change annually, and not all facies are found on all ice masses in all years. Because the distribution of snow and ice facies is directly linked to the balance between the processes of accumulation and surface melt, it can provide valuable proxy information about spatial and temporal variations in the surface mass balance.

Snow and ice facies have been mapped at regional scales using optical and microwave remote sensing. Mapping with optical sensors has had limited success, largely due to the often subtle contrast between snow and ice facies and to the occurrence of fresh snow (which conceals the underlying facies) and cloud cover (which conceals the glacier) at the end of the ablation season (Østrem, 1975a; Nolin and Payne, 2007; Dowdeswell et al., 2007). Microwave radiation is unaffected by cloud cover, but is sensitive to the surface and volumetric physical properties of snow and ice. Snow and ice facies on Arctic glaciers and ice caps have been linked to specific signatures acquired by active microwave sensors, and mapped on the glaciers Kongsvegen and Lovénbreen (Svalbard) using synthetic aperture radar (SAR; ERS-1/2) data (Engeset et al., 2002; König et al., 2002). Firn, superimposed ice, and glacier ice facies were identified

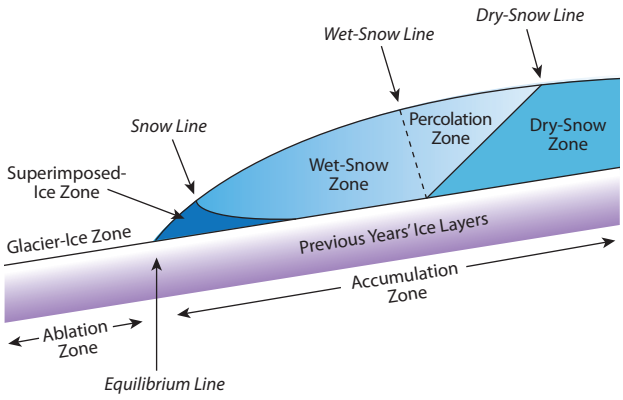

Figure 7.14. Snow and ice facies zones on a glacier or ice cap. Source: after Benson (1962).

in these studies, but the complicated nature of backscatter in the superimposed ice zone precluded the identification of the equilibrium line. Further work on Kongsvegen using *in situ* data and SAR concluded that the superimposed ice zone represents 35% of the glacier (Obleitner and Lehning, 2004). Langley et al. (2008) and Brandt et al. (2008) also investigated snow and ice facies on Kongsvegen by combining data from SAR and ground-penetrating radar (GPR) and concluded that SAR zones were in very good agreement with GPR-derived glacier facies. On Austfonna (Svalbard), Dunse et al. (2009) used GPR to determine the multi-year (2004 to 2007) snow and ice facies distribution and linked variability in facies over the study period to changes in surface mass balance.

Regional-scale mapping and monitoring of snow and ice facies have been performed using microwave scatterometer data. Wolken et al. (2009) used a classification of end-of-summer, enhanced resolution (2.225 km^2) data from QuikSCAT (tuned using available field observations) to map the distribution of snow and ice facies in the Canadian High Arctic and its interannual variability (1999 to 2005) (Figure 7.15). Increases in summer air temperature and melt duration were associated with a decrease in the areas of the percolation and saturation zones, an increase in the area of the glacier ice zone, and an increase in the elevation of inter-facies boundaries.

7.4.2.3. Equilibrium-line altitude

The equilibrium line is the line connecting points on a glacier surface where annual accumulation equals annual ablation. Above the equilibrium line (the accumulation area) there is a net gain in mass for a particular year, whereas below the equilibrium line (the ablation area) there is a net loss in mass. The equilibrium-line altitude (ELA) is the average altitude of the equilibrium line at the end of the ablation season in any balance year. The ELA is related to the surface mass balance because it rises and falls as the annual mass balance of the whole glacier becomes more or less negative (Østrem, 1975a; Hagen and Liestøl, 1990). It can be used to identify variability and trends in surface mass balance when monitored annually. The long-term ELA represents the average position of the ELA over many years. Change in the long-term ELA, generally linked to a change in glacier geometry, serves as an important indicator of regional climate change.

The ELA is most accurately determined using standard *in situ* glaciological techniques for measuring surface mass balance. Dyurgerov (2002), Dyugerov and Meier (2005) and Dyurgerov et al. (2009) compiled all available time series (around 280) of *in situ* mass balance data and related variables, including ELA, for glaciers outside the two ice sheets. For the few glaciers in the Arctic where ELAs are determined through *in situ* measurements, ELA time series are characterized by a high degree of interannual variability. However, while these measurements are robust and invaluable to the glaciological community, they are also spatially restricted and limited in their ability to provide a meaningful measure of ELA variability on a regional scale.

Alternative methods have been developed for monitoring regional-scale changes in the annual ELA, the most effective of which involve the use of satellite microwave remote sensing. In Arctic Canada, regional-scale variability in the

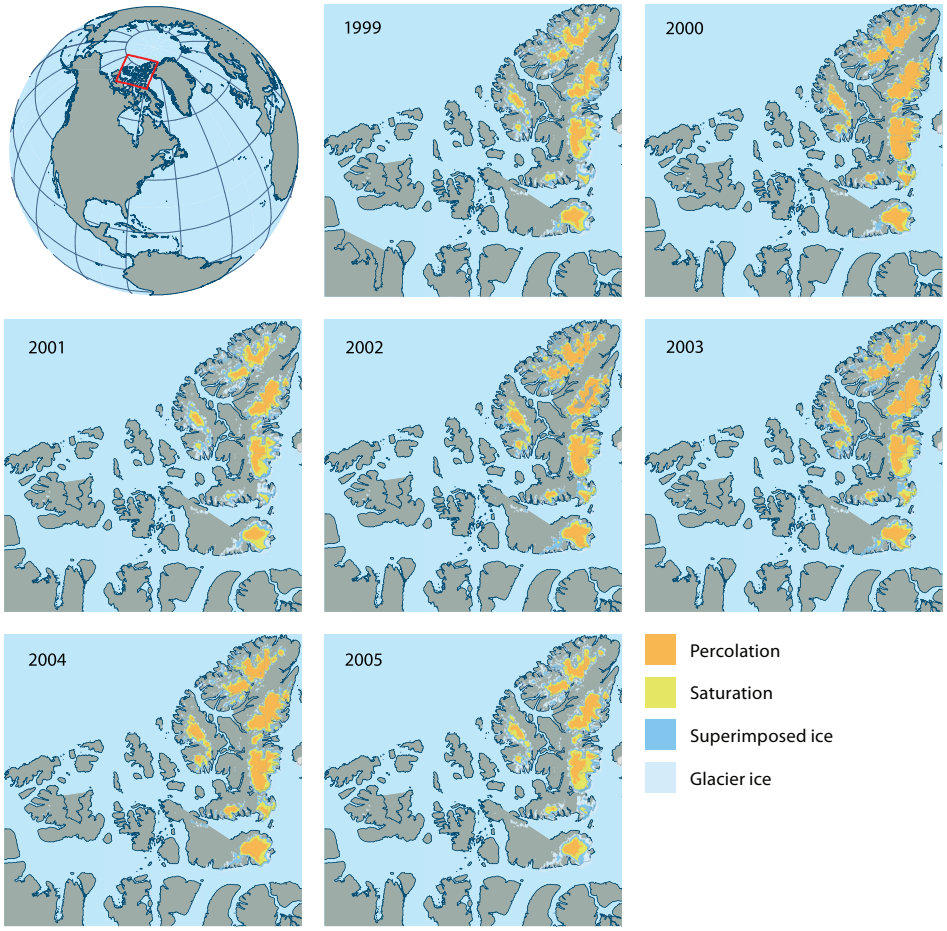

Figure 7.15. Annual distribution of snow and ice facies at the end of the melt season on ice caps in the Canadian High Arctic (1999-2005) as derived from QuikSCAT scatterometer data. Source: Wolken et al. (2009).

ELA can be inferred from changes in the lower boundary of the superimposed ice zone, which is highly correlated with changes in surface mass balance measurements (Wolken et al., 2009). Scatterometer-derived changes in the annual average ELA for each ice cap show a generally coherent pattern of change during the study period (1999 to 2005), with the highest ELAs occurring in 2001, the year with the longest melt season.

7.4.2.4. Accumulation area ratio

The accumulation area ratio (AAR) is the ratio of the area of the accumulation area to the area of the entire glacier. Because the lower limit of the accumulation area is determined by the position of the equilibrium line, the AAR and the ELA are directly related. If a record of the AAR is combined with *in situ* surface mass balance data, then it is possible to produce quantitative estimates of changes in the surface mass balance with respect to changes in the AAR (Dyurgerov et al., 1996, 2009; Hock et al., 2007b). Quantification of regional-scale changes in surface mass balance from AAR changes in the Arctic is limited by the sparseness of *in situ* surface mass balance data for use in calibration. However, regional-scale changes in surface mass balance can be qualitatively assessed based on the relative changes in the AAR between regions. Annual AARs for ice caps in the Canadian High Arctic were determined from maps of the distribution of snow and ice facies derived from QuikSCAT scatterometer data for the period 1999 to 2005 (Wolken et al., 2009). Results from this study indicate considerable spatial and temporal variability in the annual AAR during this period. For the Queen Elizabeth Islands as a whole, the mean AAR was 0.75 over the period 1999 to 2005. The smallest mean AAR (0.50) occurred in 2001and the largest (0.82) in 2004 (Wolken et al., 2009).

7.4.2.5. Albedo

The albedo (the fraction of incoming solar radiation reflected by a surface) of snow and ice is a function of snow/ice grain size, surface water content, solar incidence angle (Wiscombe and Warren, 1980), and snow impurities (Warren and Wiscombe, 1980), including black carbon from natural and industrial sources (McConnell et al., 2007; Forsstrom et al., 2009). On Arctic glaciers, solar radiation is usually the main source of energy for surface melt, and its magnitude and distribution are controlled in part by the glacier surface albedo. As a result, and because factors such as grain size and water content are coupled to surface melt rates, interannual variations in surface albedo and their spatial patterns over individual glaciers can serve as a proxy indicator of surface mass balance.

In situ observations of albedo can be scaled-up with satellite optical remote sensing measurements (Williams, 1987; Reijmer et al., 1999; Greuell and Knap, 2000; Nolin and Payne, 2007), producing data that can be used to identify reductions in albedo that provide an indication of melt onset (Hall et al., 1987; Bindschadler et al., 2001). De Ruyter de Wildt et al. (2002, 2003) used Advanced Very High Resolution Radiometer (AVHRR) data for Vatnajökull, Iceland to determine the evolution of the surface albedo over the melt season and estimate the potential absorbed radiation, which was shown to correlate well with the mean specific mass balance ($r = 0.87$ and 0.94 for different outlet glaciers). This methodology was further developed by Greuell et al. (2007), who generated estimates of mass balance for the whole of Vatnajökull.

7.4.2.6. Land (glacier) surface temperature

Because winter precipitation is consistently low in the Arctic (excluding southern Alaska, Scandinavia, Iceland, and Kamchatka), variability in glacier mass balance is largely controlled by summer temperature. While precipitation events during summer can be important as summer snowfalls result in short-term increases in surface albedo, temperature tends to drive the ablation process and control variations in surface mass balance (Koerner, 2005; Gardner and Sharp, 2007). In the absence of systematic *in situ* temperature observations, which are available for only a few areas across the Arctic, satellite-borne thermal infrared sensors can be used to monitor clear-sky land surface temperature (LST) and surface melt at regional scales over the terrestrial cryosphere (Key and Haefliger, 1992; Key et al., 1997; Stroeve and Steffen, 1998; Hall et al., 2004, 2006, 2008a,b). In the Eurasian Arctic, Sharp and Wang (2009) used Moderate-Resolution Imaging Spectroradiometer (MODIS) LST data in place of *in situ* near-surface air temperature data to tune melt detection algorithms applied to QuikSCAT scatterometer data. However, there has been little other use of LST data on Arctic glaciers and ice caps. This is probably because reliable satellite-derived LST data can only be obtained under cloud-free conditions and because there are errors and calibration inconsistencies associated with many of these data. Owing to the great potential in using LST as a proxy for regional-scale surface mass balance, there is a need for more *in situ* validation work over ice-covered regions in order to assess the accuracy of satellite-derived LST over Arctic glaciers and ice caps.

7.5. Ice dynamics and iceberg calving

- Iceberg calving from ocean-terminating glaciers can be an important process of mass loss. Rates of calving loss can change rapidly for reasons that are influenced, but not directly controlled, by climate. These changes can generate anomalously high rates of mass loss, but not anomalously high rates of mass gain.
- Possible controls on calving rates include changes in lubrication from seasonal meltwater input, changes in resistance to flow from thinning and flotation, loss of contact with a stabilizing moraine, and break-up of floating ice tongues, as well as from changes in upstream dynamics, including surging.
- A tidewater glacier cycle is recognized. It involves prolonged periods of slow (~1000 years) glacier advance into the ocean, alternating with shorter periods (around decades) of accelerated glacier flow and retreat.
- Although measurements of iceberg calving fluxes are now available for many regions of the Arctic, the ability to model the processes that determine these fluxes is rudimentary. There is currently no ability to predict how calving fluxes will evolve in the future.

- The character of a glacier terminus and the icebergs produced are linked. Small, hard-to-detect bergs are produced mainly by grounded termini and glaciers in rapid retreat, while large tabular bergs come from floating ice tongues and ice shelves.
- The largest remaining ice shelves in the Arctic fringe the northern coastline of Ellesmere Island. These entered a new phase of break-up after 2000. As a result, several fjords in the region are now free of a permanent ice cover for the first time in at least 3000 years.

7.5.1. Overview

Glaciers that terminate in the ocean or in lakes lose mass by iceberg calving as well as by melting and sublimation, and iceberg calving can be the dominant mass-loss term for many glaciers and ice caps in the Arctic. Rates of iceberg calving from marine-ending glaciers (referred to as 'tidewater glaciers' if their termini are grounded below sea level) are modulated by stress and flow conditions near the glacier's terminus, which will vary as the glacier changes shape and volume in response to climate change. Rates of calving can also change in response to internally controlled processes that alter stresses and may be entirely independent of climate. In either case, glacier mass loss through calving may be sudden and rapid, and may be far greater in magnitude than losses due to climatically controlled mass balance. Rapid dynamic changes can cause anomalously rapid mass loss, but not anomalously rapid mass gain, because alterations in flow can force fast ablation (by moving ice either to lower and warmer elevations or into the ocean), while accumulation rates are limited by precipitation.

7.5.1.1. Hydrology and basal sliding

Glaciers that slide over their beds typically exhibit significantly larger velocities and fluxes than glaciers that flow by internal (ice) deformation alone. Sliding is facilitated by the presence of water and deformable sediments at the ice/bed interface, although the relationship between water input and sliding speed is highly non-linear. Warmer surface conditions that increase surface melting in summer will accelerate glacier flow, but there is no simple relationship between the amount of warming and the magnitude of the flow acceleration. Higher water fluxes through subglacial drainage systems may result in greater enlargement of individual drainage channels, lower subglacial water pressures, and less flow enhancement than is generated by smaller fluxes. Thus, it is by no means clear that climate warming will, in the long term, result in more rapid glacier flow. As on Greenland, however, supraglacial lakes often form on Arctic glaciers in summer (Figure 7.16), and may drain suddenly when water-pressure induced fracturing creates drainage connections between the glacier surface and the glacier bed (Boon and Sharp, 2003). These lake drainage events may result in short-lived accelerations of glacier flow. As yet, however, there is no general rule to link increased sliding speed with increased englacial or subglacial water input, and no validated, reliable numerical model for basal sliding exists (Fountain and Walder, 1998; Hooke, 1998; Marshall et al., 2002).

Figure 7.16. Supraglacial lakes forming on the surface of Columbia Glacier, Alaska, during the melt season. Source: W. Tad Pfeffer, Institute for Arctic and Alpine Research, University of Colorado

7.5.1.2. Glacier surges

Glacier surges are episodes of anomalously rapid motion (about 10 to 100 times 'normal' or non-surging speeds) that last for months to a few years and alternate with longer periods (decades to centuries) of normal, or quiescent, glacier behavior. Glacier velocities during the active phase of the surge cycle may reach 100 m per day and rates of terminus advance may approach 1 km per month. Glacier surges are not a direct response to climate forcing, but surging can alter a glacier's sensitivity to climate, especially in the immediate post-surge phase when its accumulation area is anomalously depleted (Dowdeswell et al., 1995).

7.5.1.3. Calving and marine-ending outlet glacier instability

'Marine-ending' or 'ocean-terminating' glaciers reach the ocean shore with sufficient flux to maintain an ice tongue that is either grounded in water shallower than the tongue's flotation depth or may be floating under polar conditions (subfreezing and, therefore, strong when in tension). Floating tongues can also form during periods of rapid terminus retreat. The term 'tidewater glacier' is often used interchangeably with these labels, although it was originally restricted to glaciers with grounded termini. Marine-ending glaciers can undergo a periodic growth/shrinkage instability with long (roughly centuries) periods of slower motion and slow advance

alternating with shorter periods (decades) of rapid (~5 to 10 km/y) motion, high calving flux, and rapid (~1 km/y) retreat (Meier and Post, 1987) (Figure 7.17). This is significant in that during rapid retreat a glacier can lose mass into the ocean far faster (by loss of its marine-grounded tongue and drawdown of its source basin by rapid flow) than is possible by direct surface mass balance forcing alone.

In its advancing phase, a tidewater terminus is stabilized in part by back stress against a moraine at its advancing margin. If it retreats from the moraine, a tidewater glacier in an advanced position can switch abruptly (within years) into an unstable phase of rapid flow and calving accompanied by thinning in its ocean-grounded reach that results in terminus retreat. Once initiated, rapid flow and retreat appear to be generally irreversible and continue until the glacier's terminus retreats inland to a point where the water depth provides no significant buoyancy force. The causes of unstable retreat are not completely understood, but involve high basal water pressures tied to the depth of the glacier bed below sea level, rapid sliding, vertical thinning, and positive feedback between thinning and rapid flow. The processes governing the size and rate of production of icebergs are extremely poorly known. Climate-induced thinning can play a critical role in initiating unstable retreat, but once initiated, unstable retreat appears to be modulated by channel geometry and englacial and basal hydrology and is essentially independent of climate and surface mass balance. Melting of the submarine faces of grounded tidewater glaciers can be rapid (Motyka et al., 2003) and can result in undercutting of the terminal ice cliff with consequences for iceberg production and terminus stability (Rignot et al., 2010; Straneo et al., 2010).

7.5.1.4. Lake-terminating glaciers

The total area of lake-terminating calving glaciers is much smaller than the area of marine-terminating glaciers, and the dynamics of their calving appear to be significantly different. Thinning rates on lake-calving glaciers are among the highest observed anywhere (e.g., -3.0 m/y basin-averaged thinning at Yakutat Glacier, Alaska) (Larsen et al., 2007).

7.5.1.5. Ice shelf / ice tongue break-up

Stable floating ice tongues (or ice shelves) are held in place by stabilizing stresses supplied by lateral attachments to valley walls or embayment margins (and, to a lesser degree, back stress from sea ice and confined iceberg fragments: *sikkusaq*), rather than by basal drag or back stress on the glacier terminus (Dowdeswell et al., 2000; Reeh et al., 1999). Submarine melt can be a significant source of mass loss from floating tongues (Mayer et al., 2000). Spreading and thinning of floating ice produces small tensile stresses, crevassing, and calving of icebergs. Under warming conditions, a floating ice tongue can be destabilized by (i) increased submarine melt, (ii) increased internal ice temperature, and (iii) percolation of surface meltwater into open crevasses and fractures. Loss of an ice shelf or floating tongue and the associated back stress on the feeding glacier(s) affect the force balance on the ice upstream from the grounding line and in general cause an acceleration of the grounded ice and increased ice discharge to the ocean. The loss of the floating tongue has no influence on sea level, but increased discharge from the grounded part of the glacier contributes to eustatic sea-level rise.

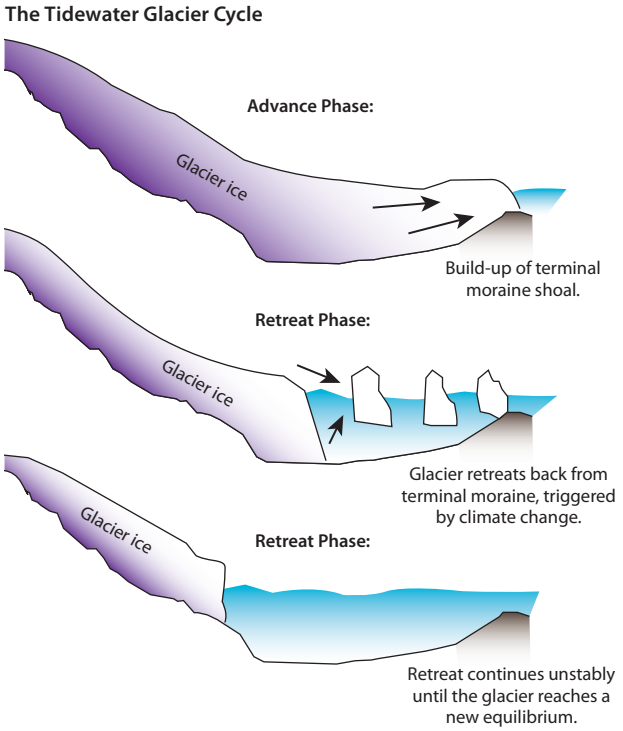

Figure 7.17. Schematic diagram showing the typical advance-retreat cycle of a tidewater glacier. Source: after Meier and Post (1987).

7.5.2. Measurement methods

Glacier dynamic changes are manifested principally in changes in speed, surface elevation, ice discharge, and iceberg calving. Consequently, surface observations to track moving features or measure surface altitude are critical to understanding the processes involved. Glacier velocity is determined from repeat measurements of the position of markers on the glacier surface made by optical survey (Harper et al., 2007), GPS (Howat et al., 2008), and by feature tracking using aerial photography (Krimmel, 2001) and ground-based photography (O'Neel et al., 2005). Velocities are also measured remotely by manual and automated feature tracking applied to a variety of visible satellite imagery (Scambos et al., 1992; Joughin, 2002; Dowdeswell and Benham, 2003) and by radar interferometry and speckle tracking (Joughin et al., 1999). Elevation changes are measured by photogrammetry, by repeat altimetry from airborne or spaceborne platforms (Arendt et al., 2002, 2006; Larsen et al., 2007; Howat et al., 2008), and to a lesser degree by ground-based GPS and optical surveys.

The terminus advance/retreat rate ($\partial x/\partial t$) is the difference between the calving rate (u_c) and the ice flow speed at the terminus (u_T): ($\partial x/\partial t = u_c - u_T$). Iceberg calving events are episodic and very short in duration, and the volume of individual icebergs is hard to determine from imagery. The calving rate is therefore difficult to measure directly, and it is typically calculated as $u_c = \partial x/\partial t + u_T$ (O'Neel et al., 2005), but this is a weak approach in predictive models where $\partial x/\partial t$ is often the variable being sought. New methods are being developed to use seismic records to identify individual calving events and estimate iceberg discharge (O'Neel and Pfeffer, 2007).

7.5.3. Calving and surging glaciers in the Arctic

Surging and marine calving glaciers are found throughout the Arctic, although there are currently none in Norway or Sweden. Table 7.2 summarizes recent estimates of mass loss by calving from major regions and/or major ice masses within the Arctic (but note that no estimates are available for some regions and ice masses).

7.5.3.1. Alaska and western Canada

The greatest concentrations of glacier area in Alaska and northwestern Canada lie along the coast of the Gulf of Alaska, where land-terminating glaciers on the interior side drain predominantly into the Matanuska, Copper, and Yukon Rivers, while seaward-facing glaciers drain into, or terminate in, the Gulf of Alaska.

7.5.3.1.1. Calving

A significant but undetermined fraction of the area of Gulf of Alaska glaciers is drained through 54 calving tidewater outlets. No estimates have been made of calving flux for the entire Gulf, but a 1982 study (Brown et al., 1982) compared geometry and calving speed for 13 of the largest tidewater glaciers and found a total flux of 7.2 Gt/y draining from an aggregate basin area of 8138 km^2, estimated for various periods within the interval 1942 to 1979. No more recent or more complete assessment has been made.

In the past 200 years, the 54 tidewater glaciers terminating in the Gulf of Alaska all retreated from extended stable positions. Columbia Glacier was the last to start retreating and as of 2009 had retreated roughly two-thirds of the way up the 30-km long fjord in which it was grounded up to about 1982. The majority of Gulf of Alaska tidewater glaciers are now either stable in retreated positions or slowly advancing (e.g., Hubbard and Mears Glaciers). Columbia Glacier is undergoing the most rapid change, calving an average 3.3 Gt/y of ice (1982 to 2001), with a maximum annual calving flux of 6.6 Gt in 2001 (O'Neel et al., 2005), and thinning in the terminus region by 20 m/y. GRACE gravity measurements suggest that the Gulf of Alaska glaciers were losing mass at a rate of 84 ± 5 Gt/y in the period 2003 to 2007 (Luthcke et al., 2008). A study of the southeastern (panhandle) Gulf of Alaska sub-region (not including Columbia Glacier) found a loss of 16.7 ± 4.4 Gt/y from 14 580 km^2. Two-thirds of this was from calving glaciers, although the fraction of this volume loss that was attributable to calving (as opposed to surface melting) is unknown (Larsen et al., 2007).

Table 7.2. Estimated mass losses by iceberg calving of mountain glaciers and ice caps. Specific balances due to calving are derived by dividing the calving mass loss by the total area of the glacier.

	Period	Area, km^2	Calving loss, Gt/y	Specific balance, m/y w.e.	Source
Alaska					
Columbia Glacier	1982 – 2001	1000	3.3	-3.3	O'Neel et al., 2005
Canadian High Arctic					
Devon Ice Cap	1960 – 1999	14 000	0.53±0.12	-0.04	Burgess et al., 2005
Prince of Wales Icefield	1963 – 2003	19 300	1.9 ±0.02	-0.10±0.00	Mair et al., 2009
Agassiz Ice Cap	1999 – 2002	19 500	0.60±0.14	-0.03±0.01	Williamson et al., 2008
W Grant Ice Cap[a]	1999 – 2003	2 000	~0.23	~ -0.12	Williamson et al., 2008
Russian Arctic					
Academy of Sciences Ice Cap	1995	5 575	0.59	-0.10	Dowdeswell et al., 2002
Franz-Josef Land	1929 – 1959	13 700	2.1	-0.15	Govorukha, 1989
	1952 – 2001		4.3	-0.31	Glazovsky and Macheret, 2006
Novaya Zemlya	1930 – 1960	23 600	1.8	-0.08	Govorukha, 1989
	1952 – 2001		1.4	-0.06	Glazovsky and Macheret, 2006
Severnaya Zemlya	1929 – 1972	19 400	0.45	-0.02	Govorukha, 1989
	1952 – 2001		0.7	-0.04	Glazovsky and Macheret, 2006
Svalbard					
All glaciers	1968 – 1998	36 600	4±1	-0.1±0.0	Hagen et al., 2003b
	2000 – 2006	36 600	6.75±1.7	-0.18±0.05	Błaszczyk et al., 2009
Austfonna	[b]	8 000	2.5±0.5	-0.31±0.06	Dowdeswell et al., 2008

[a] Calving estimates only from Otto Glacier which is likely the majority of the mass loss by calving from the ice cap; [b] a combination of various data sets from the period 1973 to 2001.

Here, and elsewhere, episodic discharges from individual glaciers can exceed the aggregate discharge from the rest of the region, making averages over time difficult to interpret or extrapolate.

7.5.3.1.2. Surging

Surging glaciers are abundant in the central Alaska Range (Denali massif), eastern Alaska Range, and throughout the St. Elias mountains, where 'Alaskan-type' surging was defined (Figure 7.18). Bering Glacier, in this region, is the largest glacier (and largest surging glacier) in Alaska (Shuchman and Josberger, 2010). Its last major surge took place in 1995 to 1996, although there was a small surge in 2009 to 2010. Bering Glacier terminates in a large proglacial lake at sea level, the size of which changes dramatically as the glacier advances and retreats. Some surging glaciers in the St. Elias Range terminate in the ocean, allowing surge behavior to influence calving discharge. No surging glaciers are known in the Chugach or Brooks Ranges.

7.5.3.2. Arctic Canada

7.5.3.2.1. Calving

There is no comprehensive summation of calving flux or inventory of calving glaciers for the Canadian Arctic Archipelago, but estimates of calving fluxes for some of the ice caps exist for mixed time periods in the interval 1960 to 2003, totaling 3.0 Gt/y (Devon Ice Cap, 0.5 Gt/y; Agassiz Ice Cap, 0.6 Gt/y; Otto Glacier (western Grant ice complex), 0.2 Gt/y; Prince of Wales Icefield, 1.9 Gt/y). As in Alaska, individual glaciers can dominate the regional flux estimates.

7.5.3.2.2. Surging

At least 51 surge-type glaciers have been identified in the Queen Elizabeth Islands (Copland et al., 2003). Of these, 15 were surging in 1959/1960 and/or 1999/2000. The largest recorded surge-type advances (4 to 7 km) were observed on Axel Heiberg Island and the Manson Icefield (Ellesmere Island). The active phase of the surge cycle of these glaciers may last more than a decade (Mueller, 1969; Copland et al., 2003), typical of 'Svalbard-type' surging (Mueller, 1969; Murray et al., 2003). Glacier velocities during the active phase of the surge cycle may range from several hundred metres to over 1 km per year. Because many of the known surge-type glaciers terminate in the ocean, surging may cause large short-term changes in the loss of mass to the oceans by iceberg calving. Little is known about the duration of the quiescent phase of the surge cycle in this region owing to the short period of observations.

7.5.3.3. Greenland (excluding the Greenland Ice Sheet)

Little is known about the history of area and volume changes of the roughly 48 600 km^2 of glaciers and ice caps that surround the Greenland Ice Sheet, or about their mass balance, calving discharge, or the fraction of their area drained through marine-terminating outlets. Mass balance estimates for these glaciers have been made (Dyurgerov and Meier, 2005) using correlated mass balance records from Svalbard and the Canadian Arctic Archipelago. Net losses from 1992 to 2002 are estimated to be about 18 Gt/y, but the fraction due to calving is completely unknown.

Figure 7.18. Hubbard Glacier, which drains into Russell Fjord in the Yakutat region of southern Alaska, is a surging tidewater glacier. Source: Anthony Arendt, University of Alaska.

7.5.3.4. Iceland

In Iceland, 26 surge-type glaciers and 80 surge advances have been identified (Björnsson et al., 2003), and surges account for a significant fraction of the mass transported by major outlet glaciers of all the main ice caps. Surges affected 38% of the area of Vatnajökull in the 1990s, and accounted for about 25% of the mass transfer from the accumulation zone of the ice cap to the ablation zone (Björnsson and Pálsson, 2008). Calving losses are unknown but probably not significant.

7.5.3.5. Svalbard

Glacier geometry, flow velocity, and front position changes of Svalbard glaciers were determined from ASTER images acquired in 2000 to 2006 (Błaszczyk et al., 2009). A total of 163 grounded tidewater glaciers drain an area of around 21 200 km^2 (more than 60% of the total glacier area of Svalbard) through a combined calving terminus length of 860 km.

7.5.3.5.1. Calving

Mass loss due to calving from the whole archipelago was initially estimated to be about 4 Gt/y for the period 1968 to 1998 (Hagen et al., 2003b), but a more recent estimate for the period 2000 to 2006 is 5.0 to 8.4 Gt/y, with a mean value of 6.75 ± 1.7 Gt/y (Błaszczyk et al., 2009). The mean retreat rate ($\partial x/\partial t$) of the calving glaciers is about 30 m/y, and terminus retreat ($\dot{M}_L$) accounts for about 30% (~2.1 Gt/y) of the total calving flux from the archipelago. Calving constitutes about 20% of the overall mass loss from Svalbard glaciers (Błaszczyk et al., 2009).

Dowdeswell et al. (2008) estimated the calving flux from Austfonna to be 2.5 ± 0.5 Gt/y from an aggregate terminus length of about 230 km. This represents 30% to 40% of the annual ablation from this ice cap. Terminus retreat reduced the ice cap area by about 10 km^2/y during the period 1991 to 2001 and accounted for about 50% of the calving loss.

7.5.3.5.2. Surging

Surge-type glaciers are very common in Svalbard and comprise a range of glacier types from small land-terminating cirque glaciers to large calving outlets. Although the overall fraction of surge-type glaciers is unknown, estimates range from 13% to 90% (Liestøl, 1969; Dowdeswell et al., 1991; Lefauconnier and Hagen, 1991; Hamilton and Dowdeswell, 1996; Jiskoot et al., 1998). Surging of marine-grounded outlets can interact with calving dynamics. The 1250-km^2 Hinlopenbreen calved about 2 km^3 of icebergs in a single year during a surge (Liestøl, 1973). Bråsvellbreen (1100 km^2) advanced up to 20 km along its 30-km marine-grounded margin during a surge in 1936 to 1938 (Schytt, 1969). In the inner part of Storfjorden, east Spitsbergen, Negribreen advanced about 12 km in less than a year (about 35 m/d) along a 15-km long section of its front during a surge in 1935 to 1936 (Liestøl, 1969). Recently, the tidewater glacier Nathorstbreen advanced about 7.6 km or about 20 m/d from September 2008 to September 2009 (Sund and Eiken, 2010).

7.5.3.6. Russian Arctic islands

7.5.3.6.1. Calving

Govorukha (1989) estimated calving fluxes of 1.8 Gt/y from Novaya Zemlya (1930 to 1960), 0.45 Gt/y from Severnaya Zemlya (1929 to 1972), and 2.1 Gt/y from Franz Josef Land during the period 1929 to 1959 (a total of 4.35 Gt/y). Using measurements of terminus ice thickness derived by radio echo sounding, ice surface velocities at glacier termini derived by radar interferometry, and measurements of terminus length and terminus advance/retreat, Glazovsky and Macheret (2006) estimated calving fluxes from the Russian Arctic islands to be 6.4 Gt/y for the period 1952 to 2001 (Novaya Zemlya = 1.4 Gt/y; Severnaya Zemlya = 0.7 Gt/y; Franz Josef Land = 4.3 Gt/y). Losses due to terminus retreat were estimated to be about 1.35 Gt/y, or roughly 21% of the total calving flux. It is not possible to determine the significance of the difference between the two calving flux estimates, so it should not be taken to imply a temporal trend in calving fluxes.

7.5.3.6.2. Surging

Surge-type glaciers are rare in the Russian Arctic Archipelago (Dowdeswell and Williams, 1997). None are known to exist in Franz Josef Land, while until recently only three had been identified in Novaya Zemlya and two in Severnaya Zemlya. However, a new analysis based on high-resolution satellite imagery identified 32 potential surge-type glaciers on Novaya Zemlya, representing 18% of the total glacier area (Grant et al., 2009). These glaciers are generally relatively long (median length 18.5 km), large (median area 106.8 km^2) outlet glaciers that terminate in water. They occupy large, complex catchment areas that may be receiving increased precipitation from the Barents Sea.

7.5.4. Recent ice shelf break-up events

Most of the largest floating ice shelves in the Arctic, fringing the northern coast of Ellesmere Island, are not predominantly glacier-fed, but form mainly by basal accretion of sea ice and surface accumulation of precipitation (Jeffries, 1992). They developed around 5500 to 3000 years BP (England et al., 2008) and have lost over 90% of their area during the 20th century, with only four major ice shelves now remaining. Much of the area loss occurred in the 1950s (Koenig et al., 1952) and 1960s (Hattersley-Smith, 1963, 1967). A new phase of disintegration began in 2000, with renewed fracturing of the Ward Hunt Ice Shelf (Mueller et al., 2003) and continued in 2005 with the abrupt loss of almost all of the Ayles Ice Shelf and major calving from the Petersen Ice Shelf (Copland et al., 2007). In summer 2008, the total ice shelf area in Arctic Canada decreased further (by 23% relative to 2007; Mueller et al., 2008) due to the loss of the entire Markham Ice Shelf and 60% of the area of the Serson Ice Shelf. As a result, several fjords on the northern coast of Ellesmere Island are now ice-free for the first time in 3000 to 5500 years (England et al., 2008). In 2010, large new fractures in the Ward Hunt Ice Shelf were first detected in Radarsat-2 images from 7 and 14 August. A MODIS image from 18 August shows that break-up of the eastern part of the ice shelf was underway (Figure 7.19), and some 65 to 70 km^2 of the shelf had been lost by the end of August. Meanwhile, fragments of the ice islands that calved from the Ayles, Serson, Peterson, Ward Hunt and Markham ice shelves in 2005 and 2008 have drifted into Canada Basin and the Sverdrup and Queen Elizabeth Islands and are beginning to enter the Northwest Passage via Barrow Strait.

Causes of ice shelf break-up appear to include rising summer air temperature and the loss of semi-permanent landfast sea ice along the northern coast of Ellesmere Island, although strong southerly winds seem to play an important role in individual break-up events. Ice shelf break-up events produce large 'ice islands' which may become a hazard to shipping and offshore resource exploration if they drift westward into the Beaufort Sea. They can also result in the drainage of epishelf lakes and the loss of their unique ecosystems (Veillette et al., 2008).

As with floating ice tongues, the loss of ice shelves does not directly influence sea-level rise. In the case of the Ellesmere ice shelves, because most of them do not interact with terrestrial glaciers, there is no indirect effect on sea level.

The Matusevich Ice Shelf in Severnaya Zemlya, the only major ice shelf in the Eurasian Arctic, has also undergone periodic calving events during roughly the past 70 years (Williams and Dowdeswell, 2001).

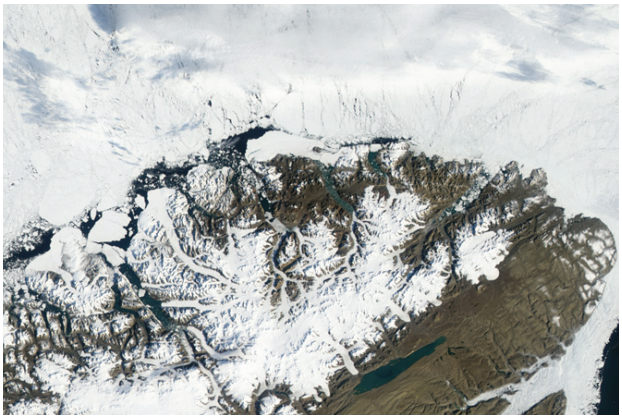

Figure 7.19. MODIS image from 18 August 2010 showing the Ward Hunt Ice Shelf, northern Ellesmere Island, and the extensive fracturing that had developed in the ice shelf to the east and south of Ward Hunt Island. Source: Canadian Ice Service.

7.5.5. Iceberg characteristics and relationship to ice dynamics

There are certain relationships between iceberg characteristics (size, number, morphological type) and parent glacier type and behavior. These relationships can be broadly described as follows (Dowdeswell, 1989; Dowdeswell et al., 1992):

- The largest tabular icebergs (large horizontal dimension relative to depth) are calved from floating glacier tongues and ice shelves. Horizontal sizes reach hundreds of metres to kilometres. The number of individual icebergs calved each year is usually small.
- Fast-flowing tidewater glaciers that are grounded have high rates of discharge, but often produce icebergs of relatively small size (tens to hundreds of metres) and irregular shape that tend to break up quickly into still smaller bergs and bergy bits (Dowdeswell and Forsberg, 1992) (Figure 7.20). Slower-flowing glaciers calve fewer icebergs, but their sizes may be larger than those of icebergs calved from more active glaciers.
- Surging glaciers and tidewater glaciers in rapid retreat tend to produce a very large number of small icebergs (10 to 50 m in length) with irregular shapes (Schytt, 1969). If such glaciers start to float, however, the mode of calving may change to one in which episodic flow-perpendicular rift formation and propagation result in the release of a few very large icebergs (Walter et al., 2010).

The systematic classification of iceberg types made by Dowdeswell for glaciers of Spitsbergen can be applied to all sources of icebergs in the Arctic. It is supported by descriptions of icebergs made at different times near Spitsbergen, Franz Josef Land, and Novaya Zemlya (Sandford, 1955; Kubyshkin et al., 2009), and by observations in the northern Barents Sea in 2003 to 2007. For example, tidewater outlet glaciers in Russkaya Gavan Bay and Inostrantsev Bay in northern Novaya Zemlya have strong fracturing of the front and produce a moderate quantity of small- and medium-sized icebergs of irregular shape (Buzin and Glazovsky, 2005). Floating margins on some of the larger ice caps of Franz Josef Land produce large tabular icebergs (Dowdeswell et al., 1994; Zubakin et al., 2007).

Figure 7.20. Small iceberg off the coast of Franz Josef Land. Note the debris-rich layers within the iceberg. Source: Photo courtesy of Arctic-shelf laboratory, AARI.

7.5.6. Controls on calving fluxes

Although the detailed physics of iceberg calving are poorly understood, certain controlling factors can be identified. The tensile strength of ice is strongly dependent on temperature, and temperate ice (ice at its pressure melting point, where water and ice exist in thermal equilibrium) has essentially no tensile strength (Schulson, 1999). Along-flow extension or compression of ice influences the opening or closing of transverse crevasses, but no clear relationship between calving rate and along-flow strain rate has been demonstrated observationally on meaningful timescales (Alley et al., 2008). A statistical relationship between water depth at grounded glacier termini and calving rate has been demonstrated (Brown et al., 1982), but this relationship is purely empirical and possibly applicable only to calving margins near steady-state. Sea ice, floating brash ice, and iceberg debris can exert substantial restraining forces (or back stresses) that are transmitted to the fjord walls and inhibit calving (Amundson et al., 2010). The presence or absence of a moraine shoal at the terminus providing resistive back stress against extension of ice in the direction of flow has a strong influence on calving rate (Meier and Post, 1987; Fischer and Powell, 1998; Nick et al., 2007). However, it is unclear whether the detachment of a glacier terminus from its terminal moraine is a cause or a consequence of thinning and retreat.

7.5.7. State of theory and modeling

A number of attempts have been made to formulate calving models, but there is still no universal theoretical framework that can explain the full suite of available observations. Using data from twelve Alaskan glaciers, Brown et al. (1982) proposed an empirical linear relationship between the calving rate and the water depth at the terminus. However, the correlation is not broadly applicable because there is no obvious physical control that can explain any depth dependency of the calving rate (Benn et al., 2007). A drawback to such empirical models is that they are often based on data from glaciers that are either in or near a steady-state (Van der Veen, 1996). Indeed, based on observations at Columbia Glacier in Alaska, Meier and Post (1987) suggested that a linear calving relationship might not be valid during periods of rapid advance or retreat. Various approaches to a mechanically based process model of calving have been pursued since the mid-1960s, based on several different lines of analysis. These include, most notably, an elastic bending beam model developed by Reeh (1968), analyses of crevasse penetration with and without water (Nye, 1957; Weertman, 1973), and analyses based on linear elastic fracture mechanics (Van der Veen, 1998a,b). Other observations and analyses include work by Holdsworth (1969) and Hughes (1992).

Based on observations from Columbia Glacier, Van der Veen (1996) proposed a flotation model, wherein the terminus of the glacier retreats to the position where the ice thickness exceeds the flotation thickness by some threshold value, H_0. On Columbia Glacier, H_0 was determined to be about 50 m. Vieli et al. (2001) pointed out that for smaller glaciers (water depths below 150 m and flow velocities less than 200 m/y), frontal cliff heights do not usually exceed 50 m, so the height above flotation will be much less than was suggested for Columbia

Glacier. As a result, they proposed a modified flotation criterion, with the minimum height above flotation, H_0, replaced by a fraction, q, of the flotation thickness at the terminus. Benn et al. (2007) noted that one significant weakness of flotation models is that they do not allow floating termini to form, thus limiting their use to certain types of calving margins. As a result, they proposed a new criterion based on a simple model of crevasse formation, in which the calving margin is located where crevasse depth is equal to the glacier surface height above sea level, and the determination of the calving rate is reduced to determining ice thickness, velocity distribution, and changes in thickness and velocity through time.

Hanson and Hooke (2000) treated calving as a multivariate problem, using water depth, longitudinal strain rate, and ice temperature as the primary factors controlling the calving rate. Nick and Oerlemans (2006) compared the water depth and flotation models using synthetic simplified glacier geometries and found the latter to be superior, but they failed to simulate a full cycle of glacier length variations when the glacier terminates in very deep water. Nick et al. (2007) elaborated on their model by including a simple sediment transport scheme in the ice flow model and concluded that sedimentation at the glacier front needs to be included for the glacier to advance into deepening water.

Most calving models presented to date are either wholly empirical or based on mechanics. Other englacial processes, including glacial hydraulics, have not been incorporated, although there is evidence that water flow along cracks may play an important role in the calving process (O'Neel and Pfeffer, 2007).

No validated, broadly applicable, and robust calving model exists at this point. The calving relationships and models proposed so far have been tailored and applied to specific glaciers and data sets, and the proposed models tend to require data that are not readily available on regional scales. Larger models, either focused glacier/ice sheet models or comprehensive coupled GCMs, tend to include calving only in an extremely simplistic fashion (e.g., specifying a fixed calving boundary location) or do not treat calving at all. Hence, there is a pressing need for robust calving formulations of intermediate complexity that are capable of being applied in a wide variety of settings and for regional-scale mass change predictions. There is also a need for the basic data required to constrain models based on such a formulation.

7.5.8. Requirements for improved predictions of calving fluxes

Because calving can deplete terrestrial ice reservoirs very rapidly, calving dynamics are a key element in understanding and predicting the mass balance and sea level rise contributions of all glaciers, ice caps, and ice sheets with calving margins. Knowledge of present-day calving rates is extremely limited owing to a lack of fundamental observations. Since changes in flow dynamics and calving are not controlled directly by externally observed variables (such as climate), robust predictions depend on an understanding of glacier physics that is still lacking and on observations that can be difficult to make. The most fundamental observations needed to better constrain potential calving losses are (i) more complete observations of calving rate and marine-ending terminus changes, and (ii) radio echo sounding of ice thicknesses and basal topography to identify marine-grounded outlets and the marine-grounded fractions of glacier and ice cap areas. Without these measurements, the potential for dynamically forced calving losses cannot be constrained let alone predicted.

7.6. Projections of Arctic glacier changes

- Most attempts to simulate the response of Arctic glaciers to future climate change involve evaluation of the response of the surface mass balance to prescribed changes in climate (usually air temperature and precipitation); simulations generally do not include changes in glacier dynamics or mass loss by iceberg calving. Climate change can be imposed as either step changes from an initial state or as transient changes over some period of time derived from climate models.
- Projections for individual glaciers throughout the Arctic show substantial mass loss or even disappearance of smaller glaciers by the end of the 21st century in response to imposed temperature and precipitation scenarios.
- Very few studies have attempted to model the response of Arctic glaciers on larger scales. A new simulation of the surface mass balance of the global population of mountain glaciers and ice caps to 2100 uses a temperature index mass balance model driven by downscaled output from ten GCMs, all forced by the IPCC A1B emissions scenario. For Arctic glaciers, projected volume loss due to surface mass balance ranges between 0.051 to 0.136 m sea-level equivalent, or 13% to 36% of their current volume by 2100 depending on the choice of GCM. Most models suggest that the largest mass losses are from glaciers in Alaska and Arctic Canada.

7.6.1. Downscaling climate model projections

General circulation models (Solomon et al., 2007) driven by standardized IPCC emissions scenarios (B1, A2, A1B; see Chapter 3) generally predict that warming and precipitation increases in the Arctic beyond 2030 will be larger than the global mean (Chapman and Walsh, 2007; Kattsov et al., 2007). Only part of the projected increases in precipitation will lead to increases in snow accumulation because the fraction of precipitation falling as rain will increase with the projected air temperature increases.

Direct use of data from GCMs for glacier mass balance projections is not currently feasible, owing to the generally large biases in model data on regional scales. Individual glaciers are typically much smaller than climate model grid boxes, and often occupy complex terrain that is only coarsely resolved in the model's underlying topography. Mass balance modeling is particularly sensitive to biases and offsets in air temperature, which controls the energy available for melt and the snow-rain ratio of precipitation (and thus controls both ablation and accumulation). Hence, some form of downscaling is required to transfer global-scale climate information to local glacier scales prior to making glacier mass balance projections.

Statistical downscaling is often used, whereby statistical relationships are established between meteorological

quantities determined at the GCM and the local scales. This can be done using either field observations or other suitable meteorological data such as data from climate re-analyses. Radić and Hock (2006) applied 'local scaling' to correct for the biases in climate model air temperature and precipitation for projecting the mass balance of Storglaciären until 2100. Downscaled temperature series were produced from GCMs and regional climate models (RCMs) by shifting the series by the averaged monthly differences between climate model and local-scale data (here ERA-40 re-analysis data) over a baseline period for which both GCM and local-scale data were available. Hence, the average seasonal cycle from ERA-40 was used as a reference by which seasonal cycles from the climate model could be 'corrected'. The results highlight the importance of including seasonally varying biases in the downscaling instead of assuming a constant bias throughout the year. Precipitation was scaled by the ratio of precipitation in the reference data set (here ERA-40) summed over the baseline period and the corresponding climate model precipitation sum. A drawback of statistical downscaling is the inherent assumption that the statistical relationships established over a baseline period will continue to hold in future climates.

An alternative approach to statistical downscaling is to use changes in GCM variables between a defined time slice in a GCM simulation of future climate and a baseline period corresponding to a period for which local climate data are available. These changes are then used to perturb the observed local climate data to drive a mass balance model and project future mass balance changes (e.g., Schneeberger et al., 2003). The changes in climate variables are often simply linearly interpolated between time slices to allow for transient simulations. Due to generally large interannual variability, however, projected climate variable changes can be sensitive to the choice of baseline period. This is especially true when large fluctuations occur around the baseline period or when the climate variable shows a trend during this period (Aðalgeirsdóttir et al., 2006).

Zhang et al. (2007a) used a dynamical downscaling approach, employing the high resolution regional model Polar MM5 driven by global atmospheric re-analysis to obtain temperature and precipitation data on a 10-km resolution grid to force a glacier mass balance model. The results of mass balance simulations using dynamically downscaled data and simulations based on observed temperature and precipitation data were in reasonably good agreement when calibration was used to minimize systematic biases in the MM5 downscaling.

7.6.2. Modeling mountain glacier and ice cap mass balance in the 21st century

While numerous studies have projected the response of individual glaciers to climate change, very few studies have attempted to project the response of Arctic glaciers on a regional scale. Zhang et al. (2007b) used dynamically downscaled daily maximum and minimum air temperatures and precipitation driven by the IPCC A1B emissions scenario of the CCSM3 climate model to force a temperature-index mass balance model for Hubbard Glacier (2460 km^2) and Bering Glacier (3630 km^2) in Alaska for the period 2010 to 2018. Both glaciers are projected to have increased accumulation, particularly on the upper reaches of the glaciers, and increased ablation, particularly on the lower parts. The modeled mass balance of Bering Glacier is projected to become more negative on average (-2.0 m w.e./y compared to -1.3 m w.e./y during the 1994 to 2004 baseline period) and the modeled mass balance of Hubbard Glacier, which was positive during the baseline period, is projected to decrease slightly (to 0.3 m w.e./y from 0.4 m w.e./y).

Hock et al. (2007a) modeled cumulative mass balance changes of the 3 km^2 Storglaciären in Sweden until 2100 in response to model-projected regional temperature changes. They predicted total changes ranging from -81 to -121 m w.e., depending on the choice of the mass balance model. A fully distributed energy balance melt model produced a greater mass balance response than simpler temperature-index models. Projections based on the IPCC B2 emissions scenario showed a 50% to 90% decrease in ice volume by 2100 (Radić and Hock, 2006) (Figure 7.21). The volume change projections vary by 40% of the initial ice volume for six different GCM inputs to the mass balance model, and by 10% depending on the details of the mass balance model used. This is in agreement with the conclusion of Oerlemans et al. (2005) that the uncertainties due to a simple representation of glacier processes are less than those associated with the output from GCMs.

Huss et al. (2008) modeled the complete disappearance of the 4.4 km^2 Laika Glacier in Arctic Canada by 2100 in response to temperature and precipitation trends derived from a climate model forced by the IPCC A1B emissions scenario. Bassford et al. (2006) modeled complete wastage of Pioneer Ice Cap (~200 km^2) and Vavilov Ice Cap (~1770 km^2) on Severnaya Zemlya within about 370 and about 1080 years, respectively, by imposing a linear change in temperature and precipitation over the period 1990 to 2100 based on the IPCC IS92a 'business-as-usual' scenario, after which the climate was held constant. Although these ice caps have quite low static sensitivities of mass balance to changes in temperature and precipitation, they are nonetheless highly sensitive to long-term climate change owing to their hypsometry and location on relatively flat beds close to sea level.

Ananicheva and Krenke (2007) modeled mass changes of 17 glacier regions in northeastern Siberia and Kamchatka (1040 km^2) for the period 2040 to 2069 using climate projections from the ECHAM4 GCM driven by the IPCC A2 emissions scenario. The equilibrium-line altitude (ELA) on these glaciers is predicted to rise by 230 m in the northern parts and 500 m in the southern parts of northeastern Siberia. The upward shift is largest in Kamchatka. Based on known correlations between the ELA and the elevation of the glacier terminus, only 22% and 31% of the glacier areas are predicted to remain in northeastern Siberia and Kamchatka, respectively, in 2070 (Ananichava et al., 2010).

On larger regional or global scales, mass changes have been projected using either an 'indirect' approach based on mass balance sensitivity, defined as the change in mass balance caused by an instantaneous change in a climatic variable such as air temperature or precipitation, or a 'direct' approach based on transient mass balance modeling. The indirect approach involves computation of sensitivities, often for each month individually ('seasonal sensitivity characteristic'; Oerlemans and Reichert, 2000), which are used to calculate the change in

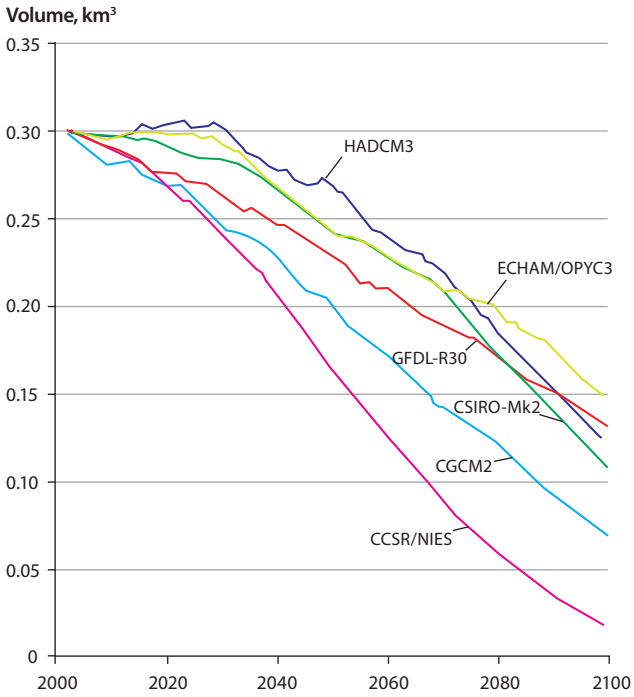

Figure 7.21. Volume projections for Storglaciären, Sweden, in the 21st century derived from six general circulation models (GCMs). Source: Radić and Hock (2006).

surface mass balance for given anomalies of temperature and precipitation. Mass balance sensitivities are determined for individual glaciers by energy balance or temperature-index modeling. Mass balance sensitivities to temperature computed on a 1° by 1° grid exhibit large spatial variations across the Arctic, with the largest sensitivities in Iceland, southern Greenland, and coastal Alaska, and the smallest sensitivities in Arctic Canada and northern Greenland (Hock et al., 2009; Figure 7.22).

Applying a regression-based temperature index model to 42 glaciers located north of 60° N, de Woul and Hock (2005) found that the mass balance sensitivity to a hypothetical temperature increase of +1 K ranged from -0.2 to -2.0 m/y. Sensitivity of the mass balance to a 10% increase in precipitation ranged from < +0.1 to +0.4 m/y. This offset the effect of a +1 K temperature increase by about 20% on average. Maritime glaciers had considerably higher mass balance sensitivities than continental glaciers. Results were extrapolated to the entire Arctic by assuming area-weighted means of sensitivity to be representative for different Arctic regions. The estimated total contribution to sea level from Arctic glaciers (including the Greenland Ice Sheet) in response to a +1 K warming was about +0.6 mm/y. This compares to an estimate of +0.53 mm/y derived using a sensitivity approach that suggested about equal contributions from the Greenland Ice Sheet and the Arctic glaciers (Oerlemans et al., 2005).

Radić and Hock (2011) computed global mass balance and volume changes for more than 120 000 mountain glaciers and roughly 2600 ice caps around the world until 2100 using an elevation-dependent temperature-index mass balance model driven by output from ten GCMs forced by the IPCC A1B emissions scenario. Future volume changes were up-scaled to all glaciers using a regionally differentiated approach. For the Arctic glaciers (including those in Greenland surrounding the ice sheet), the projected volume loss due to melt (ablation by calving is not included) ranges from 51 to 136 mm sea-level equivalent (SLE) (i.e., 13% to 36% reduction in their current volume by 2100) depending on the choice of GCM (Figure 7.23). The multi-model mean is 88 ± 28 mm SLE, or 22% ± 7% volume reduction where the uncertainty range is ±1 standard deviation. Multi-model mean volume reductions by 2100 (relative to initial volumes) vary considerably among regions, with the smallest values in Greenland (8% ± 5%) and the largest values in Svalbard (54% ± 15%); however, the spread among models for most regions is large (Figure 7.23). Most models show the largest sea level contributions coming from the Canadian Arctic and Alaska (including the Yukon), followed by the Russian Arctic and Svalbard. Contributions from Arctic Canada show a very large range from less than 10 mm SLE contribution to the largest projected contribution for any of seven Arctic regions, indicating a large spread in the projected temperature and precipitation fields among the GCMs for this region (Figure 7.24).

7.6.3. Modeling ice dynamics and ice extent

Glacier size and geometry will change as a glacier responds to climate change. Hence, projections of glacier mass balance on timescales longer than a few decades need to take into account feedbacks between the mass balance and the changing glacier surface elevation.

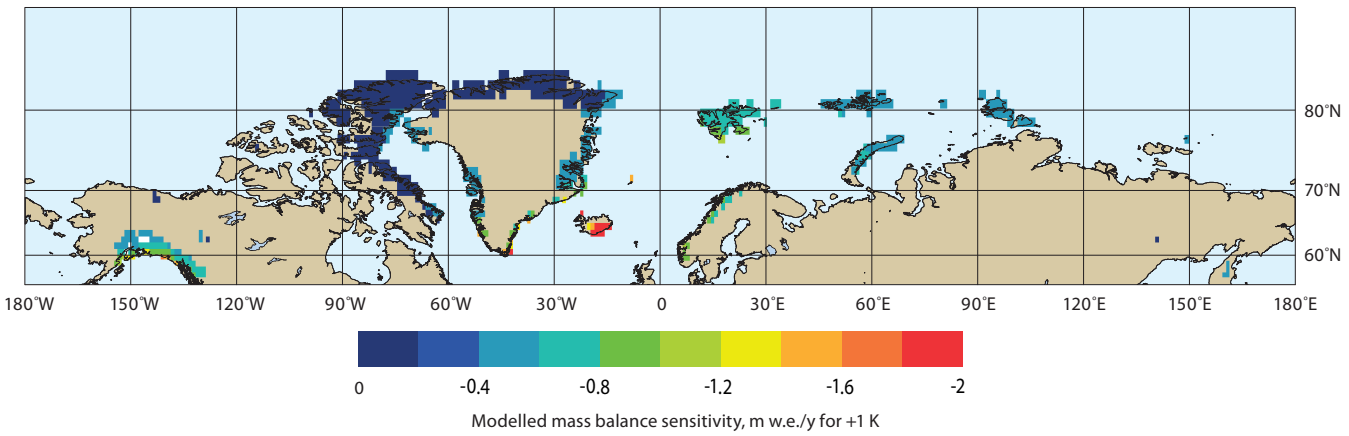

Figure 7.22. Modeled mass balance sensitivity, that is, the change in specific mass balance owing to a 1 K uniform warming. Source: Hock et al. (2009).

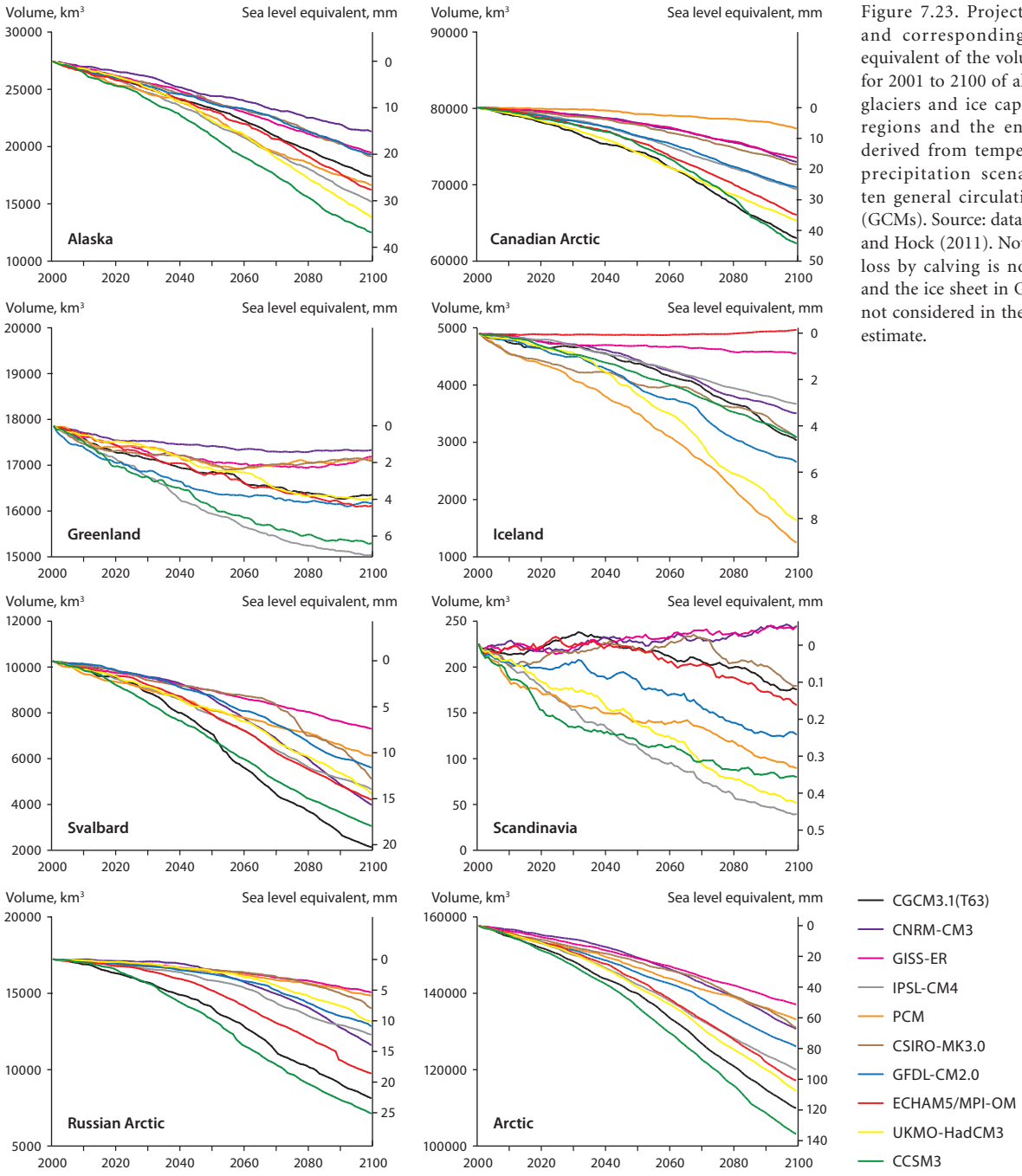

Figure 7.23. Projected volume and corresponding sea level equivalent of the volume change for 2001 to 2100 of all mountain glaciers and ice caps for seven regions and the entire Arctic derived from temperature and precipitation scenarios from ten general circulation models (GCMs). Source: data from Radić and Hock (2011). Note that mass loss by calving is not included and the ice sheet in Greenland is not considered in the Greenland estimate.

Ice flow models have been used to simulate area and thickness changes of individual glaciers (e.g., Schneeberger et al., 2003; Aðalgeirsdóttir et al., 2006). However, the detailed input data required to run such models are often not available. As a result, the effects of area changes are either simply neglected (e.g., Oerlemans et al., 2005; Zhang et al., 2007b) or approximated by scaling methods based on a functional relationship between glacier volume and glacier area (e.g., Radić and Hock, 2006). The total glacier volume is adjusted annually according to the volume changes computed from a climate-driven mass balance model. Annual area changes are then computed by inverting the volume-area relationship. Based on modeling of eleven glaciers, Schneeberger et al. (2003) showed that volume loss is overestimated by about 20% in a 100-year simulation if changes in glacier geometry are not included in the projections.

Detailed ice dynamic modeling is currently not possible on a regional scale due to a lack of the required data to run models for the vast majority of glaciers. Raper et al. (2000) developed a geometrical approach, in which the width, thickness, and length of a glacier are reduced as its volume and area decline. When applied statistically to the global population of glaciers and individually to ice caps, this approach shows that the reduction in glacier area strongly reduces ablation during the 21st century (Raper and Braithwaite, 2006). The reduction is about 45% under the IPCC A1B emissions scenario using output from two different GCMs.

A large number of glaciers in the Arctic terminate in the ocean and, therefore, lose mass through iceberg calving in addition to surface melting. Studies on a few Arctic marine-terminating ice caps (Dowdeswell et al., 2002, 2008; Burgess et al., 2005; Mair et al., 2009) indicate that calving may account for roughly 30% to 40% of total mass loss. However, model-

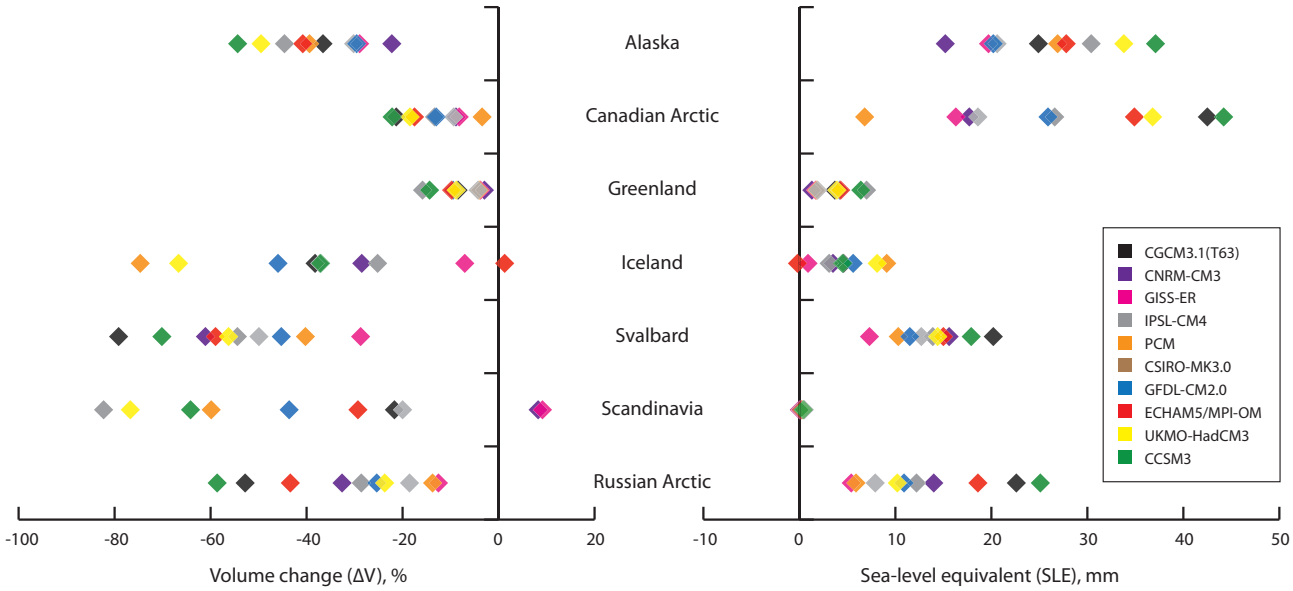

Figure 7.24. Projections of fractional volume change and sea level equivalent of the volume change by 2100 for seven regions that include all Arctic glaciers. Projections are based on temperature and precipitation modeled by ten general circulation models (GCMs). Source: Radić and Hock (2011).

based projections on regional scales neglect this effect. The current state-of-the-art in modeling does not allow meaningful projections of calving losses. However, calving rates are likely to increase as surface melting increases (Oerlemans et al., 2005).

7.7. Impacts of changes in mountain glaciers and ice caps

- The recent acceleration of mass loss from mountain glaciers and ice caps in the Arctic is such that, together with the Greenland Ice Sheet, they are likely to account for more than 60% of the current glacier wastage contribution to global sea level rise.
- Glacier wastage is likely to increase inputs of freshwater, sediment, and some nutrients to Arctic coastal waters, with potential impacts on water mass circulation, biological productivity, and ecosystem structure in affected fjord and nearshore marine environments.
- Retreat of tidewater glaciers onto land may be removing important feeding habitats that exist for seabirds and marine mammals in regions of upwelling in front of tidewater glacier termini and reducing the occurrence of grounded bergy bits that are used by seals for resting.
- Icebergs are a hazard to shipping and offshore platforms in the Arctic. The number and size distribution of bergs produced may change as tidewater glaciers retreat (e.g., more large bergs if floating ice tongues and ice shelves break up; more smaller bergs if calving from fast-flowing outlets increases). The way they circulate in Arctic waters is likely to change if sea-ice cover continues to decrease and surface water temperatures rise as a result. Bergs may become more mobile in summer as the restraining effect of sea ice declines, but disintegrate more rapidly in warmer surface waters.
- As climate warms, glacier runoff initially tends to increase due to higher melt rates, but ultimately declines as glacier area shrinks. In most regions of the Arctic, the phase of declining runoff does not yet seem to have begun, but it may begin soon in the Russian Arctic mountains.
- Changes in glacier runoff will ultimately impact the viability of hydroelectric power operations in the Arctic. They will also be associated with changes in stream temperature, sediment load, and nutrient content that will initiate changes in the ecology of downstream river and lake environments.
- As rates of mass loss increase, 'legacy pollutants' stored in firn and glacier ice will be released back into the environment.
- As glaciers retreat, there are likely to be changes in the magnitude and frequency of a range of geomorphological hazards, including mass movements from deglaciated valley walls and outburst floods from ice-marginal and proglacial (moraine-dammed) lakes.

7.7.1. Impacts on sea level

In the most recent decade for which mass balance data were available for all regions (1996 to 2006), Dyurgerov and Meier (2005) reported that Arctic glaciers collectively lost mass at a rate of 165 Gt/y (0.45 mm/y sea-level equivalent; SLE). The dataset compiled by Cogley (2009a) yields a loss rate of 180 Gt/y (0.5 mm/y SLE) for the decade 1995 to 2005, and a loss rate of as much as 282 Gt/y (0.75 mm/y SLE) for the 2000 to 2005 pentad (see Section 7.9 for a more extended discussion). For comparison, Rignot et al. (2008) calculated a mass loss from Greenland of 267 Gt/y (0.71 mm/y SLE) for 2007. These results suggest that, together, Arctic glaciers and the Greenland Ice Sheet may account for more than 60% of the current glacier wastage contribution to global sea level rise (2.1 mm/y; Cazenave et al., 2009).

The acceleration of mass loss from Arctic glaciers and ice caps for the period 1985 to 2003 calculated using data from Dyurgerov and Meier (2005) is -7.3 km^3/y^2 ice equivalent, or 6.5 Gt/y^2 (0.02 mm/y^2 SLE) (Figure 7.25). Note that at this rate

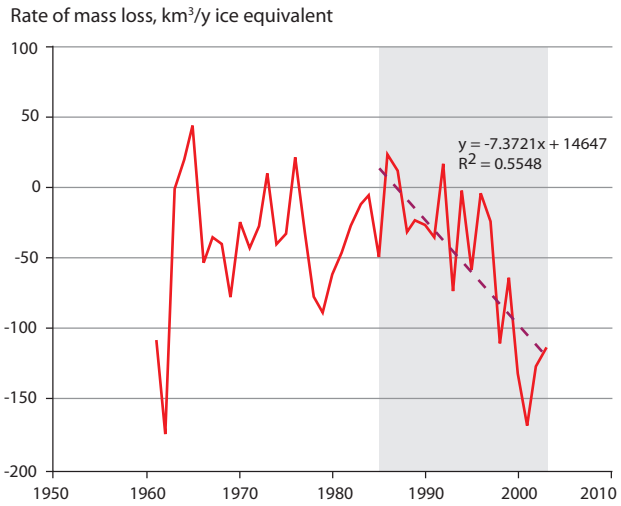

Figure 7.25. Rate of volume loss from Arctic glaciers and ice caps, derived from Dyurgerov and Meier, (2005). Source: AMAP.

of acceleration the estimated reservoir of mountain glacier and ice cap sea-level equivalent of 0.41 m (Radić and Hock, 2010) is being drawn down by only about 0.2% per year. While the current trend cannot be reliably extrapolated any significant distance into the future, depleting the reservoir is unlikely to result in a decline in annual total balance for at least the next several decades.

Analysis of the Cogley (2009a) dataset yields an estimate of mass losses from the glaciers surrounding the Greenland Ice Sheet of about 35 to 45 Gt/y for the 2000 to 2005 pentad. Some methods used to assess the mass balance of the Greenland Ice Sheet, such as most GRACE gravimetric observations, account for these losses, while other methods, such as satellite altimetric and mass flux observations, do not. It is therefore important, when combining mass loss estimates from this chapter with those in Chapter 8 on the Greenland Ice Sheet, to identify which glaciers are included in each particular method to avoid double counting.

7.7.2. Impacts on the marine environment

7.7.2.1. Freshwater and associated chemical fluxes

Glacier runoff is projected to increase in many parts of the Arctic for a period of decades or longer before declining (see also Section 7.7.3). This increased freshwater flux will influence conditions in coastal and marine waters. In fjords, freshwater discharge in summer produces a stable surface layer with low salinity (e.g., Svendsen et al., 2002), an effect that would be intensified with accelerated glacier melt. In the Gulf of Alaska, the majority (78%) of freshwater discharge occurs via a large number of smaller rivers and streams rather than a small number of point sources (Neal et al., 2010), producing baroclinic transport along the coast that is modified by wind stress (Royer, 1982). This along-coast transport is a major source of freshwater to the Bering Sea shelf and the Arctic Ocean (Weingartner et al., 2005). Runoff from glaciers and icefields contributes about half of the freshwater discharge to the Gulf of Alaska, with 10% currently from wastage (Neal et al., 2010). Because the magnitude of baroclinic transport varies with freshwater flux, future changes in glacier runoff volume and timing will have significant implications for the strength of the Alaska Coastal Current, associated marine ecosystems, and economically valuable fisheries.

In addition to changes in freshwater flux, changes in material export may influence coastal and marine ecosystems. Hood and Scott (2008) monitored three streams in southeastern Alaska and found that decreasing glacier cover was associated with decreased phosphorus export and increased export of nitrogen and dissolved organic matter, although with a decrease in the more labile forms of organic matter. Nitrogen export increases in the early stages of vegetation succession on deglaciated forelands due to the establishment of nitrogen-fixing species such as alder, but is likely to decrease with the later establishment of other species such as conifers.

Increased glacier melt may be associated with increased sediment loads, which would increase turbidity in coastal waters. Increased turbidity would reduce the penetration of solar radiation, including harmful UV-B radiation, with implications for primary production and ecosystem functioning (Hanelt et al., 2001; Erga et al., 2005).

7.7.2.2. Seabird and marine mammal habitat

Tidewater glacier fronts are known to be 'hot spots' for seabirds and marine mammals in many Arctic areas. In Svalbard, a strong preference for these habitats has been identified for ringed seals (*Phoca hispida*) and beluga (*Delphinapterus leucas*) during summer and autumn (Lydersen et al., 2001; Freitas et al., 2008). Individuals of both species spend significant amounts of their time in proximity to tidewater glacier fronts, and their diving behavior in these areas suggests that they are feeding in these locations, which are known to be areas of high productivity. Enhanced production in these areas is probably due to freshwater outflows that drive upwelling of deep water close to glacier fronts, bringing nutrients to the surface and stimulating phytoplankton blooms and zooplankton growth. In addition, the cold-water outflows from the glaciers may stun or kill invertebrates, thus attracting predators such as polar cod (*Boreogadus saida*) and capelin (*Mallotus villosus*) that are an important part of the diet of beluga and ringed seal (Dahl et al., 2000; Labansen et al., 2007), as well as a variety of seabirds and other marine mammals. In addition, ringed seals, bearded seals (*Erignathus barbatus*), and other pinnipeds use bergy bits as resting platforms. Retreat of tidewater glacier fronts onto land would decrease the availability of this preferred habitat at a time when decreases in late summer sea-ice extent are making the other preferred summer feeding habitats of Arctic pinnipeds less available. In addition, changes during glacier retreat in the lability of organic matter and the amount and types of nutrients that are delivered from land to the marine environment in meltwater runoff may reduce the productivity of these environments and their attractiveness to marine mammals and seabirds.

7.7.2.3. Iceberg production and drift

In some Arctic and sub-Arctic offshore areas, icebergs present a significant danger for marine operations including shipping

and commercial fisheries, geological exploration surveys, and production of hydrocarbons from sea surface structures such as oil rigs (Figure 7.26). The Grand Banks of Newfoundland, the Labrador Sea, offshore of West Greenland, Davis Strait, and the Barents Sea are typical examples of such areas. Damage to or even destruction of a stationary platform or its communication lines by an iceberg will result in enormous economic losses and possibly significant environmental damage. Both iceberg plan form and keel depth are important quantities to measure in this context (Woodworth-Lynas et al., 1991). Non-stationary platforms and other floating structures (e.g., floating production, storage, and offloading systems), capable of leaving their operation localities, will limit economic losses owing to interruption of hydrocarbon production for the period of shutdown due to iceberg threat.

The general direction of the drift of icebergs near the Labrador coast and the Grand Banks of Newfoundland coincides with the direction of a strong Labrador Current. Iceberg trajectories and the most dangerous drift directions are known. Over the past few decades, Canada has gained significant experience in minimizing iceberg threats and has introduced a complex system of operational practices known as the Iceberg Management System.

Currents in the Barents Sea carry icebergs from the north to the southwest (Johannessen et al., 1999; Dmitriev and Nesterov, 2007). Some may enter the central and southern regions of the area, threatening navigation and operations in the *Shtokman* gas-condensate field. An analysis of atmospheric conditions at the time of the southernmost spreading of icebergs (e.g., 1881, 1929, 1989, and 2003) has revealed that all cases were characterized by prolonged periods (three to five months) of winds from the north (Buzin et al., 2008). Under such conditions, large numbers of icebergs concentrated near Spitsbergen and Franz Josef Land (their source) are exported southward. In some years (1989, 2003), icebergs reached the *Shtokman* gas-condensate field area and in particularly extreme cases (1881, 1929) reached the coast of northern Norway and the Kola Peninsula. Sightings of an anomalously large concentration of icebergs and bergy bits (around 100 pieces) in the *Shtokman* gas-condensate field area in May 2003 (Naumov et al., 2003) significantly influenced the design concept for the production complex. The boundary of iceberg drift in the Barents Sea has been displaced to the south over the past 60 years (Zubakin et al., 2006; Buzin et al., 2008), probably related to climate warming and a corresponding increase in the production of icebergs (Figure 7.27). The tendency for the ice edge in the Barents Sea to be displaced toward the north in summer during the past 10 to 15 years (Divine and Dick, 2006) may result in earlier and easier release of icebergs stuck in the straits of Franz Josef Land. Consequently, a larger number of icebergs may be in free drift and represent a threat to shipping and platforms. However, the life expectancy of the icebergs also may be reduced in a warmer climate (Weeks and Campbell, 1973).

The iceberg discharge from the Greenland Ice Sheet is known to have increased by more than 40% from 1995 to 2005 (Rignot and Kanagaratnam, 2006). This has not, however, increased iceberg numbers on the Grand Banks or in the Labrador Sea. The number of icebergs reaching the Grand Banks has actually decreased, probably owing to increased surface water temperatures in the region and decreased ice cover (which protects icebergs from the dynamic impact of ocean waves) (McClintock et al., 2007). However, potential iceberg damage to sea-floor engineering structures is a function of iceberg keel depth as well as iceberg number. Icebergs with keel depths greater than 500 m have been observed in the Scoresby Sund fjord system of East Greenland, but few other systematic measurements of the keel depth of Arctic icebergs exist (Dowdeswell et al., 1992). The occurrence of recent plow marks on the sea floor, produced where drifting icebergs go aground, is evidence of this natural hazard, although many plow marks on Arctic continental shelves are not produced by modern icebergs (Dowdeswell et al., 1993; Syvitski et al., 2001).

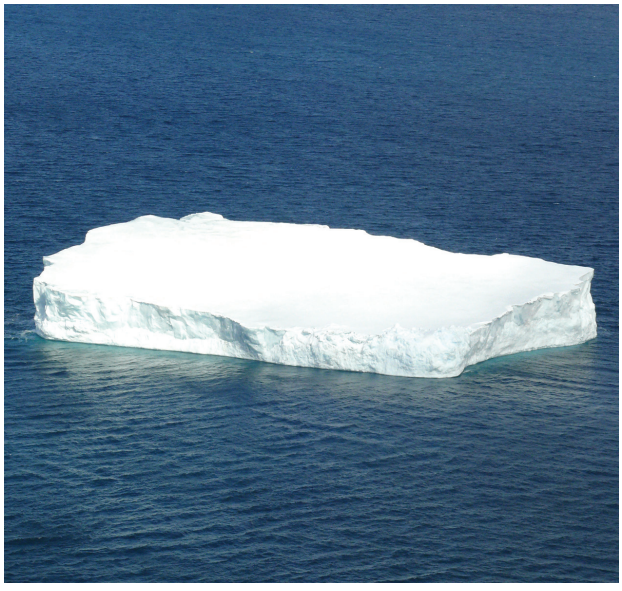

Figure 7.26. Large iceberg (100 m length, 30 m width, and 15 m height above sea surface) drifting in the Barents Sea to the southwest of Franz Josef Land on 30 May 2009. Source: Andrey Masanov, Arctic and Antarctic Research Institute, Russian Federation.

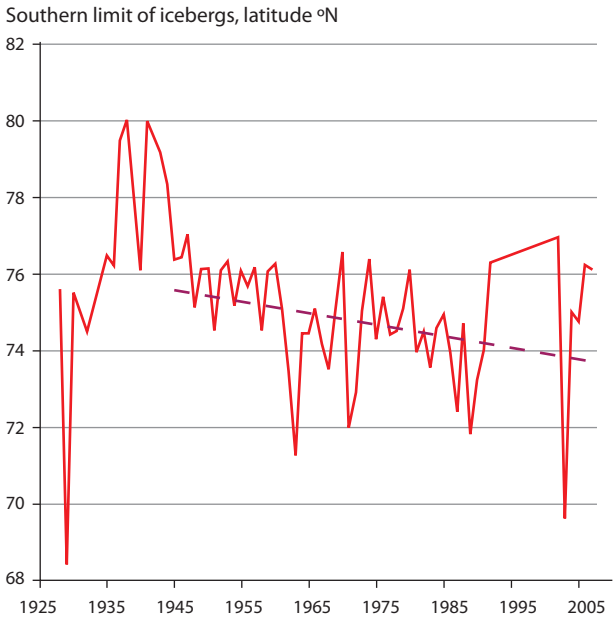

Figure 7.27. Multiyear variability of the southern limit of icebergs in the Barents Sea for the period 1928 to 2008. Source: Buzin et al. (2008).

7.7.3. Impacts on water resources

7.7.3.1. Glacier runoff

Streamflow in glacier-fed streams tends to peak later in the summer and to continue to exhibit diurnal fluctuations later in the melt season than streamflow in nival (snowmelt-dominated) streams (Church, 1974). However, the contrast between nival and proglacial regimes can be obscured by the weather patterns dominating the particular melt season, particularly when melt begins later than normal (Marsh and Woo, 1981). Research in temperate areas and in the Arctic indicates that detectable glacier melt contributions to streamflow occur in catchments with more than about 5% glacier cover, while contributions to summer flow are detectable even in catchments with as little as 2% glacier cover (e.g., Marsh and Woo, 1981; Stahl and Moore, 2006). Based on these criteria, glaciers are an important water resource throughout much of the Arctic.

Over annual or longer timescales, the influence of glaciers on streamflow can be assessed through the catchment water balance, which can be expressed as follows:

$$[1] \quad Q = P - E - f_g B + GW_{net} - \Delta S$$

where Q is streamflow, P is precipitation, E is evapotranspiration (including sublimation), f_g is the fractional glacier area within the catchment, B is the net mass balance for the glaciers, GW_{net} is the net flux of groundwater across the catchment boundaries, and ΔS represents changes in storage of seasonal snow, subsurface water, and surface water. All terms in [1] are typically expressed as a depth of water averaged over the catchment area. Negative net mass balance (glacier loss) augments streamflow relative to a basin lacking glacier cover. This contribution to streamflow ($f_g B$) is commonly referred to as 'wastage runoff'.

Table 7.3 highlights the contributions of glacier wastage (negative mass balance) to mean annual streamflow over recent decades, based on published water balance calculations and hydrological modeling. The significance of glacier melt contributions to streamflow tends to be greater than average in years with low precipitation and warm summers. At De Geerdalen, Svalbard, for example, glacier wastage contributed up to 20% of annual runoff, roughly double the average, in a year when annual precipitation was 40% below average (Killingtveit et al., 2003).

Assuming no further climate change, glaciers currently experiencing negative mass balance would recede until they achieved a hypsometry for which $B = 0$, as long as the ELA is below the top of the glacier. If the ELA lies above the maximum elevation of the glacier, the glacier would ultimately disappear. Under this assumption of constant climate, average annual runoff would ultimately decrease by an amount equal to the current contribution due to glacier wastage. Decreases in runoff would be particularly severe in years with low precipitation. Flowers et al. (2005) simulated the future evolution of Vatnajökull, Iceland, assuming a continuation of the 1961 to 1990 climatology, and found that glacier runoff would decrease by about 20% after 200 years.

Climatic warming will result in a longer melt period and more intense melt, particularly as firn cover is depleted, exposing lower-albedo glacier ice to solar radiation. As a consequence, glacier runoff will increase with the onset of a warming trend. However, increased melt is accompanied by glacier thinning and retreat, and at some point the decrease in glacier area will cause glacier runoff to decrease. While this conceptual model is widely recognized (e.g., Jansson et al., 2005; Moore et al., 2009), the timescales associated with the transition from increasing to decreasing flow are uncertain. Available studies focused on southern Alaska, northeastern British Columbia, and southwestern Yukon have reported positive trends in streamflow for glacier-fed rivers, suggesting that the glaciers in those regions are still in the initial phase of their response to warming (Fleming and Clarke, 2003; Brabets and Walvoord, 2009).

Runoff from glaciers in the temperate and sub-Arctic regions of Russia was calculated from the USSR Glacier Inventory for the period 1966 to 1980 based on the assumption that glacier systems are in equilibrium with climate. The total glacier runoff over the period 1966 to 1980 was estimated to be no more than 3 Gt (Ananicheva and Krenke, 2007). To project future changes in glacier runoff in Russia, the morphology and regime of glacier systems were adjusted on the basis of predicted changes in ELA under a climate-warming scenario derived from the ECHAM4 GCM driven by the IPCC A2 emissions scenario. Despite a significant reduction of the glacierized area, the glacier runoff from southeastern Siberia and the Sredinny Range (Kamchatka) was predicted to increase through the 21st century owing to increased ablation. Glaciers in the Kronotsky Range (Kamchatka) were predicted to almost disappear, resulting in a sharp reduction in glacier-melt runoff (Ananicheva and Krenke, 2007).

Transient responses of glacier geometry and runoff to climate warming have been simulated for Hofsjökull and

Table 7.3. Runoff contributions associated with glacier wastage.

Catchment	Location	Period	Catchment area, km^2	Glacier coverage, %	Wastage contribution to streamflow, %	Q, kg/m^2	Source
Zackenberg	Northeast Greenland	1997 – 2005	512	20	63	428	Mernild et al., 2008a
Mittivakkat	Ammassalik Island, Greenland	1993 – 2004	14.2	78	23	1970	Mernild et al., 2008b
Bayelva	Svalbard	1990 – 2001	30.9	55	23	1050	Killingtveit et al., 2003
De Geerdalen	Svalbard	1990 – 2001	34.4	17	9	539	Killingtveit et al., 2003
Endalen	Svalbard	1990 – 2001	28.8	20	19	545	Killingtveit et al., 2003

Vatnajökull, Iceland (Flowers et al., 2005; Aðalgeirsdóttir et al., 2006), and the results are consistent with the conceptual model presented above. Figure 7.28 illustrates that, as the rate of warming increases, the interval with maximum glacier runoff for Hofsjökull moves forward in time and the increase in runoff is greater. For simulations involving a warming-related increase in precipitation, the effect is to increase the magnitude of runoff increase and delay the timing of peak runoff. Flowers et al. (2005) also reported that changes in the surface topography of the ice cap would cause shifts in the hydrological divides, effectively redistributing outflow among the outlet glaciers.

Climate warming and glacier response will modify seasonal patterns of runoff in addition to changing annual totals. Jónsdóttir (2008) simulated runoff in Iceland for climate projections based on the IPCC A2 and B2 emissions scenarios and projections of glacier geometry using a dynamic glacier model (Aðalgeirsdóttir et al., 2006; Jóhannesson et al., 2006). For the period 2071 to 2100, glacier-melt contributions to streamflow are projected to increase in all seasons, while runoff from unglacierized areas increases from October to April and decreases from May to September, jointly producing a significant shift in the seasonal pattern of runoff in partially glacier-fed catchments.

The highest peak flows in proglacial streams are often associated with outburst floods (Ng et al., 2007), in which water stored on, under, or within the glacier is released suddenly, for example, by the rapid growth of a meltwater channel (e.g., Mernild et al., 2008a). There is some evidence that subglacially derived outburst events are more extreme in warmer summers when there is greater meltwater generation (Skidmore and Sharp, 1999), suggesting that flood risk in glacier-fed Arctic catchments may increase as a result of climate warming. When outburst floods are derived from ice-dammed marginal lakes, thinning of the ice dams due to increased melting may result in floods that occur earlier in the melt season and are smaller and more frequent than they are at present. Lakes will fill sooner and more rapidly than in the past and the accumulated lake water may breach the ice dam more easily than before. Earlier onset of lake drainage may allow multiple filling/drainage cycles during a melt season, especially because melt seasons will be longer in a warmer climate.

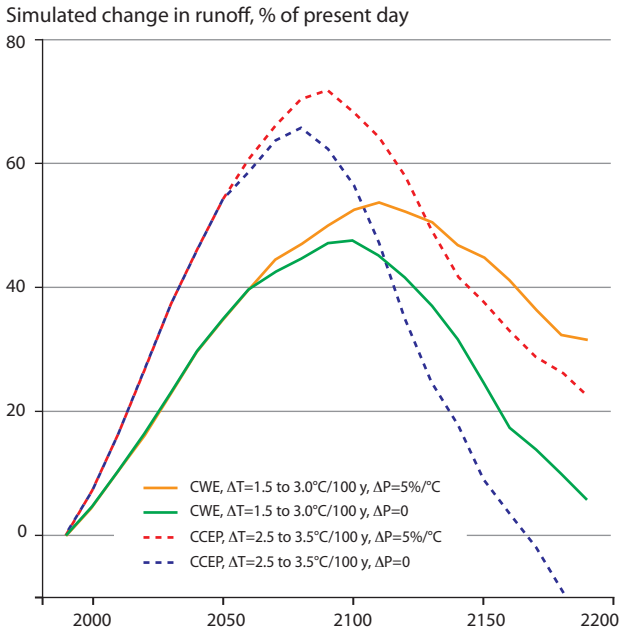

Figure 7.28. Simulated variations in glacier runoff from Hofsjökull, Iceland, under four climate scenarios. Source: Aðalgeirsdóttir et al. (2006).

7.7.3.2. Water quality

Climate warming will influence proglacial water quality as well as streamflow. Increasing meltwater runoff in the initial phases of warming should tend to moderate diurnal increases in stream temperature. However, as glaciers retreat, the length of stream exposed to solar radiation and other heat inputs will increase, potentially counteracting the effect of increased flow. In addition, the emergence of proglacial lakes can increase warming. Milner et al. (2008) found that maximum stream temperatures at Wolf Point Creek, which drains into Glacier Bay, Alaska, were 2 °C in 1977, roughly 30 years after the creek emerged due to glacier retreat. From 1996 onward, maximum temperatures have consistently exceeded 15 °C, at least in part due to the increase in size of the upstream lake, which initially formed in the 1970s. Once glaciers reach the stage of declining flow, there should be a trend to increasing stream temperature. At that point, the main factor mitigating this increase would be development of riparian forests where they do not currently exist, which would increase stream shading and enhance bank stability, resulting in a narrower, deeper stream. Both effects would tend to reduce stream warming, but would be relevant only in sub-Arctic and temperate areas such as the Gulf of Alaska.

Focusing on temperate regions, Moore et al. (2009) concluded that the onset of negative mass balance and glacier retreat would be likely to result in an initial increase in suspended sediment concentrations in proglacial streams, followed by a longer-term decrease. This long-term projection is consistent with studies that show that glacier-fed streams in the Arctic typically yield orders of magnitude more sediment than those without glacier contributions (e.g., Hasholt and Mernild, 2008). However, temporal changes in sediment concentration could vary substantially among basins due to site-specific factors, particularly the emergence of proglacial lakes, which trap sediment and thus reduce downstream transport (Hasholt et al., 2008). Future patterns of suspended sediment concentration would also be complicated in cases where glaciers shift from being cold-based or polythermal to temperate, as well as by thawing of permafrost, which could influence the erosion of stream channel beds and banks (McNamara and Kane, 2009).

Glacier retreat may be accompanied by changes in streamwater chemistry. Glacial forefields are subject to different weathering and nutrient cycling processes than those that dominate in subglacial environments, particularly as soils and vegetation develop (Anderson, 2007; Hood and Scott, 2008). Available studies, not all from Arctic areas, suggest that concentrations of nutrients and dissolved organic carbon should increase as glaciers retreat, although the forms of some nutrients and organic matter might change, possibly influencing their availability to aquatic organisms (Lafrenière and Sharp, 2005; Filippelli et al., 2006; Hood and Scott, 2008). In southeastern Alaska, decreasing basin glacier cover was found to be associated with higher concentrations of soluble reactive phosphorus and higher proportions of bioavailable (labile)

dissolved organic carbon (Hood and Berner, 2009; Hood et al., 2009). Fluvial transport of dissolved organic carbon could be influenced by changes in suspended sediment concentration, because high turbidity reduces photodegradation of dissolved organic carbon in streamwater.

7.7.3.3. Water resources and hydroelectric power generation

Most studies suggest that Arctic glaciers are currently in the initial phase of their response to warming, in which runoff increases, and that glacier runoff should continue to increase over the next few decades or so, providing an increase in water availability. However, some Russian results indicate that some areas (especially those where the glaciers are predominantly small) are likely to experience flow decreases over the next few decades as a result of glacier retreat (Ananicheva and Krenke, 2007). These contrasting behaviors could either reflect fundamental differences among glaciers in the timescale of response to warming, or suggest that glaciers are currently at different stages of their response. Further site-specific assessments are clearly warranted.

Glacier runoff is significant for hydroelectric power generation in the upper Yukon basin (at Whitehorse, Yukon, Canada), Iceland, Greenland, and in many river systems in Norway. A trend to increasing flows would also tend to increase the hydroelectric power resource. In Iceland, Jónsdóttir (2008) projected a substantial increase in hydroelectric power potential for the period 2071 to 2100, but a substantial decrease over the following century as the glaciers disappeared under the IPCC A2 and B2 emissions scenarios employed.

Reservoir operations could be influenced not only by the effects of changes in streamflow, but also by changes in sediment transport and stream temperature. Increased sediment transport would reduce the operational lifetime of a reservoir by infilling, while suspended sediment concentration and inflow temperature together would influence mixing processes and temperature profiles, in turn influencing habitat conditions for aquatic organisms as well as the temperature of water downstream.

7.7.3.4. Aquatic ecosystems

Glacier-fed rivers typically support a distinctive flora and fauna determined by physicochemical conditions, including the dominant influences of water temperature and channel stability (Milner and Petts, 1994; Milner et al., 2001). While bedload and suspended sediment transport typically peak during maximum glacial melt in summer (Østrem, 1975b), lower water levels during spring and autumn result in greater water clarity and channel stability, creating 'windows of opportunity' when algal and macroinvertebrate productivity is higher. Some of the largest runs of salmon in south-central Alaska occur in glacially influenced systems (Dorava and Milner, 2000) as glacial runoff enhances summer flow relative to rainfall- or snowmelt-dominated catchments, facilitating the migration of salmon from the ocean to their spawning grounds in tributary streams via the main channel corridor.

Since increases in glacial runoff will enhance summer flow and increase the duration of meltwater runoff, they will probably also facilitate the migration of adult salmon to their spawning grounds. Increased glacial runoff will also increase the amount of available spawning habitat and would potentially enhance winter baseflow through recharge of groundwater during the summer (Smith et al., 2001; Brown et al., 2003). The survival of young salmonids during the winter is significantly correlated with the amount of winter discharge or winter groundwater inputs (Fleming, 2005). Any changes in water source contributions that enhance winter flow should be beneficial to salmonid populations and mitigate the effect of overwintering mortality on salmonids.

In the phase of declining glacier runoff, bedload and suspended sediment transport will potentially decrease in the long term as glacial and paraglacial erosion (erosion by non-glacial processes of previously deposited glacial and fluvioglacial sediments) decrease and the stream's transport capacity decreases (Fleming and Clarke, 2005). In addition, newly formed proglacial lakes trap sediment, reducing sediment loads downstream. Fleming (2005) emphasized the potentially favorable effects of glaciers and lakes in combination on salmonid habitat: glaciers maintain late summer flow while lakes reduce sediment transport. Reduced bedload transport could allow streams to become more stable, and thus narrower and deeper. The projected reduction in suspended sediment load with ongoing glacier retreat should allow greater light penetration into the water column and increase algal productivity, particularly during certain periods of the year. The effect of increased light would be augmented by an increase in nutrient concentrations as vegetation and soils develop following glacier retreat. However, the effects of decreased turbidity on ecosystem productivity need to be considered in the context of possible decreases in late summer streamflow and increasing late summer water temperature.

There is clear evidence of a strong relationship between catchment glacierization and macroinvertebrate taxon richness in glacially influenced streams. In a stream fed by a receding glacier in southeastern Alaska, Milner et al. (2008) found that the benthic macroinvertebrate community supported only five taxa when 70% of the catchment was glacierized but 24 taxa after the glacier had disappeared two decades later. Füreder (2007) found similar trends in alpine streams with differing degrees of glacierization. This evidence suggests that changes in glacial runoff and fluvial sediment transport due to glacier shrinkage may cause an increase in the diversity of the benthic macroinvertebrate community. An increase in algal productivity will potentially enhance macroinvertebrate abundance. With a change in benthic community structure, dominant species traits will reflect a reduction in glacial contribution to flow. Macroinvertebrate body size will become larger and life cycles longer, with the benthic community dominated by habitat generalists with less omnivory and flattened forms (Ilg and Castella, 2006; Füreder, 2007). The fauna would also be less cold-adapted with reduced mobility of the adults. Enhanced abundance and increased body size will favor food availability for fish. Although an overall increase in taxonomic richness and abundance in benthic macroinvertebrate communities is predicted with decreased glacial inputs, some cold-specialist benthic species will be lost, including some endemic species. Some species will not adapt rapidly enough to survive

the anticipated rate of deglaciation in future decades (Hari et al., 2006).

The effect of shrinking glaciers on fish populations in glacially influenced rivers will depend upon whether the system is an alpine or a more lowland system. However, over time reduced glacial input into these rivers will reduce summer flow and may influence salmon migration upstream. Lower flow will also reduce the amount of habitat available adjacent to the main glacier-fed channel, including side channels and side sloughs. Side channels and sloughs are sustained by meltwaters of the main channel (Richardson and Milner, 2005). For many river systems in northerly regions, winter is a critical period when overwintering mortality for salmonids can be high if they are unable to migrate to suitable refugia, such as side channels. Water temperature is a critical variable influencing fish distribution and each species has an optimum range for different life stages. Matulla et al. (2007) predicted that the ranges of alpine stream salmonids (e.g., brown trout *Salmo trutta* and grayling *Thymallus thymallus*) would contract upstream due to changes in water temperature regimes under climate change scenarios in which the cold water input from glacial runoff decreases. Projected changes in water temperature in cold rivers can also favor non-indigenous species that have wider thermal tolerance and can out-compete indigenous taxa at higher water temperature (Ficke et al., 2007). In the Rocky Mountains, cutthroat trout (*Oncorhynchus clarkii*) have been displaced by non-indigenous brook trout (*Salvelinus fontinalis*) and brown trout that are more efficient at securing food resources at higher temperatures (Hauer et al., 1997). However, in streams that are currently colder than is optimal for salmonid growth, some degree of warming might increase salmonid production.

Large-scale glacial recession creates new habitat that can potentially be colonized by organisms including fish. The creation of new stream habitat due to glacial recession has been extensive along the coasts of southeastern and south-central Alaska due both to climate change and changing local environmental conditions (Milner et al., 2008). Although many of the recently formed streams are relatively short, the creation of new salmonid habitat is significant at a time when human activity threatens salmonid stocks in other parts of the Pacific Northwest region of North America (Nehlsen et al., 1991). Pink salmon (*Oncorhynchus gorbuscha*) can establish substantial populations from a small colonizing population of spawners within a few generations, and other species (including non-anadromous fish such as sticklebacks) colonize rapidly (Milner et al., 2008). As migrant salmon die soon after spawning, rotting of their carcasses results in a significant input of nutrients and organic matter to affected catchments, and this can promote productivity in other parts of the ecosystem.

7.7.3.5. Contaminant release from melting glaciers

Many contaminants originating from lower latitudes are carried to the Arctic by long-range atmospheric transport and stored in the firn and ice of glaciers and ice caps (Section 11.3, this volume). These contaminants include sulfate and nitrate, which have increased the acidity of snow and ice above pre-industrial levels (Koerner and Fisher, 1982), metals such as lead (Zheng et al., 2003), persistent organic pollutants such as PCBs (polychlorinated biphenyls), DDT and other organochlorine pesticides (Gregor and Gummer, 1989; Hermanson et al., 2005), as well as radionuclides associated with the Chernobyl reactor failure in 1986 and with nuclear testing dating back to 1961 to 1962 (Pinglot et al., 1999). Stored contaminants may be released back into the environment by glacier melt and the process can be accelerated if melt rates increase over time (Blais et al., 2001).

Contaminants stored in seasonal snow away from glaciers interact with soil and aquifer materials prior to their discharge to receiving waterbodies such as lakes and streams. During these interactions, a proportion of the contaminants (especially persistent organic pollutants) released via melting will be retained through sorption onto organic matter and cation exchange on clay particles in the soil. In contrast, glacier meltwater has much less interaction with organic matter and clays in soils before leaving the glacier, leading to less retention and higher rates of contaminant export to lakes and rivers downstream, as has been found in the Canadian Rockies (Blais et al., 2001; Lafreniére et al., 2006).

All the contaminants stored in glaciers would eventually be discharged in meltwater runoff regardless of climate change, but there would be significant lag times associated with the flow of ice from the accumulation to ablation zones. Climate warming accelerates melting of snow, firn, and ice, potentially releasing stored contaminants to receiving waters in a more concentrated pulse. However, thus far there has been no research in the Arctic directly addressing this impact.

7.7.4. Glacier ecosystems

Distinctive microbial ecosystems are found on and under glaciers (Hodson et al., 2008). On the glacier surface, the supraglacial ecosystem exists in the snowpack, supraglacial streams, melt pools, and cryoconites (water-filled holes on glacier surfaces that contain dust and microbial communities). It comprises a diverse array of bacteria, algae, fungi, viruses, rotifers, and tardigrades. *In situ* rates of primary production and respiration on glacier ice surfaces in summer are comparable to those encountered in soils in warmer and more nutrient-rich regions. Measurements of net production suggest that glacier ice surfaces may be largely autotrophic systems (Anesio et al., 2009), unlike most lakes and rivers, which tend to be heterotrophic systems.

At the glacier bed, a subglacial ecosystem is found in basal ice, subglacial sediments, meltwaters, and volcanic subglacial lakes (Gaidos et al., 2004, 2009; Hodson et al., 2008). It includes a mixture of aerobic and anaerobic (chemoautotrophic and heterotrophic) bacteria and probably also fungi and viruses (D'Elia et al., 2008). These microorganisms have metabolisms based on the oxidation of organic carbon, sulfide, sulfur, or hydrogen, and they use oxygen, nitrate, sulfate, iron(III), manganese(IV), or carbon as terminal electron acceptors. They play a critical role in subglacial chemical weathering (Tranter et al., 2002, 2005) and in controlling the biogeochemistry, nutrient loading, and properties of dissolved organic matter in glacial runoff (Hodson et al., 2008; Gaidos et al., 2009). They may also be involved in the production of greenhouse gases (carbon dioxide and methane), with possible feedbacks to the climate system if these gases are stored in basal ice or subglacial sediments and released to the atmosphere during deglaciation (Sharp et al., 1999; Skidmore et al., 2000; Wadham et al., 2008; Boyd et al., 2010).

The impact of climate change on these ecosystems is likely to be complicated as there will be a number of competing influences (Hodson et al., 2008). In the long term, changes in global glacier area will limit their geographical extent, and total deglaciation would be likely to eradicate these ecosystems completely. In the shorter term, increased surface melt would probably enhance supraglacial ecosystem productivity. As end-of-summer snowline elevations rise, the extent of supraglacial stream and meltwater habitats will increase at the expense of snowpack habitats. Higher ice melt rates may swamp these systems with water, continually redistributing them across the glacier surface. Increased melting of glacier ice may increase the rate of release of glacially entombed microorganisms into the supraglacial environment. This may increase the transfer of carbon, nutrients, and biota into downstream (subglacial and proglacial) aquatic environments. Increased water fluxes would be likely to increase the oxygenation of glacier beds in summer, favoring aerobic over anaerobic bacterial processes. They might also result in more rapid transit of meltwater through the subglacial ecosystem, especially as glaciers shrink, reducing the efficiency of utilization of supplies of nutrients and organic matter by subglacial microbial communities. Alternatively, increased delivery of carbon and nutrients could stimulate microbial activity, and create anoxic conditions at glacier beds in winter when surface water inputs cease.

Paradoxically, however, negative surface mass balances and glacier thinning have resulted in cooling and net freezing at the beds of some Arctic glaciers (Dowdeswell et al., 1995; Hodgkins et al., 1999; Glasser and Hambrey, 2001). Such changes would lead to isolation and cryostasis (the reversible cryopreservation of live organisms) of the subglacial ecosystem. Whether this might ultimately eliminate the subglacial ecosystem from individual glaciers or drive it deeper into unfrozen subglacial sediments is currently unknown. Elimination of the ecosystem would substantially alter the biogeochemistry of glacial runoff, with potential implications for downstream ecosystems (Hodson et al., 2004, 2005).

7.7.5. Geomorphological hazards

Glacier changes, particularly glacier retreat, can produce a range of hazards involving slope instability, increased proglacial fluvial sediment transport, and changes in water flow, particularly outburst floods. To augment the available research conducted in the Arctic, the review below draws heavily on work outside the Arctic. However, the general principles should apply throughout the Arctic region as broadly defined in this chapter.

7.7.5.1. Slope instability

Glacier down-wasting and retreat appear to be partly responsible for destabilizing adjacent terrain, leading to landslides, debris flows, rock avalanches and falls, and some catastrophic rock-slope failures in high mountains (Evans and Clague, 1994; Holm et al., 2004). Many marginally stable slopes that were buttressed by glacier ice during the Little Ice Age failed after they became deglaciated in the 20th century. A factor that has possibly contributed to such failures is steepening of rock slopes by cirque and valley glaciers during the Little Ice Age. These effects are most pronounced in mountain ranges with the largest ice cover; because it is there that ice losses in the 20th century have been greatest. An extreme example is Glacier Bay, which until the end of the 18th century was covered by glacier ice. Since then, Glacier Bay has become deglaciated, with the loss of over 1000 km^2 of ice in 200 years. The amount of ice lost is so great that the uplift of the land due to isostatic rebound is measurable (Larsen et al., 2005).

7.7.5.2. Outburst floods from moraine- and ice-dammed lakes

Lakes dammed by moraines and glaciers in high mountains have drained suddenly to produce floods orders of magnitude larger than normal nival or rainfall floods (Costa and Schuster, 1988; Clague and Evans, 1994). Lakes dammed by Neoglacial end and lateral moraines are susceptible to failure because they are steep-sided and consist of loose, poorly sorted sediment that in some cases is ice-rich (Clague and Evans, 2000). Irreversible rapid incision of a moraine dam may be caused by a large overflow triggered by an ice or snow avalanche or rockfall. Other failure mechanisms include earthquakes, slow melt of ice within the moraine, and slow removal of fine-grained sediment from the moraine by groundwater flow (piping). As climate warms, lakes impounded by glaciers may drain suddenly and unexpectedly following a long period of stability due to progressive wastage of the glacier dam and the formation of subglacial, supraglacial, or ice-marginal channels. Drainage may be initiated by hydrostatic lifting of that part of the base of the glacier facing the lake. Lakes may also form during glacier surges; they drain, often catastrophically, soon after they form.

Most outburst floods display an exponential increase in discharge, followed by a gradual or abrupt decrease to background levels as the water supply is exhausted (Clarke, 2003; Ng et al., 2007). Peak discharges are controlled by lake volume, dam height and width, the material properties of the dam, failure mechanism, and downstream topography and sediment availability. Floods from glacier-dammed lakes tend to have lower peak discharges than those from moraine-dammed lakes of similar size because enlargement of tunnels within ice is a slower process than overtopping and incision of sediment dams.

Floods resulting from failures of natural dams may transform into debris flows as they travel down steep valleys. Such flows can only form and be sustained on slopes greater than 10 to 15 degrees and only where there is an abundant supply of sediment in the valley below the dam. Entrainment of sediment and woody plant debris by floodwaters may cause peak discharge to increase down valley, which has important implications for hazard appraisal.

Outburst floods from lakes dammed by moraines and glaciers commonly alter river floodplains tens of kilometres from the flood source. The floodwaters erode, transport, and deposit huge amounts of sediment. They commonly broaden floodplains, destroy pre-flood channels, and create a new multi-channel, braided to anastomosing (channels that repeatedly branch and reconnect) plan form. The changes can persist for decades after the flood, although rivers quickly reestablish their pre-flood grades by incising the flood deposits.

Climate is an important determinant of the stability of moraine and glacier dams (O'Connor and Costa, 1993; Evans and Clague, 1994). Most moraine-dammed lakes formed

during the past century as glaciers retreated from bulky end moraines constructed during the Little Ice Age. The lake dams soon began to fail as climate warmed. With continued warming and glacier retreat, the supply of moraine-dammed lakes that are susceptible to failure will be exhausted, and the threat they pose will diminish. Glacier-dammed lakes have typically gone through a period of cyclic or sporadic outburst activity, lasting up to several decades, since climate began to warm in the late 19th century. The outburst floods from any one lake ended when the glacier dam weakened to the point that it could no longer trap water behind it. However, with continued glacier retreat, the locus of outburst activity may, in some cases, shift up-glacier to sites where new lakes develop in areas that are becoming deglaciated. Landslide damming is less clearly linked to climate.

7.7.5.3. Erosion and sedimentation

Fluctuations of glacier margins on timescales of decades and centuries can remobilize glacial sediment. During glacier advance, initial incision due to increased competence of meltwater streams is quickly followed by deposition as sediment supply increases (Maizels, 1979). Sediment stored within and beneath glaciers is delivered at an increasing rate to fluvial systems as glaciers advance (Karlén, 1976; Maizels, 1979; Leonard, 1986, 1997; Karlén and Matthews, 1992; Lamoureux, 2000). Similarly, subglacial erosion increases during glacier advance, and meltwater may carry more sediment into river valleys than at times when glaciers are more restricted. Sediment delivery to streams in the Coast Mountains of British Columbia, for example, increased during the Little Ice Age, and the streams responded by filling in their channels and braiding over distances up to tens of kilometres down valley from glaciers (Church, 1983; Gottesfeld and Johnson-Gottesfeld, 1990). Glacier retreat typically exposes large areas of unstable, unvegetated sediment that is easily entrained by meltwater (Church, 1983; Desloges and Church, 1987; Gottesfeld and Johnson-Gottesfeld, 1990; Brooks, 1994; Ashmore and Church 2001; Clague et al., 2003).

7.7.5.4. Glacier-volcano interactions and related hazards

Glaciers are found in regions of active volcanism in Alaska, Iceland, and Kamchatka, where high seismic and volcanic activity can generate significant glacier-related hazards. Consequences of volcanic activity include glacier burial by ash falls, melt-induced formation of craters and lakes on glaciers, significant mass loss by subglacial melting during subglacial eruptions, and accelerated glacier flow. Several volcanogenic *jökulhlaups* (outburst floods from glaciers) have been documented in Iceland (Russell et al., 2006).

Lahars (fluidized volcanic debris flows produced when hot pyroclastic material falls onto glaciers) can be extremely destructive owing to their high density and low viscosity while in motion, and their tendency to over-consolidate (stiffen) upon halting. Lahars are especially destructive because their mode of origin allows large volumes of material to be activated quickly, and because the topographic relief of the volcano provides abundant potential energy. In Kamchatka, lahars have caused significant damage to infrastructure and the environment. For example, the 2001 eruption of Shiveluch Volcano produced lahars which traveled about 20 km and damaged the road to Ust-Kamchatsk. The 2005 eruption of Kluchevskaya Volcano created lahars that carried blocks 3 to 4 m in size a distance of over 30 km.

It is unclear from the available literature how glacier-volcano interactions and the associated hazards will be influenced by future changes in climate and resulting changes in glaciers and ice caps. However, there is some evidence that volcanic activity may increase as ice thins (Tuffen, 2010).

7.7.5.5. Glacier surges

Surging glaciers are found in Alaska, the Yukon Territory, Arctic Canada, Greenland, Iceland, Svalbard, and Novaya Zemlya. Those in Novaya Zemlya tend to terminate in water (Grant et al., 2009), and surges of these glaciers are a potential danger to local populations and infrastructure. Some surging glaciers in Alaska, such as the Black Rapids Glacier, are a potential hazard to the Trans-Alaska (oil) Pipeline (Heinrichs et al., 1995). Surge behavior has been documented for 26 glaciers in Iceland (Björnsson et al., 2003). Surges of these glaciers are associated with an increase in proglacial stream turbidity, but not discharge. The geographical variability of surge behavior, coupled with the incomplete understanding of glacier surge mechanisms, makes it difficult to predict whether climate change will alter the frequency of surging or the impact of the phenomenon on human society.

7.7.6. Glacier-related tourism

More than 1.5 million tourists currently visit the Arctic each year, up from one million in the early 1990s. Longer and warmer summers keep Arctic seas freer of ice floes, so cruise ships can visit places that were once inaccessible. The annual number of visitors to Svalbard has surged by 33% in the period 2002 to 2006 to about 80 000 (Naik, 2007). At the beginning of the 21st century, tourism has clearly become a major engine of growth for the Alaskan economy. According to the Alaska Tourism Satellite Account (Anon, 2004), travel and tourism's economic contribution in Alaska reached USD 1.6 billion in 2002. This amount – representing sales net of related imports into the state – contributed 5.6% to Alaska Gross State Product (GSP). This includes the direct and indirect effects of all travel and tourism expenditure, but not induced (multiplier) effects. Travel and tourism's core industry – that is, only the direct impact of end-providers of goods and services to travelers – generated USD 856 million in local value added in 2002: 3.0% of Alaska's GSP. Using the core industry definition, travel and tourism was the third largest private sector employer – fourth overall – in the State, with 26 158 direct full-time-equivalent jobs (9.1% of Alaska's total employment) in 2002. Travel and tourism-generated jobs provided USD 579 million in core labor income (benefits and salaries) to Alaska. Adding public sector employment, travel and tourism's economic contribution to employment reached 39 420 full-time-equivalent jobs. Those jobs provided Alaskan workers with USD 1.15 billion in income. Glacier-related tourism is an important part of the economy in several regions of the Arctic, especially in Alaska. Every year hundreds of thousands of people visit coastal Alaska to see the glaciers. Melting of the glaciers in the warming Arctic may be a threat to this sector of the economy.

7.8. New information expected from International Polar Year projects

- Eleven projects focusing on the behavior of Arctic mountain glaciers and ice caps were initiated during the International Polar Year (IPY). They contributed to several IPY projects including GLACIODYN and 'State and Fate of the Cryosphere'.
- New regional surveys of glacier changes, which contribute to the IPY program 'State and Fate of the Arctic Cryosphere', have been conducted in Alaska, the Yukon, Labrador, Iceland, the Russian Arctic Islands, and northeastern Siberia. Surveys in Alaska and Iceland involve new mapping of glacier surface topography with LIDAR and laser altimetry. Satellite laser altimeter data from ICESat have also been used extensively in these surveys. The Yukon surveys reveal a 22% reduction in glacier area since the 1957/1958 International Geophysical Year.
- GLACIODYN projects focus on understanding and modeling the role of changing ice dynamics in the response to climate change of polythermal and calving tidewater glaciers. Target glaciers for this work are Columbia and McCall Glaciers in Alaska, Belcher Glacier on Devon Island, Canada, and Austfonna and Vestfonna in Nordaustlandet, Svalbard.
- A Russian IPY project has focused on the formation, dynamics, and decay of icebergs in the western sector of the Russian Arctic, a topic of particular interest given the increasing amount of shipping and offshore resource exploration activity in the region.

7.8.1. Alaska

Three U.S. IPY projects will contribute to knowledge of Arctic glacier changes and mechanisms of change. As part of IPY-37 GLACIODYN, there is a continuation of the 30-year record of observations on the retreat of Columbia Glacier, Alaska, which at present is the largest single Alaskan contributor to sea level change (at 3.3 Gt/y from 1982 to 2001, and 6.6 Gt/y around 2001). The ongoing work at Columbia Glacier includes re-analysis and archival of the 145-mission, 30-year sequence of aerial photography of the glacier (the longest and most detailed record of its kind ever acquired), a continuation of this aerial photogrammetric record, and a variety of additional measurements and analyses including photogrammetric feature-tracking, terrestrial time-lapse photogrammetry, airborne radar, GPS surveying, seismic observations of calving, and meteorological monitoring. Collaborative work on Svalbard with Polish colleagues is included in this project. The results will add to knowledge of the physics of calving and tidewater glaciers, and improve the ability to predict future marine-ending glacier behavior, not only on Arctic glaciers and ice caps, but on marine-ending glaciers everywhere, including the outlet glaciers of Greenland and Antarctica. Work under this funding is in progress and research supported in part by this funding is presented by O'Neel and Pfeffer (2007).

A second GLACIODYN project aims to investigate the mass balance and ice dynamics of polythermal land-terminating glaciers using McCall Glacier in Arctic Alaska as the primary field site. During the IPY, ice cores to bedrock were extracted at three locations. One complete core and selected parts of the other two cores have been returned for analyses designed to elucidate past climate conditions in the region and establish a history of pollutant deposition. Thermistor strings were installed to bedrock in the drill holes as part of a study of internal accumulation within the glacier and its effects on the glacier's mass balance and thermal regime. A program of stream hydrology measurements was initiated both at the glacier terminus and in the river that drains from the region to the Arctic Ocean (these rivers have never previously been gauged and glaciers currently contribute roughly 90% of their discharge). A full 3D higher-order ice flow model of the glacier is being run using high-resolution bedrock and surface maps. To help understand how representative the McCall Glacier measurements are of a broader region, a new LIDAR digital elevation model covering about 500 glaciers in the eastern Brooks Range was created based on surveys conducted in 2008. It will be used to measure changes in glacier volume in the region.

As part of IPY-105 'State and Fate of the Cryosphere', glacier mass loss across Alaska is assessed using airborne laser altimetry along glacier centerline profiles. Repeat profiles are compared to previous mass change estimates to address the primary question of continued acceleration of glacial wastage.

7.8.2. Arctic Canada

Two Canadian IPY projects will contribute new knowledge about the glaciers in Arctic Canada. One component of the project 'Variability and Change in the Canadian Cryosphere' (a contribution to IPY-105 'State and Fate of the Cryosphere') involves producing a multi-temporal glacier inventory and mapping changes in the extent of glaciers in the Yukon and Labrador since the International Geophysical Year (1958/1959) from aerial photography and satellite imagery. Initial results suggest a reduction of 22% in Yukon glacier area over that period (Barrand and Sharp, 2010) and a 25% reduction in the extent of Labrador glaciers between 2003 and 2007. A second goal of the project is to undertake annual mapping of melt extent, melt duration, melt onset and freeze-up dates, and the end-of-summer distribution of snow and ice facies on all large glaciers and ice caps in the Arctic (including Greenland) using enhanced resolution data from the SeaWinds scatterometer on QuikSCAT. The records extend over ten years, to the end of the 2009 melt season, and will provide new insight into the evolution of summer climate over the ice-covered areas of the Arctic land mass.

A second project is a Canadian contribution to IPY-37 GLACIODYN, which aims to investigate the role of ice dynamics in the response of Arctic glaciers and ice caps to global warming, and improve the ability to predict future changes and their impact on global sea level and fluxes of freshwater to the ocean. The Canadian contribution to GLACIODYN focuses on the Belcher Glacier in the northeastern sector of the Devon Island Ice Cap, Nunavut. This is the fastest flowing outlet from the ice cap and a major source of icebergs. The project involves an intensive field and remote sensing study of the hydrology and dynamics of the glacier linked to the development and

validation of a state-of-the-art, high-order coupled model of ice flow dynamics and glacier hydrology. The model will be used to test hypotheses about the effects of climate warming on meltwater inputs to Arctic outlet glaciers and their impact on ice flow, and to perform simulations of the response of the Belcher Glacier to recent and projected future climate change.

7.8.3. Iceland

A major Icelandic IPY project involves mapping the surface topography of Icelandic ice caps using LIDAR. The results will be used to correct digital photogrammetric maps from the 1990s, allowing an analysis of surface elevation changes of the ice caps over the past one to two decades. The LIDAR mapping is a collaboration between the Icelandic Meteorological Office and the Institute of Earth Sciences of the University of Iceland and is funded by RANNIS (the Icelandic Centre for Research), Landsvirkjun (the National Power Company of Iceland), the Icelandic Public Road Administration, the Reykjavík Energy Environmental and Energy Research Fund, and the National Land Survey of Iceland.

High-resolution LIDAR digital terrain models (DTMs) of most of Hofsjökull, Langjökull, Eiríksjökull, and Snæfellsjökull have been made from surveys conducted during the 2007/2008 IPY. DTMs of Mýrdalsjökull, Eyjafjallajökull, Hofsjökull, and southeastern Vatnajökull were completed in 2010. Mapping will be continued in 2011 to 2013 to produce DTMs of the southern, western, and northern drainage basins of the Vatnajökull ice cap.

The new LIDAR DTMs of proglacial areas and nunataks (isolated peaks protruding through the surface of the ice caps) will be used as a reference for re-analysis of the digital photogrammetric maps of glacier ablation areas in the 1990s, which should reduce systematic bias in these maps. This will make it possible to compare the photogrammetric maps with the LIDAR DTMs and quantify volume changes of the Icelandic ice caps during the past 10 to 20 years.

It is important that the glaciers are accurately mapped now when rapid changes are occurring in response to a warming climate. Accurate DTMs make it possible to pursue various lines of glaciological research, but they also have considerable economic value for the assessment and monitoring of water resources for hydroelectric power generation. Potential uses of the DTMs include modeling of surface mass balance and ice flow, mapping the boundaries of surface and subglacial watersheds, mapping subglacial water flow pathways, and quantifying rates of glacier change and their impact on global sea level. The DTMs are also important for investigations of glacier surges and isostatic uplift due to reductions in ice mass.

7.8.4. Svalbard

During the IPY, two international project consortia worked on glaciology in Svalbard: the IPY Kinnvika project and GLACIODYN. Both studied mass balance and dynamics with a focus on large ice caps. The glaciological part of the Kinnvika project focused on Vestfonna (2500 km^2) and involved studies of accumulation rates, ablation rates, ice temperatures, and ice geometry and measured ice velocity fields. Fixed mass balance stations and automatic weather stations were established across the ice cap. Shallow cores were taken to find the average point mass balance over a few decades. The data provide input to and validation of modeling and remote sensing studies.

The Norwegian part of GLACIODYN focused on Austfonna in Nordaustlandet and on Kongsvegen / Kronebreen in northwestern Spitsbergen. GLACIODYN monitored the current status of more than a dozen Arctic ice caps and glaciers with the aim of predicting the future fate of these terrestrial Arctic ice systems. The Austfonna investigations focused on (i) direct surface mass balance measurements; (ii) elevation and volume changes using satellite data, airborne laser profiles, and ground-based GPS measurements; (iii) dynamics of surge, calving and subglacial processes; and (iv) modeling of mass balance and dynamics. Five years of net surface mass balance studies on Austfonna show a slightly negative average balance (-0.1 m w.e./y), but with large interannual variations both in snow accumulation and total ablation. The calving is important (-0.30 m w.e./y) and represents 30% to 40% of the total ablation, similar to values observed on other Arctic ice caps. However, the elevation change measurements on Austfonna show a thickening in the interior of about 0.5 m/y and an increasing thinning closer to the coast of 1 to 2 m/y. A total of 230 km, or about 70%, of the ice cap margin is a calving front, at which all the ice is grounded. The calving front has been retreating at an average rate of 50 m/y since 1990 (Dowdeswell et al., 2008). There seems to be a large dynamic instability, as the measured mass flux is much less than the flux that would be expected given the observed surface mass balance.

On Spitsbergen, a Russian IPY project has used surface radio echo sounding surveys and the analysis of available multi-temporal cartographic, aerial, and satellite-derived data to determine changes in the surface elevation, thickness, ice volume, and internal structure of Fridtjovbreen resulting from a surge event in the 1990s.

7.8.5. Russian Arctic and mountains

The Russian National Program and Implementation Plan for the IPY 2007/2008 includes three projects relevant to glaciers in the Russian Arctic. The project 'Current state of glaciers and ice caps in the Eurasian Arctic' is a Russian contribution to GLACIODYN. The main goal of the project is to study the area changes, mass balance, hydrothermal state, and potential instability of glaciers and ice caps in the Russian Arctic islands and Svalbard. The main fieldwork programs in 2007 and 2008 included airborne and surface radio echo sounding surveys of ice thickness and bedrock and surface topography of ice caps and glaciers, which have been supported by the analysis of spaceborne remote sensing data. On the basis of radio echo sounding surveys of glaciers on Franz Josef Land and Novaya Zemlya and satellite altimetry data, characteristic heights and thicknesses of glacier fronts producing icebergs have been determined, including Glacier No. 1 and the Moscow Ice Cap on Hall Island, the northern part of the glacier complex on George Land (Franz Josef Land), and the glaciers in the Inostrantsev Bay area, Novaya Zemlya. New criteria for the estimation of iceberg hazards from the glaciers of Novaya Zemlya and Franz Josef Land were developed. Franz Josef Land has the greatest potential for regular formation of large icebergs (with thicknesses of up to 150 to 200 m and extents of more than 1 to 2 km) (Kubyshkin et al., 2009).

A second project, 'Formation, dynamics and decay of icebergs in the western sector of the Russian Arctic', aimed to collect new data on the formation, distribution, and properties of icebergs in the Barents and Kara Seas and to estimate the current state of outlet glacier fronts in the Russian Arctic archipelagos. During a cruise of R/V *Mikhail Somov* in September 2007, iceberg-producing glaciers on Franz Josef Land, Novaya Zemlya, and some other islands were surveyed. The survey included a wide range of iceberg studies, following their life history from calving to melting and disintegration. The study continued the survey of 2003, when an abnormally large group of icebergs (over 40, the largest of which was over 400 m long and weighed about 3 million tonnes) was discovered in the northeastern part of the Barents Sea, in the vicinity of the *Shtokman* gas-condensate field. The unusual ice conditions allowed R/V *Mikhail Somov* to circumnavigate Franz Josef Land. Helicopter radio echo sounding and aerial photography of glaciers on Prince George Land, Salisbury Island, Luigi and Champ Islands, Hall Island, and Wilczek Land allowed determination of ice thickness in potential iceberg-producing areas. Photogrammetry was used to reconstruct the geometry of glacier fronts and the above-water parts of icebergs. On some glaciers and icebergs, the vertical distribution of ice temperature (down to 20 m depth) and energy balance components of the upper 3 m layer were measured. Observations were made on the surface and in the ice (down to 3 m depth). On some glaciers, markers were installed for measurement of glacier flow. Glaciological studies were supplemented with oceanographic temperature and salinity profiling in the Franz Josef Land straits. Several groups of large tabular icebergs (more than 1 million tonnes) were found not far from their calving areas (Elena Guld Bay on Wilczek Land; the straits between Salisbury, Luigi, and Champ Islands; Geographers' Bay on Prince George Land). The majority of large icebergs were already drifting. Under favorable meteorological conditions, some may drift to the Barents Sea through the deep straits. A similar survey was undertaken of the glaciers of the northern end of the Northern Island of Novaya Zemlya (Buzin et al., 2008). This survey was repeated in autumn 2008.

The project 'Climatic factors in the contemporary evolution of North-Eastern Siberia glaciation' is another Russian contribution to GLACIODYN. This project continued studies of climate–glacier interactions in the poorly explored northeastern Siberia region. This region is of special interest because its climate is influenced both by Atlantic and Pacific air masses. It includes a part of the Northern Hemisphere where climate change (weakening of the Siberian High and warming in recent years) and cryospheric change have been detected. Meteorological parameters were measured along a transect from Magadan to Oymyakon, and in the northern massif of Suntar-Khayata. A study has been completed of glacier change in the region based on modern satellite images and data from the USSR Glacier Inventory. Infrared, visual, and aerial photo surveys were conducted for the Suntar-Khayata glaciers in order to update the Glacier Inventory (Ananichava and Kapustin, 2010).

7.9. Synthesis of the current state of Arctic mountain glaciers and ice caps

- Mass balance assessments based on field measurements and geodetic surveys indicate a marked increase in the rate of mass loss from Arctic glaciers (especially those in Alaska, the Canadian Arctic, and Greenland) since the mid-1990s. From 1961 to 2004, the mean rate of loss was in the range -91 to -141 Gt/y, but pentadal estimates for the period since 1995 range from -170 to -280 Gt/y.
- The recent increase in mass loss coincides with increases in summer air temperature and reductions in glacier area.
- Recent rates of mass loss are comparable to those from the Greenland Ice Sheet, emphasizing the importance of the Arctic as a whole as a first-order control on the rate of global sea level rise.
- Iceberg calving is an important component of mass loss in Alaska, Arctic Canada, the Russian Arctic, and Svalbard (where it accounts for about 32% of the total net mass loss). Individual tidewater glaciers can discharge very large amounts of ice into the ocean (e.g., Columbia Glacier discharged 6.6 Gt/y in 2001). However, temporal changes in this mass loss term are not well known and are not included in projections of future mass and volume change.
- Model-based projections suggest a 13% to 36% reduction in Arctic glacier volume by 2100 due to changes in surface mass balance alone. While some individual glaciers will disappear during this period (and others have already done so), mountain glaciers and ice caps in the Arctic will continue to influence change in global sea level well beyond 2100.
- Meltwater runoff from Arctic glaciers is expected to increase for a few decades at least, but will eventually decrease as the influence on melt production of decreasing glacier area becomes more significant than that of increasing melt rate.

7.9.1. Mountain glacier and ice cap mass balance

Two global mass balance datasets, one based on glaciological mass balance measurements (DM05) (Dyurgerov and Meier, 2005) and the other a combination of both glaciological and geodetic measurements (C09) (Cogley, 2009a), are subsetted to determine a pan-Arctic glacier mass balance. DM05 is a weighted arithmetic mean of single-glacier time series within a set of climatically homogeneous regions, based on data from the World Glacier Monitoring Service (WGMS, which collects standardized observations of change in the mass, volume, area, and length of glaciers worldwide; www.wgms.ch), individual published sources and, in some cases, unpublished measurements. Each time series is weighted by the area of its glacier, and then extrapolated to the climatic region based on estimates of the total glacierized area in each region. Nearly all the glaciological measurements in DM05 are derived from land-terminating glaciers (with larger glaciers underrepresented). C09 uses a nearly identical glaciological dataset to DM05, but also includes geodetic datasets that sample several tidewater glaciers. For the annual glaciological dataset,

C09 uses a spatial interpolation algorithm that fits a polynomial in geographical coordinates (centered successively on each cell of a 1° by 1° grid) to the complete (glaciological plus geodetic) set of single-glacier balances. The measured mass balances are inverse-distance weighted to the center of the grid cell, and the resulting estimate is multiplied by the total glacierized area within that cell. Estimates are averaged over five-year (pentadal) time periods. For the geodetic measurements, which usually span several years, the time-averaged mass balance during the entire period is assumed to represent the annual balances within that period. Interannual variations in the geodetic balances are accounted for by calculating a standard deviation that is a function of the warmest month's air temperature in a given year, interpolated to the glacier equilibrium line. The temperatures used are climatological means from the NCEP/NCAR Reanalysis.

While all the mass balance measurements included in the DM05 and C09 datasets are total mass balances (surface mass balance plus iceberg calving), very few are from calving glaciers. Circumstantial evidence presented by Cogley (2009a) suggests that calving glaciers may currently have more negative mass balances than land-terminating glaciers. If so, underrepresentation of calving glaciers in these datasets may result in underestimation of rates of mass loss in both global mass balance assessments. As yet, it is not understood why rates of mass loss from calving glaciers might be higher than those from land-terminating glaciers and it is not possible to properly quantify the magnitude of the bias in global mass balance assessments that arises from underrepresentation of calving glaciers in the datasets on which these assessments are based. Equally, it is not yet possible to predict how the rate of mass loss by iceberg calving will evolve under different climate change scenarios.

Both estimates derived from measurements (DM05 and C09) show that mass balances were predominantly negative during the period of record, with large interannual variability (Figure 7.29). During the period 1961 to 2004, the average mass balance of Arctic glaciers was -91 Gt/y using the DM05 data and -138.4 Gt/y using the C09 data. Estimates from DM05, based only on glaciological measurements, are more positive than the C09 estimates, possibly because they underrepresent calving glaciers. A third global mass balance estimate, derived from a surface mass balance model driven by climate station data (Hock et al., 2009), suggests that the surface mass balance of Arctic glaciers was -141 ± 65 Gt/y during the period 1961 to 2004 (Figure 7.29). Mass balances were significantly more negative in the period 1995 to 2005 than previously (of the order of -170 to -280 Gt/y according to the C09 dataset). These recent rates of mass loss are comparable in magnitude to recent estimates of mass loss from the Greenland Ice Sheet (see Chapter 8). When the mass loss rates from Arctic mountain glaciers and ice caps are combined with those from the Greenland Ice Sheet, it becomes clear that wastage of glacier ice in the Arctic is a first-order control on the rate of global sea level rise.

The regional contributions that comprise the pan-Arctic mass balance estimate derived using the combined geodetic-glaciological method (C09) are shown in Figure 7.30. This figure also shows the pentadal mean summer (June to August) 700 hPa air temperature for each region from the NCEP/NCAR Reanalysis. The time series of estimated contributions from

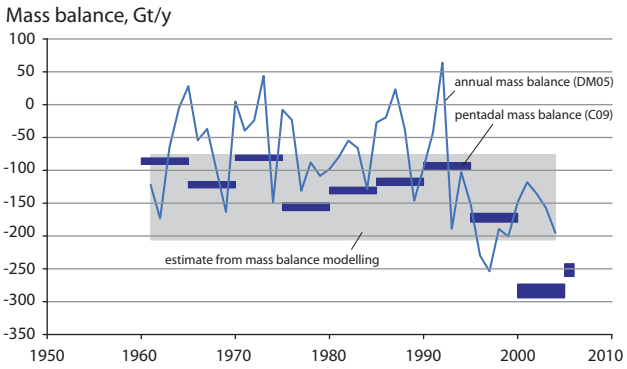

Figure 7.29. Annual mass balance (Dyurgerov and Meier, 2005) and pentadal mass balance (from data compiled by Cogley, 2009a) of Arctic glaciers as outlined in Figure 7.9. Annual estimates are extrapolated from glaciological measurements. Pentadal estimates are derived from a combination of geodetic and glaciological data. The grey box is an estimate from mass balance modeling (Hock et al., 2009) marking the error bounds around the mean estimate. Source: AMAP.

regions with observed records (such as southern Alaska, the Canadian Arctic, Scandinavia, and Iceland) are inversely related to regional summer air temperature variations. However, the time series for some regions with fewer observations (such as the Russian Arctic) are not consistent with local climate fluctuations. In these regions, the reconstructed mass balance records may be overly influenced by regional interpolation from areas with more mass balance data and different temperature histories. In general, the degree of confidence in the regional mass balance reconstructions decreases as the amount of smoothing of observed data required to generate them increases. This suggests that records from such regions need to be treated with caution and that deriving more reliable records for such regions should be a high priority.

Estimates of regional mass balance based on local measurements also illustrate the relative contribution of each region to rising sea level (Figure 7.31) over specific intervals of time. All areas with regional syntheses show mass losses during their periods of measurement, with Alaska and the Canadian Arctic being the dominant contributors to rising sea level. It is important to note that these estimates for different regions are not directly comparable owing to the differences in measurement periods.

7.9.2. Ablation due to iceberg calving

The relative proportions of ablation due to calving and surface mass balance are not well known, but available data suggest that calving plays an important role in the mass balance of glaciers in Alaska, the Canadian Arctic, Svalbard, and the Russian Arctic. There are 54 tidewater glaciers in northwestern North America, some of which are continuing their rapid retreat that commenced about 200 years ago. Among these, Columbia Glacier is undergoing the most rapid retreat exceeding 1 km/y since 2000, discharging an average of 3.3 Gt/y of calved ice during the period 1982 to 2001, with 6.6 Gt/y calved ice in 2001 (O'Neel et al., 2005). In Svalbard, calving losses accounted for about 32% of the overall glacier ablation (Błaszczyk et al., 2009). In Arctic Canada, Svalbard, and Severnaya Zemlya, calving comprises a significant fraction of the total ablation from several large ice caps including Devon Ice Cap and Prince of Wales Icefield, Austfonna, and Academy of Sciences Ice Cap

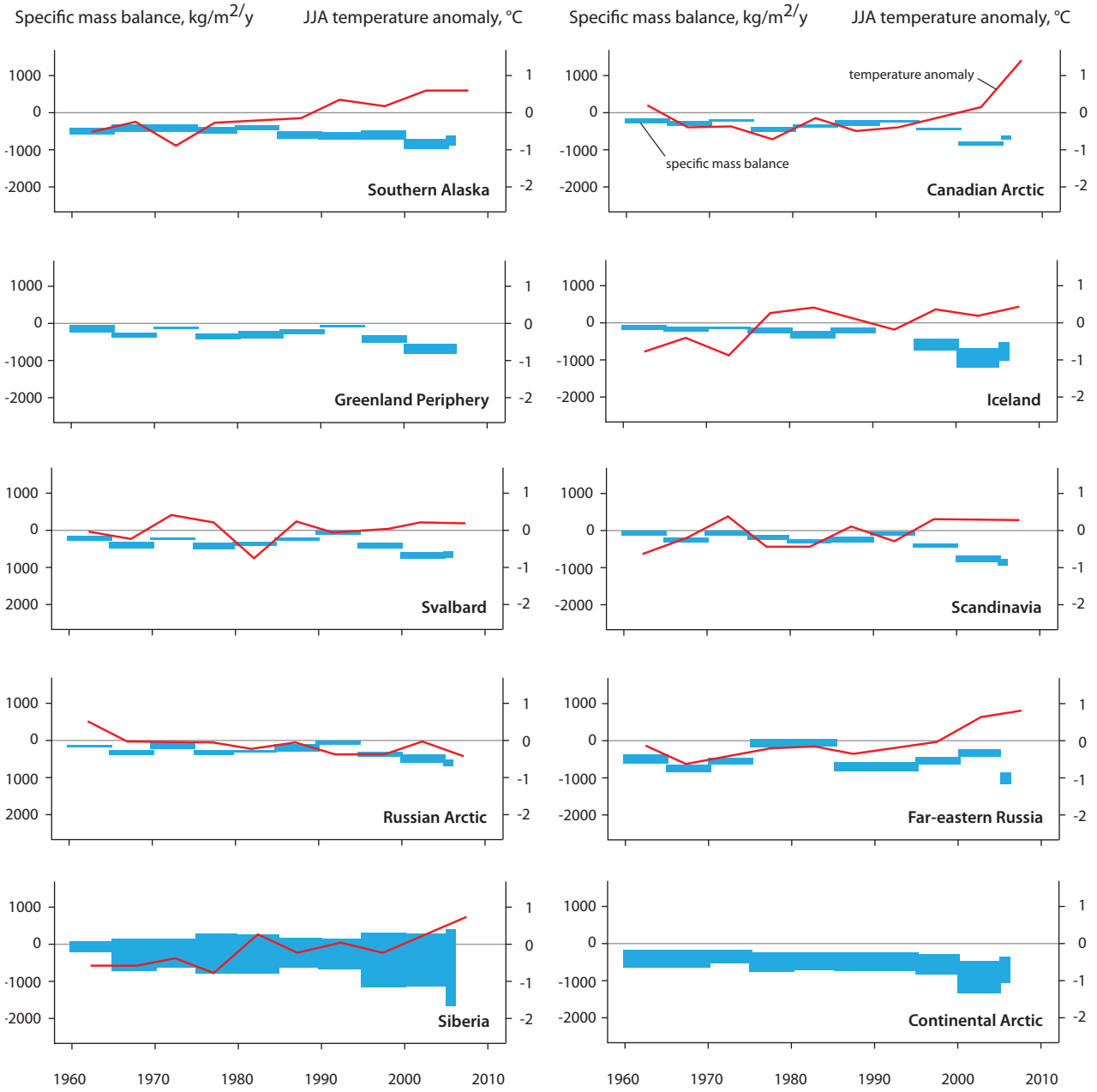

Figure 7.30. Estimates of pentadal mean annual specific mass balance for glacierized regions of the Arctic derived using the combined geodetic-glaciological dataset of Cogley (2009a) and the pentadal mean of annual anomalies in summer (June – August) air temperature at a geopotential height of 700 hPa over each region from the NCEP/NCAR Reanalysis. Temperature data are not plotted for the Greenland Periphery and Continental Arctic regions due to the non-contiguity of these regions. Source: Dan Moore, University of British Columbia.

(Dowdeswell et al., 2002, 2008; Burgess et al., 2005; Williamson et al., 2008). However, ongoing monitoring of calving fluxes is almost non-existent and, as a result, the magnitude of temporal variability and the existence and sign of any trend in calving fluxes are essentially unknown.

7.9.3. Observed trends in ice extent

Observed changes in ice extent over the past half-century are consistent with changes in mass. In nearly all regions, mass losses occurred coincidentally with decreases in glacier area. Although a small number of glaciers have advanced during this time, nearly all of these are tidewater or surge-type glaciers. The area evolution of tidewater and surge-type glaciers depends more on dynamic cycles than on direct climatic forcing, although it may be influenced by regional climate patterns.

7.9.4. Relationship to climate and circulation changes

Arctic air temperatures have increased during the past half-century (Hinzman et al., 2005), which probably explains much of the increase in rates of mass loss observed on Arctic glaciers. Increases in summer air temperature explain the accelerated losses from glaciers in northwestern North America (Arendt et al., 2009) and Arctic Canada (Gardner and Sharp, 2007), but uncertainties remain large due to the difficulties in modeling dynamic losses owing to calving.

In general, changes in synoptic-scale atmospheric circulation patterns, resulting from variations in sea-surface temperature, polar jet stream position, and other factors, correlate well with Arctic glacier mass balance time series. In northwestern North

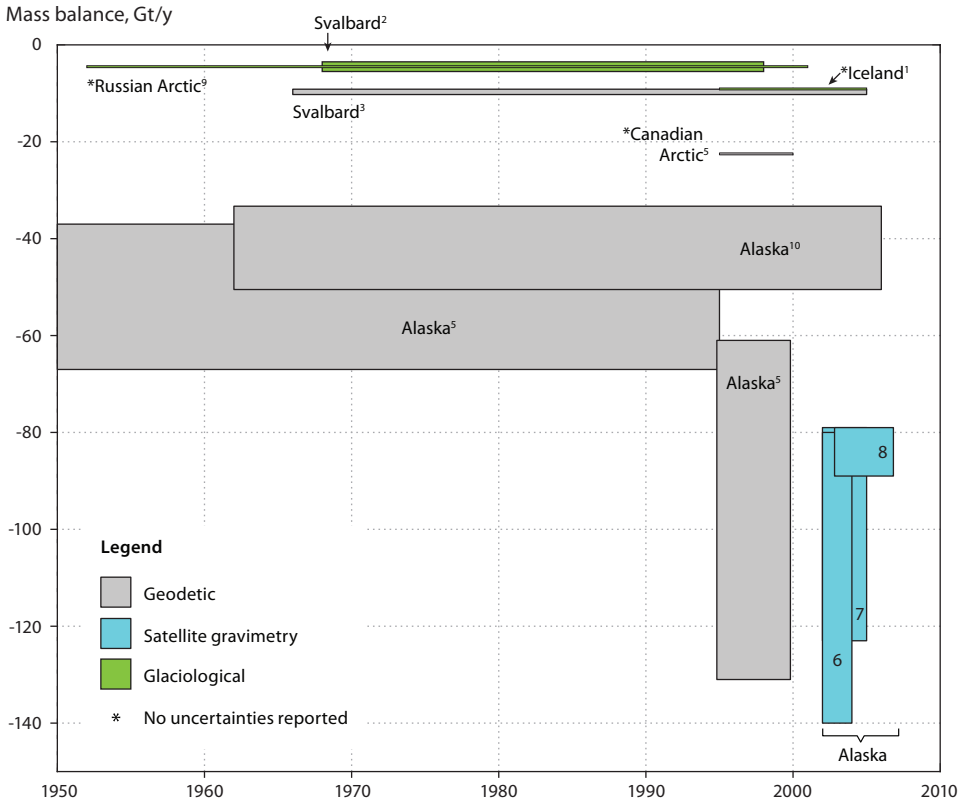

Figure 7.31. Estimates of the mass balance of Arctic glacier regions for which regional assessments have been conducted. The vertical extent of each box describes the range of uncertainty in the mass balance estimates (uncertainty estimates are not available for Iceland or the Canadian or Russian Arctic). Glaciological estimates relate only to the surface mass balance. Source: Anthony Arendt, University of Alaska, and W. Tad Pfeffer, INSTAAR, University of Colorado.

[1]Björnsson and Palsson (2008): data from two ice caps comprising 81% of the ice-covered area of Iceland; [2]Hagen et al. (2003a): surface mass balance component, Hagen et al. (2003b) calving component; [3]Nuth et al. (2010): date ranges are 1965/90 to 2003/07; [4]Abdalati et al. (2004); [5]Arendt et al. (2002); [6]Tamisiea et al. (2005); [7]Chen et al. (2006); [8]Luthcke et al. (2008); [9]Glazovsky and Macheret (2006); [10]Berthier et al. (2010).

America, two well-documented 'regime shifts' occurred in 1977 and 1989, during which temperatures abruptly shifted to more positive values and storm tracks changed direction. These shifts are evident in the mass balance time series of glaciers in Alaska (Bitz and Battisti, 1999; Josberger et al., 2007). In the Canadian Arctic, accelerated surface mass loss after 1987 was associated with changes in the position of the July circumpolar vortex. In the Russian Arctic, mass balance changes have been linked to sea-surface temperature variations in the Barents Sea.

7.9.5. Projections of future change

Modeling studies indicate that many individual glaciers may disappear by the end of the 21st century if air temperatures in the Arctic continue to rise as projected in the scenarios used by the suite of climate models employed in the Fourth Assessment of the IPCC (Solomon et al., 2007). The total volume of Arctic glaciers is projected to decline substantially by 2100. Projected reductions are of the order of 13% to 36% of current glacier volume. However, these projections vary greatly from model to model, are sensitive to the choice of climate scenario, and generally do not include mass losses by iceberg calving, which is known to be an important mode of ablation. Nonetheless, it is clear that glaciers in the Arctic are likely to continue to influence changes in global sea level well beyond the end of the 21st century.

7.9.6. Impacts

In many parts of the Arctic, climate warming should cause glacier runoff to increase for a few decades or longer, but glacier retreat will ultimately cause glacier runoff to decline. Runoff decline may already have started in some regions where most glaciers are small.

Changes in glacier runoff will influence freshwater habitat, water supply, hydroelectric power generation, flood and avalanche hazard, estuarine and coastal habitat, and patterns of ocean circulation. Glacier retreat may result in the destabilization and failure of valley-side slopes. Outburst floods from moraine-dammed lakes are likely to decrease in frequency as glaciers retreat further from moraines formed during the Little Ice Age. The frequency and magnitude of outbursts from existing glacier-dammed lakes may also change as ice dams are thinned by ice melting. However, new lakes may form further up-glacier as glacier margins recede down valley-side slopes and melt rates increase.

7.10. Knowledge gaps and recommendations

- The major gaps in knowledge that limit the ability to quantify current rates of glacier wastage in the Arctic and predict future trends are (i) the lack of a complete glacier inventory for the Arctic (including information about glacier location, area, surface topography, and ice thickness); (ii) the limited number of *in situ* mass balance measurements, the strong spatial bias in the distribution of available measurements, and the complete lack of measurements from areas such as the Russian Arctic; and (iii) the lack of ongoing monitoring programs for the iceberg calving component of mass balance, and limited knowledge of the major controls on calving fluxes.
- A coordinated effort to fill these knowledge gaps is needed in order to predict more reliably the current and future contribution of Arctic glaciers to global sea level change and better assess how glacier change will affect regional water resources.

7.10.1. Key gaps in knowledge

Despite progress since the Arctic Climate Impact Assessment (ACIA, 2005), major gaps remain in knowledge about Arctic glaciers and ice caps. The keys gaps are as follows:

1. There is a severe lack of basic information about glaciers in the Arctic. Knowledge gaps include the geographical distribution, total area and size distribution of glaciers in some regions, the distribution of area with elevation (hypsometry), and glacier thicknesses and, therefore, volume (Figure 7.32).
2. Glaciological mass balance measurements are limited to a small number of Arctic glaciers (50 in the 2000 to 2004 pentad, of which 30 were in Scandinavia), with larger glaciers and calving glaciers underrepresented. There have been no mass balance measurements conducted in Arctic Russia since 1990, and all but one measurement series from that region ended before 1980. In Arctic Canada, the number of measurement sites peaked at 13 in the early 1970s and is now only five. Given that the uncertainties associated with estimates of regional mass balance increase substantially as the number of local measurements decreases, there is a pressing need to continue (and expand) *in situ* monitoring programs and to develop alternative well-validated methods for assessing regional-scale glacier mass changes, including remote sensing observations (although a problem with these is the lack of temporal and methodological continuity between sensors and satellite missions) and numerical modeling.
3. Observations, process understanding, and modeling capabilities related to ablation by calving are severely limited, introducing large uncertainties into current and future mass balance estimates.

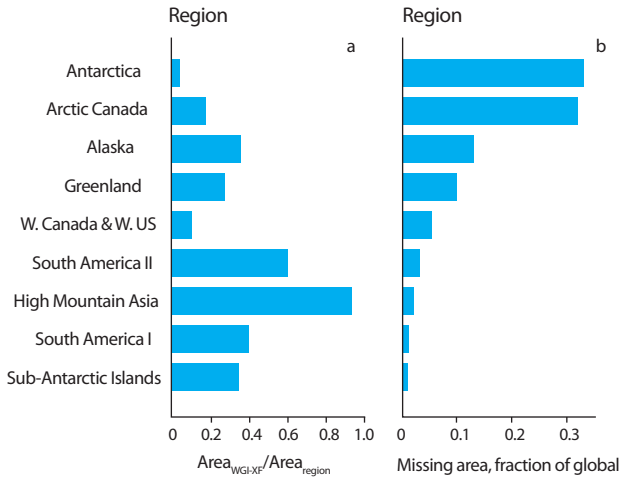

Figure 7.32. (a) Ratio between the area of Extended World Glacier Inventory (WGI-XF) glaciers (Cogley, 2009b), $A_{WGI-XF,}$ and regional glacier area, $A_{region,}$ for the nine glacierized regions that have incomplete glacier inventories. (b) Missing area in WGI-XF as a fraction of missing global glacierized area. While "a" shows the degree of completeness of each regional inventory, "b" indicates how much the different regions contribute to the global missing area. South America I refers to Bolivia, Ecuador, and Peru, while South America II refers to Argentina and Chile. Source: after Radić and Hock (2010).

7.10.2. Basic observations

Basic information about the geometry and distribution of glaciers is required to assess and model current and future mass changes and contributions of Arctic glaciers to changes in sea level, but this information is currently incomplete for the Arctic. As it is unlikely that direct volume measurements on regional scales will become available in the near future, volume estimates will continue to rely on volume-area scaling techniques. Nonetheless, more direct volume measurements, for example by airborne radio echo sounding, are required to validate scaling techniques.

Completion of high-quality Arctic-wide inventories of glacier areas and size distributions from recent optical satellite imagery is also essential to improve Arctic glacier mass balance assessments. It is important to have regional inventories based on glacier regions; regions should not be bisected by political borders.

There is need for an accurate pan-Arctic inventory of surge-type glaciers and a better understanding of surge recurrence intervals, to provide better estimates of the drawdown of ice by these unusual glaciers. The fraction of mountain glacier and ice cap area drained by marine outlets, and the size and discharge of the marine outlets (including the temporal variability in discharge), must be known if present-day estimates and future forecasts of mass loss by iceberg calving are to be improved.

7.10.3. Mass balance measurements, proxies, and modeling

Most of the uncertainties associated with mass balance estimates arise from the limited number of *in situ* observations. Because the number and distribution of *in situ* observations are unlikely to increase in the short term, there is a need to use remote sensing data to monitor ongoing changes in glacier geometry, surface mass balance, dynamics, and iceberg production. In particular, the potential for estimating mass change of Arctic ice caps using satellite gravimetry (GRACE) and repeat-track altimetry data from the Geoscience Laser Altimeter System on ICESat and its successor needs to be explored more fully. The successful launch in April 2010 of the European Space Agency's CryoSat-2 satellite will create opportunities for monitoring changes in the thickness of the larger ice masses in the Arctic.

Most indices of glacier change at regional scales can only be derived from remote sensing sources, so it is important to continue to develop and maintain long and continuous time series of remote sensing data. The development of regional-scale indicators of mass balance is currently limited by the low spatial resolution of much readily available remote sensing data. This seriously impedes the ability to map the properties of smaller ice bodies containing a significant fraction of the total glacier mass, resolve local features, and properly interpret and validate interpretations using sub-pixel *in situ* data. This is particularly the case with mapping melt duration and identifying the limits of snow and ice facies (especially the superimposed ice zone) from active microwave data that are freely available at the pan-Arctic scale. The accuracy of the results of facies mapping affects the accuracy of secondary indices (e.g., equilibrium-line altitude and accumulation area ratio) derived from facies maps. The ability to monitor regional-scale mass balance proxies at high spatial and temporal resolution is dependent on the

availability of microwave scatterometer data and enhanced resolution products (e.g., QuikSCAT SIR). It is crucial for the construction of long-term records that these data sources be replaced following the recent demise of QuikSCAT.

Uncertainties in nearly all mass balance methods are poorly quantified and rarely reported, although the latter problem is abating steadily. Often it is not clear whether reported mass balances include internal accumulation or calving, both of which can be major components of the mass balance; this makes direct comparison of different measurements problematic. The effects of internal accumulation and superimposed ice formation on glaciological mass balance measurements need to be quantified and these processes need to be included in mass balance modeling. Rigorous identification of sources and magnitudes of error is necessary through intercomparison of methods. Methods for combining mass balance datasets derived from different sampling techniques and representing different time periods and regions need to be expanded and improved to deliver firmer estimates of mass balance and contributions to sea level rise for all Arctic ice masses. The number of glaciologists with expertise in mass balance compilation and integration is also declining and a new generation of glaciologists with these skills must be trained soon.

Given the limited number of *in situ* observations, modeling will continue to play an important and growing role in the assessment of ongoing change in surface mass balance as well as in the projection of future changes. Regional-scale modeling remains a challenge because of the difficulties involved in downscaling climate re-analysis data and climate model results to the complex topography and the heterogeneous climatic conditions of mountain glacier and ice cap environments. These problems are exacerbated by the limited availability of ground measurements made on glaciers to validate the results of downscaling. Projections of future mass balance are also challenging owing to the magnitude of the uncertainty in climate projections for the Arctic that results both from the choice of forcing scenarios used to drive the climate models and large inter-model differences in climate response to the same forcing scenario.

7.10.4. Ice dynamics and ablation by iceberg calving

Although, with the possible exception of internal accumulation (but see Reeh et al., 2005 and Reeh, 2008 for recent progress), processes related to surface mass balance are relatively well understood, there is a severe gap in understanding and modeling of mass loss by calving. Glaciers that terminate in water can have dynamic instabilities that result in rapid mass losses. However, for glacier calving and glacier-marine interactions, there is a lack of both the physical understanding of critical processes and the observations necessary to validate the mathematical representation of these processes. There is also a lack of direct measurements of calving flux and its variability, and of the roles that glacier-marine interactions, bathymetry, ocean temperature, and terminus geometry and dynamics play in determining rates and patterns of glacier retreat and advance. Another area where understanding is limited involves the relationships between summer melt, the development of meltwater drainage systems on, in, and under glaciers, the delivery of water to glacier beds, and the subsequent effects on glacier sliding.

Such information would provide constraints on estimates of total dynamic mass losses and would improve modeling results. There appear to be fundamental differences between calving from tidewater glaciers that terminate in the ocean and calving from those that terminate in freshwater, but these remain poorly understood. Ablation by calving has generally been neglected in predictions of future mass balances. Hence, there is an urgent need to incorporate suitable parameterizations in Arctic-wide mass balance modeling. Since approaches developed for modeling individual glaciers are not yet suitable for application at regional scales due to the paucity of constraining observational data and the largely unresolved nature and complexity of the processes involved, there is a need to explore simpler empirical parameterizations. Given that iceberg keel plowing of sea-floor sediments is a major hazard to underwater engineering structures, there is very little knowledge of the size-frequency distribution of iceberg keel depths or the sources of large icebergs.

7.10.5. Impacts

There is a general understanding that climate warming should cause an initial increase in glacier runoff, followed by a decreasing trend. However, the magnitude of peak runoff and the timing of the shift from increasing to decreasing runoff are not known for most watersheds. Indeed, it is possible that some glaciers are currently in the phase of declining runoff, although the total stored ice volume is large enough that an Arctic-wide decline in loss will not occur in the near future. This knowledge gap is particularly critical because changes in glacier runoff control many other impacts, including those on water quality, stream channel dynamics, and circulation in estuaries and coastal waters. There is a need for further simulations of the transient response of glacier geometry and runoff, and their application to a range of drainage basins and climate scenarios, to understand better the sensitivity of runoff changes to climate forcing and its regional variability.

There is a reasonable consensus regarding the direction of stream temperature response to changing glacier runoff and glacier retreat. However, the magnitudes are uncertain. There is less certainty regarding the changes in biogeochemistry and sediment yields. Further process-based research and model development are required to address these gaps. Without predictions of these water quality responses to future climate-glacier change it is not possible to make reasonable projections of the impacts on aquatic ecosystems.

Finally, the impact of climate change on the magnitude and frequency of glacier hazards needs to be understood with a considerably greater degree of confidence to be useful.

Appendix 7.1 Glossary of glaciological terms

Definitions largely follow those proposed by Cogley et al. (2011).

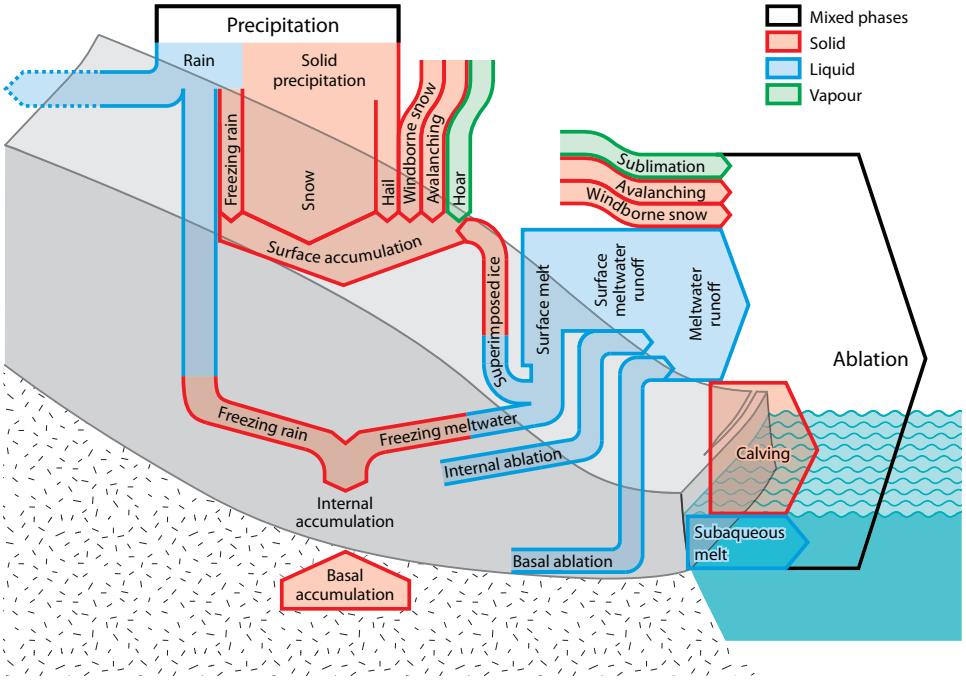

Components of the mass balance of a glacier. The arrows have arbitrary widths and do not indicate physical pathways of mass transfer. Source: after Cogley et al. (2011).

Accumulation area ratio

The *accumulation area ratio* (AAR), often expressed as a percentage, is the ratio of the area of the accumulation area to the area of the glacier. The AAR is bounded between 0.0 and 1.0 and its value often correlates well with the surface mass balance. The likelihood that mass balance will be positive increases as the AAR approaches 1.0.

Calving

Calving involves the breaking off of discrete pieces of ice from a glacier terminus into a lake or marine waters, producing icebergs. Calving of outlet glaciers is responsible for roughly half of the mass loss of the Greenland Ice Sheet (see Chapter 8), and can account for a significant part of the mass lost from glaciers in the Arctic.

Calving flux

Calving flux is the *mass flux by calving from a glacier terminus*, with dimension mass per unit time [M/T]. The calving flux can be determined from ice thickness and velocity measurements close to the terminus and the change in ice mass due to terminus advance or retreat.

Equilibrium line

The equilibrium line is defined by the set of points on the surface of the glacier where the surface mass balance is zero at the end of the melt season. The equilibrium line separates the *accumulation area* (where the annual mass balance is positive) from the *ablation area* (where the annual mass balance is negative). It coincides with the snowline (defined as the set of points on a glacier forming the lower boundary of the snow-covered area) only if all mass exchange occurs at the surface of the glacier and there is no superimposed ice. Where superimposed ice forms, the equilibrium line marks the lower limit of superimposed ice formation and occurs at a lower elevation than the snowline.

Equilibrium-line altitude

The spatially averaged altitude of the *equilibrium line* is known as the equilibrium-line altitude (ELA). The ELA is generally determined by fitting a curve to data representing *surface mass balance* as a function of altitude, although it may also be defined by direct visual observation. The ELA often correlates well with the surface mass balance.

Glacier surge

A glacier surge represents anomalously fast glacier motion (10 to 100 times non-surging speeds) sustained for a period of months to years. Surges commonly alternate with slower motion lasting for periods of years to centuries during which the glacier thickens in its upper reaches and thins in its lower reaches. Surging transfers most of the accumulated reservoir of ice from high on the glacier to its lowest reaches, and often extends the glacier terminus by significant distances (kilometres). Surges recur at fairly consistent, glacier-specific intervals. Surge-type glaciers may end on land or in the ocean and are clustered geographically for reasons that are not well understood. Surges seem to be related to changes in the subglacial hydrological regime and not primarily to climatic fluctuations. They are

controlled in some cases by thermal processes ('Svalbard-type surging', characterized by long quiescent periods) and in other cases by hydraulic processes ('Alaskan-type surging' characterized by shorter quiescent periods and higher velocities relative to Svalbard-type surges). While the processes involved in surging are understood in broad terms, many details of their behavior remain elusive (Raymond, 1987).

Internal accumulation

Internal accumulation is the refreezing of surface meltwater (or freezing of rain) that is in transit through the glacier that otherwise would have left the glacier as runoff. Water that freezes within the current year's snowpack is not counted as internal accumulation. Internal accumulation may be regarded as simply redistributing mass within the glacier. On many Arctic glaciers, internal accumulation is a major component in the mass balance and failure to account for it results in a measurement bias towards overestimation of mass loss. Typically, internal accumulation is not detected by traditional surface mass balance measurements.

Mass balance

The mass balance is the change in the mass of a glacier or ice body over a stated span of time, often expressed as a rate. Mass gain (accumulation) mainly occurs by snowfall. On some glaciers deposition of hoar, gain of blowing and drifting snow, avalanching, and basal freeze-on (usually beneath floating ice) are significant processes of accumulation. The glacier loses mass (ablation) mainly by melting and iceberg calving. On some glaciers, sublimation, evaporation, loss of blowing and drifting snow, and ice avalanching are significant processes of ablation. In some cases, a fraction of the meltwater produced (plus rainfall) can refreeze, either within snow or firn (see *internal accumulation*) or on the ice surface (see *superimposed ice*), and does not contribute to mass loss from the glacier. These processes are summarized in Figure 7.8. There are several ways to measure mass balance; these are described in Section 7.3.2.1.

The principal mass balance components are surface accumulation (C_{sfc}, usually mostly snowfall and superimposed ice formation), surface ablation (A_{sfc}, usually mostly melt), internal accumulation C_i, internal ablation A_i, basal accumulation C_b, and basal ablation A_b, and (for ocean- or lake-terminating glaciers) iceberg calving D, so the glacier-wide mass balance $\dot{M}$ expressed as a rate is given by:

$$\dot{M} = \dot{C}_{sfc} + \dot{A}_{sfc} + \dot{C}_i + \dot{A}_i + \dot{C}_b + \dot{A}_b + \dot{D}$$

All terms have the dimension mass per unit time, [M/T]. Surface accumulation and ablation tend to be major components on most land-terminating Arctic glaciers. Internal accumulation is also important on the Greenland Ice Sheet and many polythermal/cold glaciers. Basal ablation can be a dominant component of the mass balance of floating tongues of marine-terminating glaciers, while basal accumulation and internal ablation are generally negligible.

The sum $C_{sfc} + A_{sfc}$ defines the **surface mass balance,** B_{sfc} or SMB, the latter symbol often being used in ice sheet studies. In estimates of ice sheet mass balance, the term has often been extended to include internal accumulation. In addition to snowfall and superimposed ice, surface accumulation also includes deposition of hoar, freezing rain, solid precipitation in forms other than snow (e.g., hail), and snow transported by wind or avalanches.

Mass balance units

The principal dimension for mass balance is mass per unit time [M/T]. Ice sheet balances are often expressed in Gt/y (1 Gt = 10^{12} kg). However, the mass balance, especially of smaller ice bodies, is usually treated as a rate of change of mass per unit area, in which case it is referred to as *specific mass balance* and its dimension becomes [M/L^2/T], for example, kg/m^2/y, which is numerically identical to the millimetre water equivalent, mm w.e./y. While mass units (e.g., kg or Gt) are useful for hydrological or sea level calculations, specific units (e.g., kg/m^2, mm w.e.) are needed for comparisons of glaciers of different sizes, for example, when investigating glacier-climate interactions. Mass balances, in particular for larger ice bodies, are often expressed in **sea level equivalent** (SLE), which is the change in mean global sea level that would result if glacier mass were added or removed from the ocean. SLE in mm/y is often simply obtained by

$$SLE = \frac{0.001 \dot{M} A_{glacier}}{\rho_w A_{ocean}}$$

where the glacier mass change $\dot{M}$ is in kg/m^2/y and the areas of the glacier ($A_{glacier}$) and the ocean (A_{ocean}) are in m^2; ρ_w is the density of freshwater (1000 kg/m^3).

Superimposed ice

Ice accumulated on top of glacier ice by the refreezing of rain or meltwater produced during the current mass balance year is known as superimposed ice. It is different from internal accumulation, which represents refreezing within firn below the summer surface formed at the end of the summer in the previous mass balance year. Measurement of superimposed ice accumulation requires special attention in conventional mass balance programs.

Tidewater glacier

A tidewater glacier terminates in the sea, with its terminus either floating or grounded below sea level. Tidewater glaciers can undergo a periodic growth/shrinkage instability with long periods (centuries) of slower motion and slow advance alternating with shorter periods (decades) of rapid motion, high calving flux, and rapid (~1 km/y) retreat (Meier and Post, 1987).

Termed *tidewater instability*, this cyclic behavior has been documented most extensively in Alaska (Post, 1975), although it has been observed in many other regions, and the present retreat of certain Greenland Ice Sheet outlet glaciers appears to operate in a nearly identical fashion (Howat et al., 2005). During rapid retreat, a glacier can thin far faster (by loss of the marine-grounded tongue plus drawdown of an upstream basin by rapid flow) than can be accomplished by surface mass

balance alone. In its advancing phase, a tidewater terminus is stabilized by back-stress against a push moraine at its advancing margin. A tidewater glacier in an advanced position can switch abruptly (~years) to an unstable phase of thinning in its ocean-grounded reach, fast flow, and rapid calving which results in terminus retreat. Once initiated, fast flow and retreat can continue until the glacier's terminus retreats to a point where the glacier bed rises above sea level.

The causes of unstable retreat are not completely understood, but involve high basal water pressures tied to the depth of the glacier bed below sea level, rapid sliding, vertical thinning, and positive feedback between thinning and fast flow. The processes governing the size and rate of production of icebergs are extremely poorly known. Climate-induced thinning can play a critical role in initiating unstable retreat, but once initiated, unstable retreat is modulated by channel geometry and englacial and basal hydrology and is essentially independent of climate and surface mass balance.

References

Abdalati, W., W. Krabill, E. Frederick, S. Manizade, C. Martin, J. Sonntag, R. Swift, R. Thomas, J. Yungel and R. Koerner, 2004. Elevation changes of ice caps in the Canadian Arctic Archipelago. Journal of Geophysical Research-Earth Surface, 109:F04007.

ACIA, 2004. Impacts of a Warming Arctic. Arctic Climate Impact Assessment. pp. 140. Cambridge University Press.

ACIA, 2005. Arctic Climate Impact Assessment. pp. 1024. Cambridge University Press.

Aðalgeirsdóttir, G., T. Johannesson, H. Bjornsson, F. Palsson and O. Sigurosson, 2006. Response of Hofsjökull and southern Vatnajökull, Iceland, to climate change. Journal of Geophysical Research-Earth Surface, 111:F03001.

Alley, R.B., H.J. Horgan, I. Joughin, K.M. Cuffey, T.K. Dupont, B.R. Parizek, S. Anandakrishnan and J. Bassis, 2008. A simple law for ice-shelf calving. Science, 322:1344-1344.

Amundson, J.M., M. Fahnestock, M. Truffer, J. Brown, M.P. Lüthi and R.J. Motyka, 2010. Ice mélange dynamics and implications for terminus stability, Jakobshavn Isbræ Greenland. Journal of Geophysical Research-Earth Surface, 115:F01005.

Ananicheva, M.D. and G. Kapustin, 2010. Change of glacier state in mountain regions of the Russian sub-arctic: assessment by satellite imagery and aerial photography in the USSR glacier inventory [in Russian; English summary on last page]. Russian contribution into the IPY. 2007-2008. Vol.3 Cryosphere, pp. 19-26.

Ananicheva, M.D. and A.N. Krenke, 2007. Glaciation and snow cover in North Eurasia in immediate future. In: Kotlyakov, V.M. (Ed.). Glaciation in North Eurasia in the Recent Past and Immediate Future, pp. 277-293, Nauka, Moscow.

Ananicheva, M.D., G.A. Kapustin and M.M. Koreysha, 2006. Glacier changes in the Suntar-Khayata mountains and Chersky Range from the glacier inventory of the USSR and satellite images 2001-2003. Data of Glaciological Studies, 101:163-169.

Ananicheva, M.D., A.N. Krenke, and R.G. Barry, 2010. The Northeast Asia mountain glaciers in the near future by AOGCM scenarios. The Cryosphere, 4:435-445.

Anderson, S.P., 2007. Biogeochemistry of glacial landscape systems. Annual Review of Earth and Planetary Sciences, 35:375-399.

Anderson, R.K., G.H. Miller, J.P. Briner, N.A. Lifton and S.B. DeVogel, 2008. A millennial perspective on Arctic warming from C-14 in quartz and plants emerging from beneath ice caps. Geophysical Research Letters, 35:L01502.

Andreassen, L.M., H. Elvehøy, B. Kjøllmoen, R.V. Engeset and N. Haakensen, 2005. Glacier mass-balance and length variation in Norway. Annals of Glaciology, 42:317-325.

Anesio, A.M., A.J. Hodson, A. Fritz, R. Psenner and B. Sattler, 2009. High microbial activity on glaciers: importance to the global carbon cycle. Global Change Biology, 15:955-960.

Anon, 2004. The Alaska Tourism Satellite Account. A comprehensive analysis of the economic contribution of travel and tourism. 24 pp. Global Insight,

Arendt, A.A., K.A. Echelmeyer, W.D. Harrison, C.S. Lingle and V.B. Valentine, 2002. Rapid wastage of Alaska glaciers and their contribution to rising sea level. Science, 297:382-386.

Arendt, A., K. Echelmeyer, W. Harrison, C. Lingle, S. Zirnheld, V. Valentine, B. Ritchie and M. Druckenmiller, 2006. Updated estimates of glacier volume changes in the western Chugach Mountains, Alaska, and a comparison of regional extrapolation methods. Journal of Geophysical Research-Earth Surface, 111:F03019.

Arendt, A., J. Walsh and W. Harrison, 2009. Changes of glaciers and climate in northwestern North America during the late twentieth century. Journal of Climate, 22:4117-4134.

Ashmore, P. and M. Church, 2001. The impact of climate change on rivers and river processes in Canada. Geological Survey of Canada Bulletin, 555:58.

Bahr, D.B., M.F. Meier and S.D. Peckham, 1997. The physical basis of glacier volume-area scaling. Journal of Geophysical Research-Solid Earth, 102:20355-20362.

Bakke, J., S.O. Dahl, Ø. Paasche, R. Løvlie and A. Nesje, 2005. Glacier fluctuations, equilibrium-line altitudes and palaeoclimate in Lyngen, northern Norway, during the Lateglacial and Holocene. The Holocene, 15:518-540.

Bamber, J.L., S. Ekholm and W.B. Krabill, 2001. A new, high-resolution digital elevation model of Greenland fully validated with airborne laser altimeter data. Journal of Geophysical Research-Solid Earth, 106:6733-6745.

Bamber, J., W. Krabill, V. Raper and J. Dowdeswell, 2004. Anomalous recent growth of part of a large Arctic ice cap: Austfonna, Svalbard. Geophysical Research Letters, 31:L12402.

Barkov, N.I., D.Y. Bolshiyanov, O.A. Gvozdik, O.L. Klementyev, V.M. Makeyev, I.G. Maksimenko, V.Y. Potapenko and K.R.I. Yuna, 1992. New data on structure and development of Vavilov Glacier on Severnaya Zemlya [in Russian]. Data of Glaciological Studies, 75:35-41.

Barrand, N.E. and M.J. Sharp, 2010. Sustained rapid shrinkage of Yukon glaciers since the 1957-1958 International Geophysical Year. Geophysical Research Letters, 37:L07501.

Bassford, R.P., M.J. Siegert and J.A. Dowdeswell, 2006. Quantifying the mass balance of ice caps on Severnaya Zemlya, Russian High Arctic. III: Sensitivity of ice caps in Severnaya Zemlya to future climate change. Arctic, Antarctic and Alpine Research, 38:21-33.

Benn, D.I., C.R. Warren and R.H. Mottram, 2007. Calving processes and the dynamics of calving glaciers. Earth-Science Reviews, 82:143-179.

Benson, C.S., 1962. Stratigraphic studies in the snow and firn of Greenland ice sheet. CRREL (SIPRE) Research Report, 70, 93 pp.

Berthier, E., E. Schiefer, G.K.C. Clarke, B. Menounos and F. Rémy, 2010. Contribution of Alaskan glaciers to sea-level rise derived from satellite imagery. Nature Geoscience, 3:92-95.

Bindschadler, R., J. Dowdeswell, D. Hall and J.G. Winther, 2001. Glaciological applications with Landsat-7 imagery: early assessments. Remote Sensing of Environment, 78:163-179.

Bitz, C.M. and D.S. Battisti, 1999. Interannual to decadal variability in climate and the glacier mass balance in Washington, western Canada, and Alaska. Journal of Climate, 12:3181-3196.

Björnsson, H. and F. Palsson, 2008. Icelandic glaciers. Jökull, 58:365-386.

Björnsson, H., F. Palsson, O. Sigurðsson and G.E. Flowers, 2003. Surges of glaciers in Iceland. Annals of Glaciology, 36:82-90.

Blais, J.M., D.W. Schindler, D.C.G. Muir, M. Sharp, D. Donald, M. Lafrenière, E. Braekevelt and W.M.J. Strachan, 2001. Melting glaciers: A major source of persistent organochlorines to subalpine Bow Lake in Banff National Park, Canada. Ambio, 30:410-415.

Blake, W., 1981. Neoglacial fluctuations of glaciers, southeastern Ellesmere Island, Canadian Arctic Archipelago. Geografiska Annaler Series a-Physical Geography, 63:201-218.

Blake, W.J., 1989. Radiocarbon dating by accelerator mass spectrometry: A contribution to the chronology of Holocene events in Nordaustlandet, Svalbard. Geografiska Annaler 71A:51-74.

Blaszczyk, M., J.A. Jania and J.O. Hagen, 2009. Tidewater glaciers of Svalbard: Recent changes and estimates of calving fluxes. Polish Polar Research, 30:85-142.

Bolch, T., B. Menounos and R. Wheate, 2010. Landsat-based inventory of glaciers in western Canada, 1985-2005. Remote Sensing of Environment, 114:127-137.

Boon, S. and M. Sharp, 2003. The role of hydrologically-driven ice fracture in drainage system evolution on an Arctic glacier. Geophysical Research Letters, 30:1916.

Boyd, E.S., M. Skidmore, A.C. Mitchell, C. Bakermans and J.W. Peters, 2010. Methanogenesis in subglacial sediments. Environmental Microbiology Reports 2:685-692.

Brabets, T.P. and M.A. Walvoord, 2009. Trends in streamflow in the Yukon River Basin from 1944 to 2005 and the influence of the Pacific Decadal Oscillation. Journal of Hydrology, 371:108-119.

Braithwaite, R.J., 2005. Mass-balance characteristics of arctic glaciers. Annals of Glaciology, 42:225-229.

Brandt, O., J. Kohler and M. Luthje, 2008. Spatial mapping of multi-year superimposed ice on the glacier Kongsvegen, Svalbard. Journal of Glaciology, 54:73-80.

Briner, J.P., P.T. Davis and G.H. Miller, 2009. Latest Pleistocene and Holocene glaciation of Baffin Island, Arctic Canada: key patterns and chronologies. Quaternary Science Reviews, 28:2075-2087.

Brooks, G.R., 1994. The fluvial reworking of late Pleistocene drift, Squamish River drainage basin, southwest British Columbia. Géographie physique et Quaternaire, 48:51-68.

Brown, C.S., M.F. Meier and A. Post, 1982. Calving speed of Alaska tidewater glaciers, with application to Columbia Glacier. USGS Professional Paper, 1258-C, 20 pp.

Brown, L.E., D.M. Hannah and A.M. Milner, 2003. Alpine stream habitat classification: An alternative approach incorporating the role of dynamic water source contributions. Arctic, Antarctic and Alpine Research, 35:313-322.

Burgess, D.O. and M.J. Sharp, 2004. Recent changes in areal extent of the Devon Ice Cap, Nunavut, Canada. Arctic, Antarctic and Alpine Research, 36:261-271.

Burgess, D.O., M.J. Sharp, D.W.F. Mair, J.A. Dowdeswell and T.J. Benham, 2005. Flow dynamics and iceberg calving rates of Devon Ice Cap, Nunavut, Canada. Journal of Glaciology, 51:219-230.

Buzin, I.V. and A.F. Glazovsky, 2005. Icebergs of Shokalsky glacier, Novaya Zemlya. Data of Glaciological Studies, 99:39-44.

Buzin, I.V., A.F. Glazovsky, Y.P. Gudoshnikov, A.I. Danilov, N.Y. Dmitiev, G.K. Zubakin, N.V. Kubyshkin, A.K. Naumov, A.V. Nesterov, A.A. Skutin, E.A. Skutina and S.I. Shibakin, 2008. Icebergs and glaciers of the Barents Sea. Results of the most recent research. Part.1. Main producing glaciers, their propagation and morphometric properties. [in Russian with English summary]. Problems of the Arctic and Antarctic, 78:66-80.

Cazenave, A., K. Dominh, S. Guinehut, E. Berthier, W. Llovel, G. Ramillien, M. Ablain and G. Larnicol, 2009. Sea level budget over 2003-2008: A reevaluation from GRACE space gravimetry, satellite altimetry and Argo. Global and Planetary Change, 65:83-88.

Chapman, W.L. and J.E. Walsh, 2007. Simulations of Arctic temperature and pressure by global coupled models. Journal of Climate, 20:609-632.

Chen, J.L., C.R. Wilson and B.D. Tapley, 2006. Satellite gravity measurements confirm accelerated melting of Greenland ice sheet. Science, 313:1958-1960.

Church, M., 1974. Hydrology and permafrost with reference to North America. – Paper presented at Proceedings of Workshop Seminar 1974, Permafrost Hydrology, pp. 7-20. Canadian National Committee for the International Hydrological Decade, Ottawa

Church, M., 1983. Pattern of instability in a wandering gravel bed channel. In: Collinson, J.D. and J. Lewin (Eds.). Modern and Ancient Fluvial Systems, pp. 169-180, International Association of Sedimentologists Special Publication,

Citterio, M., F. Paul, A.P. Ahlstrom, H.F. Jepsen and A. Weidick, 2009. Remote sensing of glacier change in West Greenland: accounting for the occurrence of surge-type glaciers. Annals of Glaciology, 50:70-80.

Clague, J.J. and S.G. Evans, 1994. Formation and failure of natural dams in the Canadian Cordillera. Geological Survey of Canada, Bulletin 464.

Clague, J.J. and S.G. Evans, 2000. A review of catastrophic drainage of moraine-dammed lakes in British Columbia. Quaternary Science Reviews, 19:1763-1783.

Clague, J., J.R. Harper, R.J. Hebda and D.E. Howes, 1982. Late Quaternary sea levels and crustal movements, coastal British Columbia. Canadian Journal of Earth Sciences, 19:597-618.

Clague, J.J., R.J.W. Turner and A.V. Reyes, 2003. Record of recent river channel instability, Cheakamus Valley, British Columbia. Geomorphology, 53:317-332.

Clarke, G.K.C., 2003. Hydraulics of subglacial outburst floods: new insights from the Spring-Hutter formulation. Journal of Glaciology, 49:299-313.

Cogley, J.G., 2005. Mass and energy balances of glaciers and ice sheets. In: Anderson, M.G. (Ed.). Encyclopedia of Hydrological Sciences, pp. 2555-2573, Wiley.

Cogley, J.G., 2009a. Geodetic and direct mass-balance measurements: comparison and joint analysis. Annals of Glaciology, 50:96-100.

Cogley, J.G., 2009b. A more complete version of the World Glacier Inventory. Annals of Glaciology, 50:32-38.

Cogley, J.G. and W.P. Adams, 1998. Mass balance of glaciers other than the ice sheets. Journal of Glaciology, 44:315-325.

Cogley, J.G., W.P. Adams, M.A. Ecclestone, F. JungRothenhausler and C.S.L. Ommanney, 1996. Mass balance of White Glacier, Axel Heiberg island, NWT, Canada, 1960-91. Journal of Glaciology, 42:548-563.

Cogley, J.G., R. Hock, L.A. Rasmussen, A.A. Arendt, A. Bauder, R.J. Braithwaite, P. Jansson, G. Kaser, M. Moller, L. Nicholson and M. Zemp, 2011. Glossary of Glacier Mass Balance and Related Terms. IHPVII Technical Documents in Hydrology No. 86, IACS Contribution No. 2, UNESCO-IHP.

Colgan, W. and M. Sharp, 2008. Combined oceanic and atmospheric influences on net accumulation on Devon Ice Cap, Nunavut, Canada. Journal of Glaciology, 54:28-40.

Copland, L., D.R. Mueller and L. Weir, 2007. Rapid loss of the Ayles ice shelf, Ellesmere Island, Canada. Geophysical Research Letters, 34:L21501.

Copland, L., M.J. Sharp and J.A. Dowdeswell, 2003. The distribution and flow characteristics of surge-type glaciers in the Canadian High Arctic. Annals of Glaciology, 36:73-81.

Costa, J.E. and R.L. Schuster, 1988. The formation and failure of natural dams. Geological Society of America Bulletin, 100:1054-1068.

D'Elia, T., R. Veerapaneni and S.O. Rogers, 2008. Isolation of microbes from Lake Vostok accretion ice. Applied and Environmental Microbiology, 74:4962-4065.

Dahl, T.M., C. Lydersen, K.M. Kovacs, S. Falk-Petersen, J. Sargent, I. Gjertz and B. Gulliksen, 2000. Fatty acid composition of the blubber in white whales (Delphinapterus leucas). Polar Biology, 23:401-409.

De Ruyter de Wildt, M.S. and J. Oerlemans, 2003. Satellite retrieval of mass balance: comparing SAR images with albedo images and in situ mass-balance observations. Journal of Glaciology, 49:437-448.

De Ruyter de Wildt, M.S., J. Oerlemans and H. Björnsson, 2002. A method for monitoring glacier mass balance using satellite albedo measurements: application to Vatnajökull, Iceland. Journal of Glaciology, 48:267-278.

de Woul, M. and R. Hock, 2005. Static mass-balance sensitivity of Arctic glaciers and ice caps using a degree-day approach. Annals of Glaciology, 42:217-224.

Desloges, J.R. and M. Church, 1987. Channel and floodplain facies in a wandering gravel-bed river. In: Ethridge, F.G. and R.M. Flores (Eds.). Recent Developments in Fluvial Sedimentology, pp. 99-109.

Divine, D.V. and C. Dick, 2006. Historical variability of sea ice edge position in the Nordic Seas. Journal of Geophysical Research-Oceans, 111:C01001.

Dmitriev, N.Y. and A.V. Nesterov, 2007. Iceberg drift in the Barents Sea according to observation data and simulation results. – Paper presented at The 17th International Offshore and Polar Engineering Conference (ISOPE-2007), pp. 633-638. The International Society of Offshore and Polar Engineers, Lisbon, Portugal, July 1-6, 2007.

Dorava, J.M. and A.M. Milner, 2000. Role of lake regulation on glacier-fed rivers in enhancing salmon productivity: the Cook Inlet watershed, south-central Alaska, USA. Hydrological Processes, 14:3149-3159.

Dowdeswell, J.A., 1986. Remote sensing of ice cap outlet glacier fluctuations on Nordaustlandet, Svalbard. Polar Research, 4:25-32.

Dowdeswell, J.A., 1989. On the nature of Svalbard icebergs. Journal of Glaciology, 35:224-234.

Dowdeswell, J.A. and T.J. Benham, 2003. A surge of Perseibreen, Svalbard, examined using aerial photographs and ASTER high-resolution satellite imagery. Polar Research, 22:373-383.

Dowdeswell, J.A. and R. L. Collin, 1990. Fast-flowing outlet glaciers on Svalbard ice caps. Geology, 18:778-781.

Dowdeswell, J.A. and S. Evans, 2004. Investigations of the form and flow of ice sheets and glaciers using radio-echo sounding. Reports on Progress in Physics, 67:1821-1861.

Dowdeswell, J.A. and C.F. Forsberg, 1992. The size and frequency of icebergs and bergy bits from tidewater glaciers in Kongsfjorden, northwest Spitsbergen. Polar Research, 11:81-91.

Dowdeswell, J.A. and J.-O. Hagen, 2004. Arctic ice caps and glaciers. In: Bamber, J.L. and A.J. Payne (Eds.). Mass Balance of the Cryosphere: Observations and Modelling of Contemporary and Future Changes, pp. 527- 557, Cambridge University Press.

Dowdeswell, J.A. and M. Williams, 1997. Surge-type glaciers in the Russian High Arctic identified from digital satellite imagery. Journal of Glaciology, 43:489-494.

Dowdeswell, J.A., G.S. Hamilton and J.O. Hagen, 1991. The duration of the active phase on surge-type glaciers - contrasts between Svalbard and other regions. Journal of Glaciology, 37:388-400.

Dowdeswell, J.A., R.J. Whittington and R. Hodgkins, 1992. The sizes, frequencies, and freeboards of East Greenland icebergs observed using ship radar and sextant. Journal of Geophysical Research-Oceans, 97:3515-3528.

Dowdeswell, J.A., H. Villinger, R. J. Whittington and P. Marienfeld, 1993. Iceberg scouring in Scoresby Sund and on the East Greenland continental shelf. Marine Geology, 111:37-53.

Dowdeswell, J.A., M.R. Gorman, A.F. Glazovsky and Y.Y. Macheret, 1994. Evidence for floating ice shelves in Franz Josef Land, Russian High Arctic. Arctic and Alpine Research, 26:86-92.

Dowdeswell, J.A., R. Hodgkins, A.M. Nuttall, J.-O. Hagen and G.S. Hamilton, 1995. Mass balance change as a control on the frequency and occurrence of glacier surges in Svalbard, Norwegian High Arctic. Geophysical Research Letters, 22:2909-2912.

Dowdeswell, J.A., J.O. Hagen, H. Björnsson, A.F. Glazovsky, W.D. Harrison, P. Holmlund, J. Jania, R.M. Koerner, B. Lefauconnier, C.S.L. Ommanney and R.H. Thomas, 1997. The mass balance of circum-Arctic glaciers and recent climate change. Quaternary Research, 48:1-14.

Dowdeswell, J.A., R.J. Whittington, A. E. Jennings, J.T. Andrews, A. Mackensen and P. Marienfeld, 2000. An origin for laminated glacimarine sediments through sea-ice build-up and suppressed iceberg rafting. Sedimentology, 47:557-576.

Dowdeswell, J.A., R.P. Bassford, M.R. Gorman, M. Williams, A.F. Glazovsky, Y.Y. Macheret, A.P. Shepherd, Y.V. Vasilenko, L.M. Savatyuguin, H.W. Hubberten and H. Miller, 2002. Form and flow of the Academy of Sciences Ice Cap, Severnaya Zemlya, Russian High Arctic. Journal of Geophysical Research-Solid Earth, 107:2076.

Dowdeswell, J.A., T.J. Benham, M.R. Gorman, D. Burgess and M.J. Sharp, 2004. Form and flow of the Devon Island Ice Cap, Canadian Arctic. Journal of Geophysical Research-Earth Surface, 109:F02002.

Dowdeswell, E.K., J.A. Dowdeswell and F. Cawkwell, 2007. On the glaciers of Bylot Island, Nunavut, Arctic Canada. Arctic, Antarctic and Alpine Research, 39:402-411.

Dowdeswell, J.A., T.J. Benham, T. Strozzi and J.O. Hagen, 2008. Iceberg calving flux and mass balance of the Austfonna ice cap on Nordaustlandet, Svalbard. Journal of Geophysical Research-Earth Surface, 113:F03022.

Dunse, T., T.V. Schuler, J.O. Hagen, T. Eiken, O. Brandt and K.A. Hogda, 2009. Recent fluctuations in the extent of the firn area of Austfonna, Svalbard, inferred from GPR. Annals of Glaciology, 50:155-162.

Dwyer, J.L., 1995. Mapping tide-water glacier dynamics in east Greenland using LANDSAT data. Journal of Glaciology, 41:584-595.

Dyke, A.S., 1978. Indications of neoglacierization on Somerset Island, District of Franklin. Scientific and Technical Notes, Current Research, Part B. Geological Survey of Canada, 78-1B:215-217.

Dyurgerov, M.B., 2002. Glacier mass balance and regime: data of measurements and analysis. Occasional Paper 55, 268 pp. Institute of Arctic and Alpine Research, University of Colorado, Boulder,

Dyurgerov, M.B. and M.F. Meier, 2005. Glaciers and the changing earth system: a 2004 snapshot. Occasional Paper 58, 118 pp. Institute of Arctic and Alpine Research, University of Colorado, Boulder,

Dyurgerov, M., V.N. Uvarov and T.E. Kostjashkina, 1996. Mass balance and runoff of Tuyuksu glacier and the north slope of the Zailiyskiy Alatau Range, Tien Shan. Zeitschrift für Gletscherkunde und Glazialgeologie, 32:41-54.

Dyurgerov, M., M.F. Meier and D.B. Bahr, 2009. A new index of glacier area change: a tool for glacier monitoring. Journal of Glaciology, 55:710-716.

Early, D.S. and D.G. Long, 2001. Image reconstruction and enhanced resolution imaging from irregular samples. Ieee Transactions on Geoscience and Remote Sensing, 39:291-302.

Echelmeyer, K.A., W.D. Harrison, C.F. Larsen, J. Sapiano, J.E. Mitchell, J. DeMallie, B. Rabus, G. Aðalgeirsdóttir and L. Sombardier, 1996. Airborne surface profiling of glaciers: A case-study in Alaska. Journal of Glaciology, 42:538-547.

Eisen, O., W.D. Harrison and C.F. Raymond, 2001. The surges of Variegated Glacier, Alaska, USA, and their connection to climate and mass balance. Journal of Glaciology, 47:351-358.

Engeset, R.V., J. Kohler, K. Melvold and B. Lunden, 2002. Change detection and monitoring of glacier mass balance and facies using ERS SAR winter images over Svalbard. International Journal of Remote Sensing, 23:2023-2050.

England, J., N. Atkinson, J. Bednarski, A.S. Dyke, D.A. Hodgson and C.O. Cofaigh, 2006. The Innuitian Ice Sheet: configuration, dynamics and chronology. Quaternary Science Reviews, 25:689-703.

England, J.H., T.R. Lakeman, D.S. Lemmen, J.M. Bednarski, T.G. Stewart and D.J.A. Evans, 2008. A millennial-scale record of Arctic Ocean sea ice variability and the demise of the Ellesmere Island ice shelves. Geophysical Research Letters, 35:L19502.

Erga, S.R., K. Aursland, O. Frette, B. Hamre, J.K. Lotsberg, J.J. Stamnes, J. Aure, F. Rey and K. Stamnes, 2005. UV transmission in Norwegian marine waters: controlling factors and possible effects on primary production and vertical distribution of phytoplankton. Marine Ecology Progress Series, 305:79-100.

ESRI, 2003. Digital Chart of the World: for use with ARC/INFO software. 4 laser optical disks. 220 pp. Environmental Systems Research Institute, USA.

Evans, S.G. and J.J. Clague, 1994. Recent climatic change and catastrophic geomorphic processes in mountain environments. Geomorphology, 10:107-128.

Ficke, A.D., C.A. Myrick and L.J. Hansen, 2007. Potential impacts of global climate change on freshwater fisheries. Reviews in Fish Biology and Fisheries, 17:581-613.

Filippelli, G.M., C. Souch, B. Menounos, S. Slater-Atwater, A.J.T. Jull and O. Slaymaker, 2006. Alpine lake sediment records of the impact of glaciation and climate change on the biogeochemical cycling of soil nutrients. Quaternary Research, 66:158-166.

Fischer, M.P. and R.D. Powell, 1998. A simple model for the influence of push-morainal banks on the calving and stability of glacial tidewater termini. Journal of Glaciology, 44:31-41.

Fisher, D.A., 2002. High-resolution multiproxy climatic records from icecores, tree-rings, corals and documentary sources using eigenvector techniques and maps: assessment of recovered signal and errors. The Holocene, 12:401-419.

Fisher, D.A., R.M. Koerner, W.S.B. Paterson, W. Dansgaard, N. Gundestrup and N. Reeh, 1983. Effect of wind scouring on climatic records from ice-core cxygen-isotope profiles. Nature, 301:205-209.

Fisher, D.A., R.M. Koerner and N. Reeh, 1995. Holocene climatic records from Agassiz Ice Cap, Ellesmere Island, NWT, Canada. The Holocene, 5:19-24.

Fisher, D.A., R.M. Koerner, J.C. Bourgeois, G. Zielinski, C. Wake, C.U. Hammer, H.B. Clausen, N. Gundestrup, S. Johnsen, K. Goto-Azuma, T. Hondoh, E. Blake and M. Gerasimoff, 1998. Penny ice cap cores, Baffin Island, Canada, and the Wisconsinan Foxe Dome connection: Two states of Hudson Bay ice cover. Science, 279:692-695.

Fisher, D., E. Osterberg, A. Dyke, D. Dahl-Jensen, M. Demuth, C. Zdanowicz, J. Bourgeois, R.M. Koerner, P. Mayewski, C. Wake, K. Kreutz, E. Steig, J. Zheng, K. Yalcin, K. Goto-Azuma, B. Luckman and S. Rupper, 2008. The Mt Logan Holocene–late Wisconsinan isotope record: tropical Pacific–Yukon connections. The Holocene, 18:667-677.

Fleming, S.W., 2005. Comparative analysis of glacial and nival streamflow regimes with implications for lotic habitat quantity and fish species richness. River Research and Applications, 21:363-379.

Fleming, S.W. and G.K.C. Clarke, 2003. Glacial control of water resource and related environmental responses to climatic warming, empirical analysis using historical streamflow data from northwestern Canada. Canadian Water Resources Journal 28:69-86.

Fleming, S.W. and G.K.C. Clarke, 2005. Attenuation of high-frequency interannual streamflow variability by watershed glacial cover. ASCE-Journal of Hydraulic Engineering, 131:615-618.

Flowers, G.E., S.J. Marshall, H. Björnsson and G.K.C. Clarke, 2005. Sensitivity of Vatnajökull ice cap hydrology and dynamics to climate warming over the next 2 centuries. Journal of Geophysical Research-

Earth Surface, 110:F02011.

Førland, E.J. and I. Hanssen-Bauer, 2003. Past and future climate variations in the Norwegian Arctic: overview and novel analyses. Polar Research, 22:113-124.

Forsstrom, S., J. Strom, C.A. Pedersen, E. Isaksson and S. Gerland, 2009. Elemental carbon distribution in Svalbard snow. Journal of Geophysical Research-Atmospheres, 114:8.

Fountain, A.G. and J.S. Walder, 1998. Water flow through temperate glaciers. Reviews of Geophysics, 36:299-328.

Fox, A.J. and A.P.R. Cooper, 1994. Measured properties of the Antarctic Ice Sheet derived from the SCAR Antarctic digital database. Polar Record, 30:201-206.

Freitas, C., K.M. Kovacs, R.A. Ims, M.A. Fedak and C. Lydersen, 2008. Ringed seal post-moulting movement tactics and habitat selection. Oecologia, 155:193-204.

Fritzsche, D., R. Schütt, H. Meyer, H. Miller, F. Wilhelms, T. Opel and L.M. Savatyugin, 2005. A 275 year ice-core record from Akademii Nauk ice cap, Severnaya Zemlya, Russian Arctic. Annals of Glaciology, 42:361-366.

Füreder, L., 2007. Life at the edge: Habitat condition and bottom fauna of Alpine running waters. International Review of Hydrobiology, 92:491-513.

Gaidos, E., B. Lanoil, T. Thorsteinsson, A. Graham, M. Skidmore, S.K. Han, T. Rust and B. Popp, 2004. A viable microbial community in a subglacial volcanic crater lake, Iceland. Astrobiology, 4:327-344.

Gaidos, E., V. Marteinsson, T. Thorsteinsson, T. Jóhannesson, A.R. Runarsson, A. Stefansson, B. Glazer, B. Lanoil, M. Skidmore, S. Han, M. Miller, A. Rusch and W. Foo, 2009. An oligarchic microbial assemblage in the anoxic bottom waters of a volcanic subglacial lake. Isme Journal, 3:486-497.

Gardner, A.S. and M. Sharp, 2007. Influence of the arctic circumpolar vortex on the mass balance of Canadian High Arctic glaciers. Journal of Climate, 20:4586-4598.

Gardner, A.S. and M. Sharp, 2009. Sensitivity of net mass-balance estimates to near-surface temperature lapse rates when employing the degree-day method to estimate glacier melt. Annals of Glaciology, 50:80-86.

Gardner, A.S., M.J. Sharp, R.M. Koerner, C. Labine, S. Boon, S.J. Marshall, D.O. Burgess and D. Lewis, 2009. Near-surface temperature lapse rates over Arctic glaciers and their implications for temperature downscaling. Journal of Climate, 22:4281-4298.

Geirsdóttir, A., G.H. Miller, Y. Axford and S. Olafsdóttir, 2009. Holocene and latest Pleistocene climate and glacier fluctuations in Iceland. Quaternary Science Reviews, 28:2107-2118.

Glasser, N.F. and M.J. Hambrey, 2001. Styles of sedimentation beneath Svalbard valley glaciers under changing dynamic and thermal regimes. Journal of the Geological Society, 158:697-707.

Glazovsky, A.F., 2003. Glacier dynamics. In: Bobylev, L.P., K.Y. Kondratyev and O.M. Johannessen (Eds.). Arctic Environmental Variability in the Context of Global Change, pp. 251-270, Praxis Publishing Ltd.

Glazovsky, A. and Y. Macheret, 2006. Eurasian Arctic. In: Kotlyakov, V.M. (Ed.). Glaciation in north and central Eurasia in present time. [in Russian with English summary], pp. 97-114 and 438-445, Nauka, Moscow.

Glazovsky, A.F., G.A. Nosenko and D.G. Tsvetkov, 2007. Glaciers of Urals. Current and future state. Data of Glaciological Studies 98:207-214.

Gottesfeld, A.S. and L.M. Johnson-Gottesfeld, 1990. Floodplain dynamics of a wandering river, dendrochronology of the Morice River, British Columbia, Canada. Geomorphology, 3:159-179.

Govorukha, L.S., 1989. Modern glaciation of the Soviet Arctic. 256 pp. Gidrometeoizdat / Hydrometeoizdat, Leningrad.

Grant, K.L., C.R. Stokes and I.S. Evans, 2009. Identification and characteristics of surge-type glaciers on Novaya Zemlya, Russian Arctic. Journal of Glaciology, 55:960-972.

Gregor, D.J. and W.D. Gummer, 1989. Evidence of atmospheric transport and deposition of organochlorine pesticides and polychlorinated biphenyls in Canadian Arctic snow. Environmental Science & Technology, 23:561-565.

Greuell, W. and W.H. Knap, 2000. Remote sensing of the albedo and detection of the slush line on the Greenland ice sheet. Journal of Geophysical Research-Atmospheres, 105:15567-15576.

Greuell, W., J. Kohler, F. Obleitner, P. Glowacki, K. Melvold, E. Bernsen and J. Oerlemans, 2007. Assessment of interannual variations in the surface mass balance of 18 Svalbard glaciers from the Moderate Resolution Imaging Spectroradiometer/Terra albedo product. Journal of Geophysical Research-Atmospheres, 112:D07105.

Grinsted, A., J.C. Moore, V. Pohjola, T. Martma and E. Isaksson, 2006. Svalbard summer melting, continentality, and sea ice extent from the Lomonosovfonna ice core. Journal of Geophysical Research-Atmospheres, 111:D07110.

Hagen, J.O. and O. Liestøl, 1990. Long-term glacier mass-balance investigations in Svalbard, 1950-88. Annals of Glaciology, 14:102-106.

Hagen, J.O., O. Liestøl, E. Roland and T. Jørgensen, 1993. Glacier Atlas of Svalbard and Jan Mayen. Norsk Polarinstitutt Meddelelser 129, 160 pp.

Hagen, J.O., J. Kohler, K. Melvold and J.G. Winther, 2003a. Glaciers in Svalbard: mass balance, runoff and fresh water flux. Polar Research 22:145-159.

Hagen, J.O., K. Melvold, F. Pinglot and J.A. Dowdeswell, 2003b. On the net mass balance of the glaciers and ice caps in Svalbard, Norwegian Arctic. Arctic Antarctic and Alpine Research, 35:264-270.

Hall, D.K., J.P. Ormsby, R.A. Bindschadler and H. Siddalingaiah, 1987. Characterization of snow and ice reflectance zones on glaciers using Landsat thematic mapper data. Annals of Glaciology, 9:104-108.

Hall, D.K., R.S. Williams, K. Steffen and J.Y.L. Chien, 2004. Analysis of summer 2002 melt extent on the Greenland ice sheet using MODIS and SSM/I data. Paper presented at IEEE International Symposium on Geoscience and Remote Sensing (IGARSS), pp. 3029-3032. Anchorage, Alaska, September 20-24 2004.

Hall, D.K., R.S. Williams, K.A. Casey, N.E. DiGirolamo and Z. Wan, 2006. Satellite-derived, melt-season surface temperature of the Greenland Ice Sheet (2000-2005) and its relationship to mass balance. Geophysical Research Letters, 33:L11501.

Hall, D.K., J.E. Box, K.A. Casey, S.J. Hook, C.A. Shuman and K. Steffen, 2008a. Comparison of satellite-derived and in-situ observations of ice and snow surface temperatures over Greenland. Remote Sensing of Environment, 112:3739-3749.

Hall, D.K., R.S. Williams, S.B. Luthcke and N.E. Digirolamo, 2008b. Greenland ice sheet surface temperature, melt and mass loss: 2000-06. Journal of Glaciology, 54:81-93.

Hamilton, G.S. and J.A. Dowdeswell, 1996. Controls on glacier surging in Svalbard. Journal of Glaciology, 42:157-168.

Hammer, C.U., S.J. Johnsen, H.B. Clausen, D. Dahl-Jensen, N. Gundestrup and J.-P. Steffensen, 2001. The palaeoclimatic record from a 345m long ice core from the Hans Tausen Iskappe. Meddelelser om Grønland, Geoscience 39:87-95.

Hanelt, D., H. Tug, K. Bischof, C. Gross, H. Lippert, T. Sawall and C. Wiencke, 2001. Light regime in an Arctic fiord: a study related to stratospheric ozone depletion as a basis for determination of UV effects on algal growth. Marine Biology, 138:649-658.

Hanson, B. and R.L. Hooke, 2000. Glacier calving: a numerical model of forces in the calving-speed/water-depth relation. Journal of Glaciology, 46:188-196.

Hari, R.E., D.M. Livingstone, R. Siber, P. Burkhardt-Holm and H. Guttinger, 2006. Consequences of climatic change for water temperature and brown trout populations in Alpine rivers and streams. Global Change Biology, 12:10-26.

Harper, J.T., N.F. Humphrey, W.T. Pfeffer and B. Lazar, 2007. Two modes of accelerated glacier sliding related to water. Geophysical Research Letters, 34:L12503.

Hasholt, B. and S.H. Mernild, 2008. Hydrology, sediment transport and water resources of Ammassalik Island, SE Greenland. Geografisk Tidsskrift-Danish Journal of Geography, 108:73-95.

Hasholt, B., J. Kruger and L. Skjernaa, 2008. Landscape and sediment processes in a proglacial valley, the Mittivakkat Glacier area, Southeast Greenland. Geografisk Tidsskrift-Danish Journal of Geography, 108:97-110.

Hattersley-Smith, G., 1963. The Ward Hunt Ice Shelf: recent changes in the ice front. Journal of Glaciology, 4:415-424.

Hattersley-Smith, G., 1967. Note on ice shelves off the north coast of Ellesmere Island. Arctic Circular, 17:13-14.

Hauer, F.R., J.S. Baron, D.H. Campbell, K.D. Fausch, S.W. Hostetler, G.H. Leavesley, P.R. Leavitt, D.M. McKnight and J.A. Stanford, 1997. Assessment of climate change and freshwater ecosystems of the Rocky Mountains, USA and Canada. Hydrological Processes, 11:903-924.

Heinrichs, T., I. Mayo, D. Trabant and R. March, 1995. Observations of the

surge-type Black Rapids Glacier, Alaska, during a quiescent period, 1970-92. US Geological Survey, Earth Science Information Center, Open-File Report, 94-512, 131 pp.

Hermanson, M.H., E.H. Isaksson, C. Teixeira, D.C.G. Muir, K.M. Compher, Y.F. Li, I. Igarashi and K. Kamiyama, 2005. Current-use and legacy pesticide history in the Austfonna ice cap, Svalbard, Norway. Environmental Science & Technology, 39:8163-8169.

Hinzman, L.D. and 34 others, 2005. Evidence and implications of recent climate change in northern Alaska and other arctic regions. Climatic Change, 72:251-298.

Hock, R., V. Radiđand M. de Woul, 2007a. Climate sensitivity of Storglaciären - An inter-comparison of mass balance models using ERA-40 reanalysis and regional climate model data. Annals of Glaciology, 46:342-348.

Hock, R., D. Kootstra and C. Reijmer, 2007b. Deriving glacier mass balance from accumulation area ratio on Storglaciären, Sweden. IAHS Publication, 318:163-170.

Hock, R., M. de Woul, V. Radiđand M. Dyurgerov, 2009. Mountain glaciers and ice caps around Antarctica make a large sea-level rise contribution. Geophysical Research Letters, 36:L07501.

Hodgkins, R., J.O. Hagen and S.E. Hamran, 1999. 20th century mass balance and thermal regime change at Scott Turnerbreen, Svalbard. Annals of Glaciology, 28:216-220.

Hodson, A., P. Murnford and D. Lister, 2004. Suspended sediment and phosphorus in proglacial rivers: bioavailability and potential impacts upon the P status of ice-marginal receiving waters. Hydrological Processes, 18:2409-2422.

Hodson, A.J., P.N. Mumford, J. Kohler and P.M. Wynn, 2005. The High Arctic glacial ecosystem: new insights from nutrient budgets. Biogeochemistry, 72:233-256.

Hodson, A., A.M. Anesio, M. Tranter, A. Fountain, M. Osborn, J. Priscu, J. Laybourn-Parry and B. Sattler, 2008. Glacial ecosystems. Ecological Monographs, 78:41-67.

Holdsworth, G., 1969. Flexure of a floating ice tongue. Journal of Glaciology, 8:385-397.

Holland, D.M., R.H. Thomas, B. De Young, M.H. Ribergaard and B. Lyberth, 2008. Acceleration of Jakobshavn Isbræ triggered by warm subsurface ocean waters. Nature Geoscience, 1:659-664.

Holm, K., M. Bovis and M. Jakob, 2004. The landslide response of alpine basins to post-Little Ice Age glacial thinning and retreat in southwestern British Columbia. Geomorphology, 57:201-216.

Holmlund, P., 1993. Surveys of post-Little Ice Age glacier fluctuations in northern Sweden. Zeitschrift für Gletscherkunde und Glazialgeologie 29:1-13.

Holmlund, P., P. Jansson and R. Pettersson, 2005. A re-analysis of the 58 year mass-balance record of Storglaciaren, Sweden. Annals of Glaciology, 42:389-394.

Holtzscherer, J.-J. and A. Bauer, 1954. Contributions á la connaissance de l' Indlandsis du Groenland. IAHS Publication 39:244-296.

Hood, E. and L. Berner, 2009. Effects of changing glacial coverage on the physical and biogeochemical properties of coastal streams in southeastern Alaska. Journal of Geophysical Research-Biogeosciences, 114:G03001.

Hood, E. and D. Scott, 2008. Riverine organic matter and nutrients in southeast Alaska affected by glacial coverage. Nature Geoscience, 1:583-587.

Hood, E., J. Fellman, R.G.M. Spencer, P.J. Hernes, R. Edwards, D. D'Amore and D. Scott, 2009. Glaciers as a source of ancient and labile organic matter to the marine environment. Nature, 462:1044-1047.

Hooke, R.L., 1998. Principles of Glacier Mechanics. pp. 248. Prentice-Hall.

Hooke, R.L. and H.B. Clausen, 1982. Wisconsin and holocene delta-18-O variations, Barnes Ice Cap, Canada. Geological Society of America Bulletin, 93:784-789.

Hooke, R.L., G.W. Johnson, K.A. Brugger, B. Hanson and G. Holdsworth, 1987. Changes in mass balance, velocity, and surface profile along a flow line on Barnes Ice Cap, 1970-1984. Canadian Journal of Earth Sciences, 24:1550-1561.

Howat, I.M., I. Joughin, S. Tulaczyk and S. Gogineni, 2005. Rapid retreat and acceleration of Helheim Glacier, east Greenland. Geophysical Research Letters, 32:L22502.

Howat, I.M., I. Joughin, M. Fahnestock, B.E. Smith and T.A. Scambos, 2008. Synchronous retreat and acceleration of southeast Greenland outlet glaciers 2000-06: ice dynamics and coupling to climate. Journal of Glaciology, 54:646-660.

Hughes, T.J., 1992. Theoretical calving rates from glaciers along ice walls grounded in water of variable depths. Journal of Glaciology, 38:282-294.

Humlum, O., B. Elberling, A. Hormes, K. Fjordheim, O.H. Hansen and J. Heinemeier, 2005. Late-Holocene glacier growth in Svalbard, documented by subglacial relict vegetation and living soil microbes. The Holocene, 15:396-407.

Huss, M., R. Stöckil, G. Kappenberger and H. Blatter, 2008. Temporal and spatial changes of Laika Glacier, Canadian Arctic, since 1959, inferred from satellite remote sensing and mass-balance modelling. Journal of Glaciology, 54:857-866.

Ilg, C. and E. Castella, 2006. Patterns of macroinvertebrate traits along three glacial stream continuums. Freshwater Biology, 51:840-853.

Isaksson, E., D. Divine, J. Kohler, T. Martma, V. Pohjola, H. Motoyama and O. Watanabe, 2005. Climate oscillations as recorded in Svalbard ice core delta O-18 records between AD 1200 and 1997. Geografiska Annaler Series a-Physical Geography, 87A:203-214.

Isaksson, E., M. Hermanson, H.C. Sheila, M. Igarashi, K. Kamiyama, J. Moore, H. Motoyama, D. Muir, V. Pohjola, R. Vaikmäe, R.S.W. van de Wal and O. Watanabe, 2003. Ice cores from Svalbard - useful archives of past climate and pollution history. Physics and Chemistry of the Earth, 28:1217-1228.

Jansson, P., G. Rosqvist and T. Schneider, 2005. Glacier fluctuations, suspended sediment flux and glacio-lacustrine sediments. Geografiska Annaler Series a-Physical Geography, 87A:37-50.

Jeffries, M.O., 1992. Arctic ice shelves and ice islands: Origin, growth and disintegration, physical characteristics, structural-stratigraphic variability, and dynamics. Reviews of Geophysics, 30:245-267.

Jiskoot, H. and D.T. Juhlin, 2009. Surge of a small East Greenland glacier, 2001-2007, suggests Svalbard-type surge mechanism. Journal of Glaciology, 55:567-570.

Jiskoot, H., P. Boyle and T. Murray, 1998. The incidence of glacier surging in Svalbard: Evidence from multivariate statistics. Computers & Geosciences, 24:387-399.

Jiskoot, H., A.K. Pedersen and T. Murray, 2001. Multi-model photogrammetric analysis of the 1990s surge of Sortebræ, East Greenland. Journal of Glaciology, 47:677-687.

Johannessen, K., S. Loset and P. Strass, 1999. Simulation of Iceberg Drift. – Paper presented at The 15th International Conference on Port and Ocean Engineering Under Arctic Conditions, (POAC-99), pp. 97-105. Espoo, Finland, August 23-27 1999.

Jóhannesson, T., G. Aðalgeirsdóttir, A. Ahlstrøm, L.M. Andreassen, H. Björnsson, M. de Woul, H. Elvehøy, G.E. Flowers, S. Guðmundsson, R. Hock, P. Holmlund, F. Pálsson, V. Radiđ O. Sigurðsson and T. Thorsteinsson, 2006. The impact of climate change on glaciers and glacial runoff in the Nordic countries. Paper presented at The European Conference on Impacts of Climate Change on Renewable Energy Sources, pp. 30. CE-2, Hydrological Service, National Energy Authority, Reykjavik, Iceland, May 31 - June 2.

Jónsdóttir, J.F., 2008. A runoff map based on numerically simulated precipitation and a projection of future runoff in Iceland. Hydrological Sciences Journal-Journal Des Sciences Hydrologiques, 53:100-111.

Josberger, E.G., W.R. Bidlake, R.S. March and B.W. Kennedy, 2007. Glacier mass balance fluctuations in the Pacific Northwest and Alaska, USA. Annals of Glaciology, 46:291-296.

Joughin, I., 2002. Ice-sheet velocity mapping: a combined interferometric and speckle-tracking approach. Annals of Glaciology, 34:195-201.

Joughin, I., L. Gray, R. Bindschadler, S. Price, D. Morse, C. Hulbe, K. Mattar and C. Werner, 1999. Tributaries of West Antarctic Ice streams revealed by RADARSAT interferometry. Science, 286:283-286.

Kalnay, E., M. Kanamitsu, R. Kistler, W. Collins, D. Deaven, L. Gandin, M. Iredell, S. Saha, G. White, J. Woollen, Y. Zhu, M. Chelliah, W. Ebisuzaki, W. Higgins, J. Janowiak, K.C. Mo, C. Ropelewski, J. Wang, A. Leetmaa, R. Reynolds, R. Jenne and D. Joseph, 1996. The NCEP/NCAR 40-year reanalysis project. Bulletin of the American Meteorological Society, 77:437-471.

Karlén, W., 1976. Lacustrine sediments and tree limit variations as indicators of Holocene climatic fluctuations in Lappland, northern Sweden. Geografiska Annaler Series a-Physical Geography, 58:1-34.

Karlén, W., 1988. Scandinavian glacial and climatic fluctuations during the Holocene. Quaternary Science Reviews, 7:199-209.

Karlén, W. and J.A. Matthews, 1992. Reconstructing Holocene glacier variations from glacial lake sediments: studies from Nordvestlandet

and Jostedalsbreen-Jotunheimen, southern Norway. Geografiska Annaler 74:327-348.

Kaser, G., J.G. Cogley, M.B. Dyurgerov, M.F. Meier and A. Ohmura, 2006. Mass balance of glaciers and ice caps: Consensus estimates for 1961-2004. Geophysical Research Letters, 33:L19501.

Kattsov, V.M., J.E. Walsh, W.L. Chapman, V.A. Govorkova, T.V. Pavlova and X.D. Zhang, 2007. Simulation and projection of arctic freshwater budget components by the IPCC AR4 global climate models. Journal of Hydrometeorology, 8:571-589.

Kaufman, D.S. and 28 others, 2004. Holocene thermal maximum in the western Arctic (0-180 degrees W). Quaternary Science Reviews, 23:529-560.

Kaufman, D.S., D.P. Schneider, N.P. McKay, C.M. Ammann, R.S. Bradley, K.R. Briffa, G.H. Miller, B.L. Otto-Bliesner, J.T. Overpeck, B.M. Vinther and M. Arctic Lakes 2k Project, 2009. Recent warming reverses long-term Arctic cooling. Science, 325:1236-1239.

Kelly, M.A. and T.V. Lowell, 2009. Fluctuations of local glaciers in Greenland during latest Pleistocene and Holocene time. Quaternary Science Reviews, 28:2088-2106.

Key, J. and M. Haefliger, 1992. Arctic ice surface temperature retrieval from AVHRR thermal channels. Journal of Geophysical Research-Atmospheres, 97:5885-5893.

Key, J.R., J.B. Collins, C. Fowler and R.S. Stone, 1997. High-latitude surface temperature estimates from thermal satellite data. Remote Sensing of Environment, 61:302-309.

Killingtveit, Å., L.E. Pettersson and K. Sand, 2003. Water balance investigations in Svalbard. Polar Research, 22:161-174.

Kinnard, C., R.M. Koerner, C.M. Zdanowicz, D.A. Fisher, J. Zheng, M.J. Sharp, L. Nicholson and B. Lauriol, 2008. Stratigraphic analysis of an ice core from the Prince of Wales Icefield, Ellesmere Island, Arctic Canada, using digital image analysis: High-resolution density, past summer warmth reconstruction, and melt effect on ice core solid conductivity. Journal of Geophysical Research-Atmospheres, 113:D24120.

Koenig, L.S., K.R. Greenaway, M. Dunbar and G. Hattersley-Smith, 1952. Arctic ice islands. Arctic 5:67-103.

Koerner, R.M., 1970. Some observations on superimposition of ice on the Devon Island Ice Cap, N. W.T., Canada. Geografiska Annaler, 52A:57-67.

Koerner, R.M., 1997. Some comments on climatic reconstructions from ice cores drilled in areas of high melt. Journal of Glaciology, 43:90-97.

Koerner, R.M., 2005. Mass balance of glaciers in the Queen Elizabeth Islands, Nunavut, Canada. Annals of Glaciology, 42:417-423.

Koerner, R.M. and D.A. Fisher, 1982. Acid snow in the Canadian High Arctic. Nature, 295:137-140.

Koerner, R.M. and D.A. Fisher, 1990. A record of Holocene summer climate from a Canadian High-Arctic ice core. Nature, 343:630-631.

Koerner, R.M. and D.A. Fisher, 2002. Ice-core evidence for widespread Arctic glacier retreat in the Last Interglacial and the early Holocene. Annals of Glaciology, 35:19-24.

Kohler, J., T.D. James, T. Murray, C. Nuth, O. Brandt, N.E. Barrand, H.F. Aas and A. Luckman, 2007. Acceleration in thinning rate on western Svalbard glaciers. Geophysical Research Letters, 34:L18502.

König, M., J. Wadham, J.-G. Winther, J. Kohler and A.-M. Nuttall, 2002. Detection of superimposed ice on the glaciers Kongsvegen and Midre Lovènbreen, Svalbard, using SAR satellite imagery. Annals of Glaciology, 34:335-342.

Kononov, Y.M., M.D. Ananicheva and I.C. Willis, 2005. High-resolution reconstruction of Polar Ural glacier mass balance for the last millennium. Annals of Glaciology, 42:163-170.

Kotlyakov, V.M., V.I. Nikolaev, I.M. Korotkov and O.L. Klementyev, 1991. Climate-stratigraphy of Severnaya Zemlya ice domes in the Holocene. In: Khudyakov, G.I. (Ed.). Stratigraphy and Correlation of Quaternary deposits of Asia and Pacific region, pp. 100-112, Nauka, Moscow.

Krenke, A.N., 1982. Mass exchange of glacier systems over the USSR territory [in Russian with English summary]. Hydrometeoizdat, 5.1:93-101.

Krimmel, R.M., 2001. Photogrammetric data set, 1957- 2000, and bathymetric measurements for Columbia Glacier, Alaska. U.S. Geological Survey Water Resources Investigation Report, 01-4089, 49 pp. U.S. Geological Survey,

Kubyshkin, N.V., O.M. Andreev, V.V. Borodulin, A.F. Glazovsky, Y.P. Gudoshnikov, G.K. Zubakin, Y.Y. Macheret and A.A. Skutin, 2009. Characteristics of icebergs in their calving sites in the Russian Arctic: Results of airborne and direct studies during the IPY 2007/08. Paper presented at The 19th International Offshore and Polar Engineering Conference (ISOPE-2009), pp. 539-543. Osaka, Japan, June 21-26, 2009.

Labansen, A.L., C. Lydersen, T. Haug and K.M. Kovacs, 2007. Spring diet of ringed seals (Phoca hispida) from northwestern Spitsbergen, Norway. ICES Journal of Marine Science, 64:1246-1256.

Lafrenière, M.J. and M.J. Sharp, 2005. A comparison of solute fluxes and sources from glacial and non-glacial catchments over contrasting melt seasons. Hydrological Processes, 19:2991-3012.

Lafrenière, M.J., J.M. Blais, M.J. Sharp and D.W. Schindler, 2006. Organochlorine pesticide and polychlorinated biphenyl concentrations in snow, snowmelt, and runoff at Bow Lake, Alberta. Environmental Science & Technology, 40:4909-4915.

Lamoureux, S., 2000. Five centuries of interannual sediment yield and rainfall-induced erosion in the Canadian High Arctic recorded in lacustrine varves. Water Resources Research, 36:309-318.

Landvik, J.Y., A. Weidick and A. Hansen, 2001. The glacial history of the Hans Tausen Iskappe and the last glaciation of Peary Land, North Greenland. Meddelelser om Grønland, Geoscience 39:27-44.

Langley, K., S.E. Hamran, K.A. Hogda, R. Storvold, O. Brandt, J. Kohler and J.O. Hagen, 2008. From glacier facies to SAR backscatter zones via GPR. IEEE Transactions on Geoscience and Remote Sensing, 46:2506-2516.

Larsen, C.F., R.J. Motyka, J.T. Freymueller, K.A. Echelmeyer and E.R. Ivins, 2005. Rapid viscoelastic uplift in southeast Alaska caused by post-Little Ice Age glacial retreat. Earth and Planetary Science Letters, 237:548-560.

Larsen, C.F., R.J. Motyka, A.A. Arendt, K.A. Echelmeyer and P.E. Geissler, 2007. Glacier changes in southeast Alaska and northwest British Columbia and contribution to sea level rise. Journal of Geophysical Research-Earth Surface, 112:F01007.

Lefauconnier, B. and J.O. Hagen, 1991. Surging and calving glaciers in eastern Svalbard. Norsk Polarinstitut Meddelelser, 116, 130 pp.

Leonard, E.M., 1986. Varve studies at Hector Lake, Alberta, Canada, and the relationship between glacial activity and sedimentation. Quaternary Research, 25:199-214.

Leonard, E.M., 1997. The relationship between glacial activity and sediment production: Evidence from a 4450-year varve record of neoglacial sedimentation in Hector Lake, Alberta, Canada. Journal of Paleolimnology, 17:319-330.

Liestøl, O., 1969. Glacier surges in west Spitsbergen. Canadian Journal of Earth Sciences, 6:895-897.

Liestøl, O., 1973. Glaciological work in 1971. Aarbok Norsk Polarinstitut pp. 67- 76, Norsk Polarinstitutt.

Lingle, C.S., A.A. Arendt, W.D. Harrison, K.A. Echelmeyer and C.F. Larsen, 2008. Is glacier wastage continuing to accelerate in NW North America? E0S Transactions of the American Geophysical Union, 90, Fall Meeting Supplement:C22A-05.

Long, D.G. and B.R. Hicks, 2005. Standard Brigham Young University QuikSCAT/SeaWinds land/ice image products. Brigham Young University, Microwave Environmental Remote Sensing Technical Report MERS 05-04 and Electrical and Computer Engineering Department Report TR-L130-05.04, 30 pp.

Lubinski, D.J., S.L. Forman and G.H. Miller, 1999. Holocene glacier and climate fluctuations on Franz Josef Land, Arctic Russia, 80°N. Quaternary Science Reviews, 18:85-108.

Luthcke, S.B., A.A. Arendt, D.D. Rowlands, J.J. McCarthy and C.F. Larsen, 2008. Recent glacier mass changes in the Gulf of Alaska region from GRACE mascon solutions. Journal of Glaciology, 54:767-777.

Lydersen, C., A.R. Martin, K.M. Kovacs and I. Gjertz, 2001. Summer and autumn movements of white whales Delphinapterus leucas in Svalbard, Norway. Marine Ecology Progress Series, 219:265-274.

Lythe, M.B., D.G. Vaughan and B. Consortium, 2001. BEDMAP: A new ice thickness and subglacial topographic model of Antarctica. Journal of Geophysical Research-Solid Earth, 106:11335-11351.

Mair, D., D. Burgess and M. Sharp, 2005. Thirty-seven year mass balance of Devon Ice Cap, Nunavut, Canada, determined by shallow ice coring and melt modeling. Journal of Geophysical Research-Earth Surface, 110:F01011.

Mair, D., D. Burgess, M. Sharp, J.A. Dowdeswell, T. Benham, S. Marshall and F. Cawkwell, 2009. Mass balance of the Prince of Wales Icefield,

Ellesmere Island, Nunavut, Canada. Journal of Geophysical Research-Earth Surface, 114:F02011.

Maizels, J.K., 1979. Proglacial aggradation and changes in braided channel patterns during a period of glacier advance: An Alpine example. Geografiska Annaler 61:87-101.

Mangerud, J. and J.Y. Landvik, 2007. Younger Dryas cirque glaciers in western Spitsbergen: smaller than during the Little Ice Age. Boreas, 36:278-285.

Marsh, P. and M.K. Woo, 1981. Snowmelt, glacier melt, and high arctic streamflow regimes. Canadian Journal of Earth Sciences, 18:1380-1384.

Marshall, S.J., T.S. James and G.K.C. Clarke, 2002. North American Ice Sheet reconstructions at the Last Glacial Maximum. Quaternary Science Reviews, 21:175-192.

Matulla, C., S. Schmutz, A. Melcher, T. Gerersdorfer and P. Haas, 2007. Assessing the impact of a downscaled climate change simulation on the fish fauna in an Inner-Alpine River. International Journal of Biometeorology, 52:127-137.

Mayer, C., N. Reeh, F. Jung-Rothenhausler, P. Huybrechts and H. Oerter, 2000. The subglacial cavity and implied dynamics under Nioghalverdsfjorden Glacier, NE Greenland. Geophysical Research Letters, 27:2289-2292.

McClintock, J., R. McKenna and C. Woodworth-Lynas, 2007. Grand Banks Iceberg Management. Report prepared for PERD/CHC, National Research Council Canada, Ottawa, ON. Report prepared by AMEC Earth & Environmental, St. John's, NL, R.F. McKenna & Associates, Wakefield, QC, and PETRA International Ltd., Cupids, NL. PERD/CHC Report, 20-84, 92 pp.

McConnell, J.R., R. Edwards, G.L. Kok, M.G. Flanner, C.S. Zender, E.S. Saltzman, J.R. Banta, D.R. Pasteris, M.M. Carter and J.D.W. Kahl, 2007. 20th-century industrial black carbon emissions altered arctic climate forcing. Science, 317:1381-1384.

McNamara, J.P. and D.L. Kane, 2009. The impact of a shrinking cryosphere on the form of arctic alluvial channels. Hydrological Processes, 23:159-168.

Meier, M.F. and A. Post, 1987. Fast tidewater glaciers. Journal of Geophysical Research-Solid Earth and Planets, 92:9051-9058.

Meier, M.F., M.B. Dyurgerov, U.K. Rick, S. O'Neel, W.T. Pfeffer, R.S. Anderson, S.P. Anderson and A.F. Glazovsky, 2007. Glaciers dominate Eustatic sea-level rise in the 21st century. Science, 317:1064-1067.

Menounos, B., G. Osborn, J.J. Clague and B.H. Luckman, 2009. Latest Pleistocene and Holocene glacier fluctuations in western Canada. Quaternary Science Reviews, 28:2049-2074.

Mernild, S.H., B. Hasholt and G.E. Liston, 2008a. Climatic control on river discharge simulations, Zackenberg River drainage basin, northeast Greenland. Hydrological Processes, 22:1932-1948.

Mernild, S.H., D.L. Kane, B.U. Hansen, B.H. Jakobsen, B. Hasholt and N.T. Knudsen, 2008b. Climate, glacier mass balance and runoff (1993-2005) for the Mittivakkat Glacier catchment, Ammassalik Island, SE Greenland, and in a long term perspective (1898-1993). Hydrology Research, 39:239-256.

Milner, A.M. and G.E. Petts, 1994. Glacial rivers - physical habitat and ecology. Freshwater Biology, 32:295-307.

Milner, A.M., J.E. Brittain, E. Castella and G.E. Petts, 2001. Trends of macroinvertebrate community structure in glacier-fed rivers in relation to environmental conditions: a synthesis. Freshwater Biology, 46:1833-1847.

Milner, A.M., A.L. Robertson, K.A. Monaghan, A.J. Veal and E.A. Flory, 2008. Colonization and development of an Alaskan stream community over 28 years. Frontiers in Ecology and the Environment, 6:413-419.

Moholdt, G., J.O. Hagen, T. Eiken and T.V. Schuler, 2010a. Geometric changes and mass balance of the Austfonna ice cap, Svalbard. The Cryosphere, 4:21-34.

Moholdt, G., C. Nuth, J.-O. Hagen and J. Kohler, 2010b. Recent elevation changes of Svalbard glaciers derived from ICESat laser altimetry. Remote Sensing of Environment, 114:2756-2767.

Moore, R.D., S.W. Fleming, B. Menounos, R. Wheate, A. Fountain, K. Stahl, K. Holm and M. Jakob, 2009. Glacier change in western North America: influences on hydrology, geomorphic hazards and water quality. Hydrological Processes, 23:42-61.

Motyka, R., L. Hunter, K. Echelmeyer and C. Connor, 2003. Submarine melting at the terminus of a tidewater glacier, Leconte Glacier, Alaska, USA. Annals of Glaciology, 36:57-65.

Mueller, F., 1969. Was the Good Friday Glacier on Axel Heiberg Island surging? Canadian Journal of Earth Sciences, 6:891-894.

Mueller, D.R., W.F. Vincent and M.O. Jeffries, 2003. Break-up of the largest Arctic ice shelf and associated loss of an epishelf lake. Geophysical Research Letters, 30:2031.

Mueller, D.R., L. Copland, A. Hamilton and D. Stern, 2008. Examining Arctic ice shelves prior to the 2008 breakup. EOS, Transactions of the American Geophysical Union 89:502-503.

Murray, T., T. Strozzi, A. Luckman, H. Jiskoot and P. Christakos, 2003. Is there a single surge mechanism? Contrasts in dynamics between glacier surges in Svalbard and other regions. Journal of Geophysical Research-Solid Earth, 108:2237.

Naik, G., 2007. Arctic becomes tourism hot spot, but is that cool? The Wall Street Journal: A1. September 24.

Naumov, A.K., G.K. Zubakin, Y.P. Gudoshnikov, I.V. Buzin and A.A. Skutin, 2003. Glaciers and icebergs in the region of Shtokmanovskoe gas consendate deposit. [in Russian with Enghlish summary]. Paper presented at Proceedings of RAO-03, pp. 337-342. St.Petersburg, Russia, 16-19 September.

Neal, E.G., E. Hood and K. Smikrud, 2010. Contribution of glacier runoff to freshwater discharge into the Gulf of Alaska. Geophysical Research Letters, 37:L06404.

Nehlsen, W., J.E. Williams and J.A. Lichatowich, 1991. Pacific salmon at the crossroads: stocks at risk from California, Oregon, Idaho and Washington. Fisheries, 16:4-21.

Nesje, A., 2005. Briksdalsbreen in western Norway: AD 1900-2004 frontal fluctuations as a combined effect of variations in winter precipitation and summer temperature. The Holocene, 15:1245-1252.

Nesje, A., 2009. Latest Pleistocene and Holocene alpine glacier fluctuations in Scandinavia. Quaternary Science Reviews, 28:2119-2136.

Ng, F., S. Liu, B. Mavlyudov and Y. Wang, 2007. Climatic control on the peak discharge of glacier outburst floods. Geophysical Research Letters, 34:L21503.

Nick, F.M. and J. Oerlemans, 2006. Dynamics of tidewater glaciers: comparison of three models. Journal of Glaciology, 52:183-190.

Nick, F.M., C.J. van der Veen and J. Oerlemans, 2007. Controls on advance of tidewater glaciers: Results from numerical modeling applied to Columbia Glacier. Journal of Geophysical Research-Earth Surface, 112:F03S24.

Nolin, A.W. and M.C. Payne, 2007. Classification of glacier zones in western Greenland using albedo and surface roughness from the Multi-angle Imaging SpectroRadiometer (MISR). Remote Sensing of Environment, 107:264-275.

Nuth, C., J. Kohler, H.F. Aas, O. Brandt and J.O. Hagen, 2007. Glacier geometry and elevation changes on Svalbard (1936-90). Annals of Glaciology, 46:106-116.

Nuth, C., G. Moholdt, J. Kohler, J.O. Hagen and A. Kääb, 2010. Svalbard glacier elevation changes and contribution to sea level rise. Journal of Geophysical Research-Earth Surface, 115:F01008.

Nye, J.F., 1957. The distribution of stress and velocity in glaciers and ice sheets. Proceedings of the Royal Society of London, Series A, 239:113-133.

O'Connor, J.E. and J.E. Costa, 1993. Geologic and hydrologic hazards in glacierized basins in North America resulting from 19th and 20th century global warming. Natural Hazards 8:121-140.

O'Neel, S. and W.T. Pfeffer, 2007. Source mechanics for monochromatic icequakes produced during iceberg calving at Columbia Glacier, AK. Geophysical Research Letters, 34:L22502.

O'Neel, S., W.T. Pfeffer, R. Krimmel and M. Meier, 2005. Evolving force balance at Columbia Glacier, Alaska, during its rapid retreat. Journal of Geophysical Research-Earth Surface, 110:F03012.

Obleitner, F. and M. Lehning, 2004. Measurement and simulation of snow and superimposed ice at the Kongsvegen glacier, Svalbard (Spitzbergen). Journal of Geophysical Research-Atmospheres, 109:D04106.

Oerlemans, J. and B.K. Reichert, 2000. Relating glacier mass balance to meteorological data by using a seasonal sensitivity characteristic. Journal of Glaciology, 46:1-6.

Oerlemans, J., R.P. Bassford, W. Chapman, J.A. Dowdeswell, A.F. Glazovsky, J.O. Hagen, K. Melvold, M.D. de Wildt and R.S.W. van de Wal, 2005. Estimating the contribution of Arctic glaciers to sea-level change in the next 100 years. Annals of Glaciology, 42:230-236.

Ommanney, C.S.L., 1970. The Canadian glacier inventory. Paper presented at Glaciers, Proceedings of Workshop Seminar, pp. 23-30. Canadian National Committee, the International Hydrological Decade, Ottawa.

Opel, T., D. Fritzsche, H. Meyer, R. Schutt, K. Weiler, U. Ruth, F. Wilhelms and H. Fischer, 2009. 115 year ice-core data from Akademii Nauk ice cap, Severnaya Zemlya: high-resolution record of Eurasian Arctic climate change. Journal of Glaciology, 55:21-31.

Osipova, G.B., 2006. General state of mountain glaciers. In: Kotlyakov, V.M. (Ed.). Glaciation in North and Central Eurasia at Present Time, pp. 115-126, Nauka, Moscow.

Østrem, G., 1975a. ERTS data in glaciology - An effort to monitor glacier mass balance from satellite imagery. Journal of Glaciology, 15:403-415.

Østrem, G., 1975b. Sediment transport in glacial meltwater streams. Glaciofluvial and Glaciolacustrine Sedimentation. SEPM Special Publication, 23:101-122.

Østrem, G. and M.M. Brugman, 1991. Glacier mass-balance measurements: a manual for field and office work. NHRI Science Report 4, 224 pp.

Østrem, G., K.D. Selvig and K. Tandberg, 1988. Atlas over breer i Sør-Norge. Meddelelser fra Hydrologisk Avdeling 61, 248 pp. Norges Vassdrags- og Energiverk, Oslo.

Østrem, G., N. Haakensen and O. Melander, 1973. Atlas over breer i Nord-Skandinavia. Meddelelser fra Hydrologisk Avdeling 22, 315 pp. Norges Vassdrags-og Energiverk, Oslo and Stockholm.

Overpeck, J., K. Hughen, D. Hardy, R. Bradley, R. Case, M. Douglas, B. Finney, K. Gajewski, G. Jacoby, A. Jennings, S. Lamoureux, A. Lasca, G. MacDonald, J. Moore, M. Retelle, S. Smith, A. Wolfe and G. Zielinski, 1997. Arctic environmental change of the last four centuries. Science, 278:1251-1256.

Paterson, W.S.B., R.M. Koerner, D. Fisher, S.J. Johnsen, H.B. Clausen, W. Dansgaard, P. Bucher and H. Oeschger, 1977. An oxygen-isotope climatic record from Devon Island Ice Cap, Arctic Canada. Nature, 266:508-511.

Paul, F. and F. Svoboda, 2009. A new glacier inventory on southern Baffin Island, Canada, from ASTER data: II. Data analysis, glacier change and applications. Annals of Glaciology, 50:22-31.

Pinglot, J.F., M. Pourchet, B. Lefauconnier, J.O. Hagen, E. Isaksson, R. Vaikmae and K. Kamiyama, 1999. Accumulation in Svalbard glaciers deduced from ice cores with nuclear tests and Chernobyl reference layers. Polar Research, 18:315-321.

Pohjola, V.A. and J.C. Rogers, 1997. Atmospheric circulation and variations in Scandinavian glacier mass balance. Quaternary Research, 47:29-36.

Pohjola, V.A., T.A. Martma, H.A.J. Meijer, J.C. Moore, E. Isaksson, R. Vaikmäe and R.S.W. Van de Wal, 2002. Reconstruction of three centuries of annual accumulation rates based on the record of stable isotopes of water from Lomonosovfonna, Svalbard. Annals of Glaciology, 35:57-62.

Polyakov, I.V., R.V. Bekryaev, G.V. Alekseev, U.S. Bhatt, R.L. Colony, M.A. Johnson, A.P. Maskshtas and D. Walsh, 2003. Variability and trends of air temperature and pressure in the maritime Arctic, 1875-2000. Journal of Climate, 16:2067-2077.

Polyak, L., I. Murdmaa and E. Ivanova, 2004. A high-resolution, 800-year glaciomarine record from Russkaya Gavan', a Novaya Zemlya Fjord, Eastern Barents Sea. The Holocene, 14:628-634.

Post, A., 1975. Preliminary hydrography and historic terminal changes of Columbia Glacier, Alaska. Hydrological Investigations Atlas, HA-559, 3 pp. U.S. Geological Survey, Tacoma, Washington.

Radić, V. and R. Hock, 2006. Modeling future glacier mass balance and volume changes using ERA-40 reanalysis and climate models: A sensitivity study at Storglaciären, Sweden. Journal of Geophysical Research-Earth Surface, 111:F03003.

Radić, V. and R. Hock, 2010. Regional and global volumes of glaciers derived from statistical upscaling of glacier inventory data. Journal of Geophysical Research-Earth Surface, 115:F01010.

Radić, V. and R. Hock, 2011. Regional differentiated contribution of mountain glaciers and ice caps to future sea-level rise. Nature Geoscience, 4:91-94.

Radić, V., R. Hock and J. Oerlemans, 2008. Analysis of scaling methods in deriving future volume evolutions of valley glaciers. Journal of Glaciology, 54:601-612.

Raper, S.C.B. and R.J. Braithwaite, 2006. Low sea level rise projections from mountain glaciers and icecaps under global warming. Nature, 439:311-313.

Raper, S.C.B., O. Brown and R.J. Braithwaite, 2000. A geometric glacier model for sea-level change calculations. Journal of Glaciology, 46:357-368.

Rasmussen, L.A., 2004. Altitude variation of glacier mass balance in Scandinavia. Geophysical Research Letters, 31:L13401.

Raymond, C.F., 1987. How do glaciers surge? A review. Journal of Geophysical Research-Solid Earth and Planets, 92:9121-9134.

Reeh, N., 1968. On the calving of ice from floating glaciers and ice shelves. Journal of Glaciology, 7:215-232.

Reeh, N., 2008. A non-steady-state firn-densification model for the percolation zone of a glacier. Journal of Geophysical Research, 113:F03023.

Reeh, N., C. Mayer, H. Miller, H.H. Thomsen and A. Weidick, 1999. Present and past climate control on fjord glaciations in Greenland: implications for IRD-deposition in the sea. Geophysical Research Letters, 26:1039-1042.

Reeh, N., O.B. Olesen, H.H. Thomsen, W. Starzer and C.E. Bøggild, 2001. Mass balance parameterisation for Hans Tausen Iskappe, Peary Land, North Greenland. Meddelelser om Grønland, Geosciences, 39:57-69.

Reeh, N., D.A. Fisher, R.M. Koerner and H.B. Clausen, 2005. An empirical firn densification model comprising ice lenses. Annals of Glaciology, 42:101-106.

Reichert, B.K., L. Bengtsson and J. Oerlemans, 2001. Midlatitude forcing mechanisms for glacier mass balance investigated using general circulation models. Journal of Climate, 14:3767-3784.

Reijmer, C.H., W.H. Knap and J. Oerlemans, 1999. The surface albedo of the Vatnajokull ice cap, Iceland: A comparison between satellite-derived and ground-based measurements. Boundary-Layer Meteorology, 92:125-144.

Rennermalm, A.K., L.C. Smith, J.C. Stroeve and V.W. Chu, 2009. Does sea ice influence Greenland ice sheet surface-melt? Environmental Research Letters, 4:1-6.

Richardson, J.C. and A.M. Milner, 2005. Rivers of Pacific Canada and Alaska. In: Benke, A. and B. Cushing (Eds.). Rivers of North America, pp. 735-775, Academic Press.

Rignot, E. and P. Kanagaratnam, 2006. Changes in the velocity structure of the Greenland ice sheet. Science, 311:986-990.

Rignot, E., J.E. Box, E. Burgess and E. Hanna, 2008. Mass balance of the Greenland ice sheet from 1958 to 2007. Geophysical Research Letters, 35:L20502.

Rignot, E., M. Koppes and I. Velicogna, 2010. Rapid submarine melting of the calving faces of West Greenland glaciers. Nature Geoscience, 3:187-191.

Royer, T.C., 1982. Coastal fresh water discharge in the northeast Pacific. Journal of Geophysical Research-Oceans and Atmospheres, 87:2017-2021.

Russell, A.J., M.J. Roberts, H. Fay, P.M. Marren, N.J. Cassidy, F.S. Tweed and T. Harris, 2006. Icelandic jökulhlaup impacts: Implications for ice-sheet hydrology, sediment transfer and geomorphology. Geomorphology, 75:33-64.

Sandford, K.S., 1955. Tabular icebergs between Spitsbergen and Franz-Josef Land. Geographical Journal, 121:164-170.

Scambos, T.A., M.J. Dutkiewicz, J.C. Wilson and R.A. Bindschadler, 1992. Application of image cross-correlation to the measurement of glacier velocity using satellite image data. Remote Sensing of Environment, 42:177-186.

Schiefer, E., B. Menounos and R. Wheate, 2007. Recent volume loss of British Columbian glaciers, Canada. Geophysical Research Letters, 34:L16503.

Schneeberger, C., H. Blatter, A. Abe-Ouchi and M. Wild, 2003. Modelling changes in the mass balance of glaciers of the northern hemisphere for a transient 2 x CO2 scenario. Journal of Hydrology, 282:145-163.

Schulson, E.M., 1999. The structure and mechanical behavior of ice. JOM-Journal of the Minerals Metals & Materials Society, 51:21-27.

Schytt, V., 1969. Glacier surge in eastern Svalbard. Canadian Journal of Earth Sciences 6:875-882.

Serreze, M.C., A.P. Barrett, J.C. Stroeve, D.N. Kindig and M.M. Holland, 2009. The emergence of surface-based Arctic amplification. The Cryosphere, 3:11-19.

Sharp, M. and L.B. Wang, 2009. A five-year record of summer melt on Eurasian Arctic ice caps. Journal of Climate, 22:133-145.

Sharp, M. and G. Wolken, 2009. Glaciers outside Greenland. Bulletin of the American Meteorological Society, State of the Climate in 2008:107-108.

Sharp, M. and G. Wolken, 2010. Glaciers outside Greenland. Bulletin of the American Meteorological Society, State of the Climate 2009: 91:94-97.

Sharp, M., J. Parkes, B. Cragg, I.J. Fairchild, H. Lamb and M. Tranter, 1999. Widespread bacterial populations at glacier beds and their relationship to rock weathering and carbon cycling. Geology, 27:107-110.

Sharp, M.J., L. Copland, K. Filbert, D. Burgess and S. Williamson, 2003. Recent changes in the extent and volume of Canadian Arctic glaciers. Paper presented at Snow Watch 2002 Workshop and Assessing Global Glacier Recession, Glaciological Data Report, pp. 73-75. NSIDC/WDC for Glaciology, Boulder, Colorado.

Sharp, M., D.O. Burgess, F. Cawkwell, L. Copland, J.A. Davis, E.K. Dowdeswell, J.A. Dowdeswell, A.S. Gardner, D. Mair, L. Wang, S.N. Williamson, G.J. Wolken and F. Wyatt, 2011, in press. Recent glacier changes in the Canadian Arctic. In: Kargel, J.S., M.P. Bishop, A. Kääb, B.H. Raup and G. Leonard (Eds.). Global Land Ice Measurements from Space: Satellite Multispectral Imaging of Glaciers, pp. 20 pp, Praxis-Singer,

Shuchman, R.A. and E.G. Josberger (Eds.), 2010. Bering Glacier: Interdisciplinary Studies of Earth's Largest Temperate Surging Glacier. 384 pp.

Sigurðsson, O., T. Jónsson and T. Jóhannesson, 2007. Relations between glacier termini variations and summer temperature in Iceland since 1930. Annals of Glaciology, 46:170-176.

Skidmore, M.L. and M.J. Sharp, 1999. Drainage system behaviour of a High-Arctic polythermal glacier. Annals of Glaciology, 28:209-215.

Skidmore, M.L., J.M. Foght and M.J. Sharp, 2000. Microbial life beneath a high Arctic glacier. Applied and Environmental Microbiology, 66:3214-3220.

Smith, B.P.G., D.M. Hannah, A.M. Gurnell and G.E. Petts, 2001. A hydrogeomorphological context for ecological research on alpine glacial rivers. Freshwater Biology, 46:1579-1596.

Smith, L.C., Y.W. Sheng, R.R. Forster, K. Steffen, K.E. Frey and D.E. Alsdorf, 2003. Melting of small Arctic ice caps observed from ERS scatterometer time series. Geophysical Research Letters, 30:2034.

Sneed, W.A., R.L. Hooke and G.S. Hamilton, 2008. Thinning of the south dome of Barnes Ice Cap, Arctic Canada, over the past two decades. Geology, 36:71-74.

Solomon, S., D. Qin, M. Manning, Z. Chen, M. Marquis, K.B. Averyt, M. Tignor and H.L. Miller (Eds.), 2007. Climate Change 2007. The Physical Science Basis. Contribution of Working Group I to the Fourth Assessment Report of the Intergovernmental Panel on Climate Change. 996 pp. Cambridge University Press.

Stahl, K. and R.D. Moore, 2006. Influence of watershed glacier coverage on summer streamflow in British Columbia, Canada. Water Resources Research, 42:W06201.

Straneo, F., G.S. Hamilton, D.A. Sutherland, L.A. Stearns, F. Davidson, M.O. Hammill, G.B. Stenson and A. Rosing-Asvid, 2010. Rapid circulation of warm subtropical waters in a major glacial fjord in East Greenland. Nature Geoscience, 3:182-186.

Stroeve, J. and K. Steffen, 1998. Variability of AVHRR-derived clear-sky surface temperature over the Greenland ice sheet. Journal of Applied Meteorology, 37:23-31.

Sund, M. and T. Eiken, 2010. Recent surges on Blomstrandbreen, Comfortlessbreen and Nathorstbreen, Svalbard. Journal of Glaciology, 56:182-184.

Svendsen, J.I. and J. Mangerud, 1997. Holocene glacial and climatic variations on Spitsbergen, Svalbard. The Holocene, 7:45-57.

Svendsen, H., A. Beszczynska-Moller, J.O. Hagen, B. Lefauconnier, V. Tverberg, S. Gerland, J.B. Orbaek, K. Bischof, C. Papucci, M. Zajaczkowski, R. Azzolini, O. Bruland, C. Wiencke, J.G. Winther and W. Dallmann, 2002. The physical environment of Kongsfjorden-Krossfjorden, an Arctic fjord system in Svalbard. Polar Research, 21:133-166.

Syvitski, J.P.M., A.B. Stein, J.T. Andrews and J.D. Milliman, 2001. Icebergs and the sea floor of the East Greenland (Kangerlussuaq) continental margin. Arctic, Antarctic and Alpine Research, 33:52-61.

Tamisiea, M.E., E.W. Leuliette, J.L. Davis and J.X. Mitrovica, 2005. Constraining hydrological and cryospheric mass flux in southeastern Alaska using space-based gravity measurements. Geophysical Research Letters, 32:L20501.

Thomsen, T. and A. Weidick, 1992. Climate change impact on northern water resources in Greenland. Paper presented at the 9th International Northern Research Basins Symposium, pp. 749-781. Government of Canada, Yukon & Northwest Territories.

Tranter, M., M.J. Sharp, H.R. Lamb, G.H. Brown, B.P. Hubbard and I.C. Willis, 2002. Geochemical weathering at the bed of Haut Glacier d'Arolla, Switzerland - a new model. Hydrological Processes, 16:959-993.

Tranter, M., M. Skidmore and J. Wadham, 2005. Hydrological controls on microbial communities in subglacial environments. Hydrological Processes, 19:995-998.

Trouet, V., J. Esper, N.E. Graham, A. Baker, J.D. Scourse and D.C. Frank, 2009. Persistent positive North Atlantic Oscillation mode dominated the Medieval climate anomaly. Science, 324:78-80.

Tuffen, H., 2010. How will melting of ice affect volcanic hazards in the twenty first century. Philosophical Transactions of the Royal Society A, 368:2535-2558.

Van der Veen, C.J., 1996. Tidewater calving. Journal of Glaciology, 42:375-385.

Van der Veen, C.J., 1998a. Fracture mechanics approach to the penetration of surface crevasses on glaciers. Cold Regions Science and Technology, 27:31-47.

Van der Veen, C.J., 1998b. Fracture mechanics approach to the penetration of bottom crevasses on glaciers. Cold Regions Science and Technology, 27:213-223.

VanLooy, J., R. Forster and A. Ford, 2006. Accelerating thinning of Kenai Peninsula glaciers, Alaska. Geophysical Research Letters, 33:L21307.

Vare, L.L., G. Massé, T.R. Gregory, C.W. Smart and S.T. Belt, 2009. Sea ice variations in the central Canadian Arctic Archipelago during the Holocene. Quaternary Science Reviews, 28:1354-1366.

Veillette, J., D.R. Mueller, D. Antoniades and W.F. Vincent, 2008. Arctic epishelf lakes as sentinel ecosystems: Past, present and future. Journal of Geophysical Research-Biogeosciences, 113:G04014.

Vieli, A., M. Funk and H. Blatter, 2001. Flow dynamics of tidewater glaciers: a numerical modelling approach. Journal of Glaciology, 47:595-606.

Vinther, B.M., S.L. Buchardt, H.B. Clausen, D. Dahl-Jensen, S.J. Johnsen, D.A. Fisher, R.M. Koerner, D. Raynaud, V. Lipenkov, K.K. Andersen, T. Blunier, S.O. Rasmussen, J.P. Steffensen and A.M. Svensson, 2009. Holocene thinning of the Greenland ice sheet. Nature, 461:385-388.

Wadham, J.L., M. Tranter, S. Tulaczyk and M. Sharp, 2008. Subglacial methanogenesis: A potential climatic amplifier? Global Biogeochemical Cycles, 22:GB2021.

Walter, F., S. O'Neel, D. McNamara, W.T. Pfeffer, J.N. Bassis and H.A. Fricker, 2010. Iceberg calving during transition from grounded to floating ice: Columbia Glacier, Alaska. Geophysical Research Letters, 37:L15501.

Wang, L., M.J. Sharp, B. Rivard, S. Marshall and D. Burgess, 2005. Melt season duration on Canadian Arctic ice caps, 2000-2004. Geophysical Research Letters, 32:L19502.

Wang, L., M. Sharp, B. Rivard and K. Steffen, 2007. Melt season duration and ice layer formation on the Greenland ice sheet, 2000-2004. Journal of Geophysical Research-Earth Surface, 112:F04013.

Warren, S.G. and W.J. Wiscombe, 1980. A model for the spectral albedo of snow. II: snow containing atmospheric aerosols. Journal of the Atmospheric Sciences, 37:2734-2745.

Weeks, W.F. and W.J. Campbell, 1973. Icebergs as a freshwater source: An appraisal. Journal of Glaciology, 12:207-233.

Weertman, J., 1973. Can a water-filled crevasse reach the bottom surface of a glacier? Paper presented at the Symposium on the Hydrology of Glaciers, pp. 139-145. Union Geodesique et Geophysique Internationale. Association Internationale d'Hydrologie Scientifique. Commission de Neiges et Glaces, Cambridge, September 7-13, 1969.

Weidick, A., 1995. Greenland. Satellite Image Atlas of Glaciers of the World, USGS Professional Paper. 1386-C, 153 pp.

Weidick, A. and E. Morris, 1998. Local glaciers surrounding the continental ice sheets. Paper presented at Into the second century of world glacier monitoring - prospects and strategies, pp. 197-205. UNESCO, Paris.

Weingartner, T.J., S.L. Danielson and T.C. Royer, 2005. Freshwater variability and predictability in the Alaska Coastal Current. Deep-Sea Research Part II-Topical Studies in Oceanography, 52:169-191.

Weng, W.L., 1995. The area of Greenland and ice cap, Letter to the editor. Arctic, 48:206-206.

WGMS, 2009. Glacier Mass Balance Bulletin (2006-2007). Glacier Mass Balance Bulletin, 10, 108 pp. World Glacier Monitoring Service, Zürich.

Williams, R.S., 1987. Satellite remote sensing of the Vatnajökull, Iceland. Annals of Glaciology, 9:127-165.

Williams, M. and J.A. Dowdeswell, 2001. Historical fluctuations of the Matusevich Ice Shelf, Severnaya Zemlya, Russian High Arctic. Arctic, Antarctic and Alpine Research, 33:211-222.

Williamson, S., M. Sharp, J. Dowdeswell and T. Benham, 2008. Iceberg calving rates from northern Ellesmere Island ice caps, Canadian Arctic, 1999-2003. Journal of Glaciology, 54:391-400.

Winkler, S., 2003. A new interpretation of the date of the 'Little Ice Age' glacier maximum at Svartisen and Okstindan, northern Norway. The Holocene, 13:83-95.

Wiscombe, W.J. and S.G. Warren, 1980. A model for the spectral albedo of snow, I: Pure snow. Journal of the Atmospheric Sciences, 37:2712-2733.

Wolken, G.J., J.H. England and A.S. Dyke, 2008. Changes in late-Neoglacial perennial snow/ice extent and equilibrium-line altitudes in the Queen Elizabeth Islands, Arctic Canada. The Holocene, 18:615-627.

Wolken, G.J., M. Sharp and L.B. Wang, 2009. Snow and ice facies variability and ice layer formation on Canadian Arctic ice caps, 1999-2005. Journal of Geophysical Research-Earth Surface, 114:F03011.

Woodworth-Lynas, C.M.T., H.W. Josenhans, J.V. Barrie, C.F.M. Lewis and D.R. Parrott, 1991. The physical processes of seabed disturbance during iceberg grounding and scouring. Continental Shelf Research, 11:939-951.

Zdanowicz, C.M., D.A. Fisher, I. Clark and D. Lacelle, 2002. An ice-marginal delta O-18 record from Barnes Ice Cap, Baffin Island, Canada. Annals of Glaciology, 35:145-149.

Zeeberg, J., 2001. Climate and glacial history of the Novaya Zemlya Archipelago, Russian Arctic, with notes on the region's history of exploration. pp. 174. Rosenberg Publishers, Amsterdam.

Zeeberg, J. and S.L. Forman, 2001. Changes in glacier extent on north Novaya Zemlya in the twentieth century. The Holocene, 11:161-175.

Zhang, J., U.S. Bhatt, W.V. Tangborn and C.S. Lingle, 2007a. Climate downscaling for estimating glacier mass balances in northwestern North America: Validation with a USGS benchmark glacier. Geophysical Research Letters, 34:L21505.

Zhang, J., U.S. Bhatt, W.V. Tangborn and C.S. Lingle, 2007b. Response of glaciers in northwestern North America to future climate change: an atmosphere/glacier hierarchical modeling approach. Annals of Glaciology, 46:283-290.

Zheng, J., C. Zdanowicz, D. Fisher, G. Hall and J. Vaive, 2003. A new 155-year record of Pb pollution from Devon Ice Cap, Canada. Journal de Physique IV France, 107:1405-1408.

Zubakin, G.K., A.K. Naumov and E.A. Skutina, 2006. Spreading and morphometric peculiarities of icebergs in the Barents Sea. Paper presented at The 18th IAHR International Symposium on Ice, pp. 79-87.

Zubakin, G.K., Y.P. Gudoshnikov, A.K. Naumov, A.F. Glazovsky, N.V. Kubyshkin, I.V. Buzin, V.V. Borodulin and E.A. Skutina, 2007. Results of investigation of icebergs, glaciers and their frontal zones in the North-Eastern part of the Barents Sea. In: Yue, Q.J. (Ed.). Recent Development of Offshore Engineering in Cold Regions, pp. 548-564, POAC-07.